UNIVERSITY OF CALIFORNIA, SAN DIEGO

Localization and activation of CaMKII delta isoforms and their involvement in heart failure

A dissertation submitted in partial satisfaction of the
requirements for the degree Doctor of Philosophy

in

Biomedical Sciences

by

Shikha Mishra

Committee in charge:

Professor Joan Heller Brown, Chair
Professor Wolfgang Dillmann
Professor Steve Hedrick
Professor Andrew McCulloch
Professor Alexandra Newton

2010

The Dissertation of Shikha Mishra is approved, and it is acceptable in quality and form for publication on microfilm and electronically:

Chair

University of California, San Diego
2010

Dedication

This dissertation is dedicated to my family, especially my parents, Dr. Raja and Sandhya Mishra who stood beside me to hold my hands as I took my first steps and who now once again stand beside me as I step into my future. My parents have devoted their lives to ensuring my success and making my dreams and visions reality and they have provided me with endless love, support and encouragement. My family's unwavering belief in my capabilities and the knowledge that were I to ever lose my footing, I wouldn't have far to fall because they would be right there, have been my greatest motivation for pursuing my paramount goal of education and all of my dreams.

For everything, I thank you, Daddy, Mama, Nam and Pooh

Epigraph

It is our responsibility as scientists, knowing the great progress which comes from a satisfactory philosophy of ignorance, the great progress which is the fruit of freedom of thought, to proclaim the value of this freedom; to teach how doubt is not to be feared but welcomed and discussed; and to demand this freedom as our duty to all coming generations.

Richard Feynman

Table of Contents

List of Abbreviations

AIP	Autocamtide-2 related inhibitory peptide
AMVM	Adult mouse ventricular myocyte
ANF	Atrial natriuretic factor
AP-1	Activator protein 1
βMHC	Beta myosin heavy chain
BNP	B-type natriuretic protein
BSA	Bovine serum albumin
BW	Body weight
CaM	Calmodulin
CaMKII	Ca^{2+}/Calmodulin dependent protein kinase II
CICR	Ca^{2+} induced Ca^{2+} release
Csq	Calsequestrin
Cx43	Connexin - 43
Cyp D	Cyclophilin D
Cyto	Cytosol
DMEM	Dulbecco's Modified Eagle's Medium
DNA	Deoxyribonucleic acid
dUTP	2'-deoxuridine 5'-triphophate
E-C	Excitation-contraction
EDTA	Ethylenediaminetetraacetic acid
ELISA	Enzyme-linked immunosorbent assay
E-T	Excitation - transcription

FS	Fractional shortening
GAPDH	Glyceraldehyde 3-phosphate dehydrogenase
GFP	Green fluorescent protein
H_2O_2	Hydrogen peroxide
HA	Hemagglutinin
HDAC	Histone deacetylase
HW	Heart weight
$IP_3(R)$	Inositol triphosphate (receptor)
kD	Kilodalton
KO	Knockout
KO/TG	Phospholamban knockout / CaMKII δ_C transgenic
LIF	Leukemia inhibitory factor
LVIDs	Left ventricular internal diameter systole
LW	Lung weight
M	Molar
MEF2	Myocyte enhancer factor 2
MEM	Minimum essential medium
Mito	Mitochondria
MOI	Multiplicity of infection
mPTP	Mitochondrial permeability transition pore
NCX	Na/Ca^{2+} exchanger
NLS	Nuclear localization sequence
NRVM	Neonatal rat ventricular myocyte

Nuc	Nucleus
PBS	Phosphate buffered saline
P-CaMKII	Phosphorylated CaMKII
PE	Phenylephrine
PLN	Phospholamban
PPIF	Peptidylprolyl isomerase F
P-RyR2	Phosphorylated ryanodine receptor 2
PT	Permeability transition
Rho GDI	Rho guanine nucleotide dissociation inhibitor
RIPA	Radio-immunoprecipitation assay
ROS	Reactive oxygen species
RyR2	Ryanodine receptor 2
SDS PAGE	Sodium dodecyl sulfate polyacrilamide gel electrophoresis
Ser	Serine
SERCA	Sarco/endoplasmic reticulum Ca^{2+}-ATPase
siRNA	Small interfering ribonucleic acid
SR	Sarcoplasmic reticulum
SR/mem	Sarcoplasmic reticulum/membrane
TAC	Transverse aortic constriction
TBS	Tris buffered saline
TG	Transgenic
Thr	Threonine
TUNEL	Terminal deoxynucleotidyl transferase dUTP nick end labeling

VDAC	Voltage-dependent anion channel
WGA	Wheat germ agglutinin
WT	Wild type

List of Figures

Acknowledgements

I would like to thank my thesis advisor, Professor Joan Heller Brown, for her support and encouragement over the past six years. In allowing me to join her lab, Joan gave me the honor of training under her guidance and an opportunity to receive one of the highest levels of graduate mentorship possible. Her sincere consideration to teaching me how to do science and the generous amount of time that she devoted to my training never ceased to amaze me. Under her mentorship I have gained an in-depth understanding of pharmacology through classes she taught, courses that she directed, and chats we had during our weekly meetings. Under her direction, I have learned how to conduct science with the highest level of integrity, analyze data from an objective and multidimensional perspective and communicate with the scientific community, all of which have contributed to my success in graduate school. I am fully confident that my success in the future will be attributable to the exceptional training and foundation that Joan has given to me as an advisor, mentor and friend.

I would like to extend a special thank you to all of the members of the Heller Brown lab, past and current, for their help and support. The training I received in the laboratory was incomparable and I am thankful for having the opportunity to learn in an environment where a high level of scientific integrity and inquisitiveness is maintained. Without the help of Katherine Huang, I wouldn't have been able to complete several seminal studies of my research project, and I am eternally grateful for her help. I would especially like to thank Dr. Tong Zhang and Dr. Shigeki Miyamoto for their mentorship starting my first day in the lab. Under their guidance, I learned the basis of my project and many of the techniques I used to complete my degree.

Thank you to my thesis committee members, Drs. Andrew McCulloch, Steve Hedrick, Alexandra Newton and Wolfgang Dillmann for advice, suggestions and guidance in helping me formulate and complete my thesis work. My committee meetings were thought provoking, and helped to focus and add perspective to my projects.

I would like to sincerely thank Dr. Don Bers, from UC Davis, for his mentorship, insight, discussions, suggestions and generosity in allowing me to learn and execute experiments within his lab as well as meet to discuss results and potential projects. I consider Dr. Bers an honorary member of my committee, and his input in my projects was imperative. I would like to thank Dr. Maya Kunkel and Dr. Alexandra Newton for their exceptional mentorship; while working in the Newton lab, I learned fluorescence reporter and imaging techniques and received advice and assistance on the FRET reporter project. Both Maya and Alexandra have been encouraging and supportive throughout graduate school, and I highly value their involvement in my training. I would also like to acknowledge Dr. Anne Murphy and her lab for assisting me with mitochondrial experiments and answering a multitude of questions with an open door and a smile. For their mentorship, advice, discussions and friendship along the way, I'd also like to say thank you to Professors Larry Brunton and Paul Insel.

I would like to thank the Biomedical Sciences Graduate program, especially Gina Butcher and Leanne Nordeman for all of their help and support.

On a personal note, I would like to say a heartfelt thank you to all of my friends who have kept me happy and motivated throughout this journey – you know who you are! My success thus far is largely due to my amazing support system I proudly call my family. My parents, to whom I dedicated this thesis, have devoted their lives to providing

me with everything necessary to guarantee my success. They are the role models that I strive to emulate in all aspects of my life. I have no words to describe the support and help that my sister and other half, Deepa, and my "little" brother, Deepak, have given me. Each victory we celebrate together, and each failure we fight together. Lastly, I'd like to thank my best friend, Shibin Parameswaran, who is an integral part of my achievement of this degree and is a continuous source of joy, love, and happiness in my life. I couldn't have done this without you.

Professionally and in all other aspects of my life, I thank you all for contributing to and sharing in my achievement.

The text and figures in Chapter III and IV are, in part, a reprint of material as it appears in:

Mishra S., Bers D.M., Brown J.H. Location matters: Clarifying the concept of nuclear and cytosolic CaMKII subtypes *Circ Res* Submitted December 2010

Huke S, DeSantiago J, Kaetzel MA, Mishra S, Brown JH, Dedman JR and Bers DM SR-targeted CaMKII inhibition improves SR Ca handling, but accelerates cardiac remodeling in mice overexpressing CaMKIIδ_C *J Mol Cell Cardiol.* 2010 Oct 21

Elrod J, Wong R, Mishra S, Vagnozzi RJ, Sakthievel, B, Karch J, Gabel S, Farber J, Force T, Brown JH, Murphy E, Molkentin JD Cyclophilin-D controls mitochondrial pore-dependent Ca^{2+} exchange, metabolic flexibility and predisposition to heart failure.

J Clin Invest. 2010 Oct 1;120(10):3680-7

Zhang T, Guo T, Mishra S, Dalton ND, Kranias EG, Peterson KL, Bers DM, Brown JH. Phospholamban ablation rescues sarcoplasmic reticulum Ca(2+) handling but exacerbates cardiac dysfunction in CaMKIIdelta(C) transgenic mice. *Circ Res*. 2010 Feb 5;106(2):354-62.

Zhang T, Kohlhaas M, Backs J, Mishra S, Phillips W, Dybkova N, Chang S, Ling H, Bers DM, Maier LS, Olson EN, Brown JH CaMKIIdelta isoforms differentially affect calcium handling but similarly regulate HDAC/MEF2 transcriptional responses. *J Biol Chem.* 2007 Nov 30;282(48):35078-87.

Vita

2004 B.S. Biomedical Engineering, The Johns Hopkins University

2010 Ph.D. Biomedical Sciences, University of California San Diego

Publications

Mishra S, Bers DM, Brown JH. Subcellular localization and activation of CaMKII δ splice variants governs activation and functional consequences. (Circ Res Submitted November 2010)

Guo T, Zhang T, Ginsburg KS, Mishra S, Brown JH, Bers DM. Modulation of resting Ca^{2+} sparks in intact myocytes by endogenous CaMKIIδ_C (Submitted 2010)

Huke S, DeSantiago J, Kaetzel MA, Mishra S, Brown JH, Dedman JR and Bers DM. ***SR-*** targeted CaMKII inhibition improves SR Ca handling, but accelerates cardiac remodeling in mice overexpressing CaMKIIδ_C (J Mol Cell Cardiol. 2010 Oct 21)

Elrod J, Wong R, Mishra S, Vagnozzi RJ, Sakthievel, B, Karch J, Gabel S, Farber J, Force T, Brown JH, Murphy E, Molkentin JD. Cyclophilin-D controls mitochondrial pore-dependent Ca^{2+} exchange, metabolic flexibility and predisposition to heart failure. J Clin Invest. 2010 Oct 1;120(10):3680-7

Mishra S, Ling H, Grimm M, Zhang T, Bers DM, Brown JH. Cardiac Hypertrophy and Heart Failure Development Through Gq and CaM Kinase II Signaling. J Cardiovasc Pharmacol. 2010 Jun 7 2010

Zhang T, Guo T, Mishra S, Dalton ND, Kranias EG, Peterson KL, Bers DM, Brown JH. Phospholamban ablation rescues sarcoplasmic reticulum Ca(2+) handling but exacerbates cardiac dysfunction in CaMKIIdelta(C) transgenic mice. Circ Res. 2010 Feb 5;106(2):354-62.

Rubio M, Avitabile D, Fischer K, Emmanuel G, Gude N, Miyamoto S, Mishra S, Schaefer EM, Brown JH, Sussman MA. Cardioprotective stimuli mediate phosphoinositide 3-kinase and phosphoinositide dependent kinase 1 nuclear accumulation in cardiomyocytes. J Mol Cell Cardiol. 2009 Jul;47(1):96-103.

Zhang T, Kohlhaas M, Backs J, Mishra S, Phillips W, Dybkova N, Chang S, Ling H, Bers DM, Maier LS, Olson EN, Brown JH. CaMKIIdelta isoforms differentially affect calcium handling but similarly regulate HDAC/MEF2 transcriptional responses. J Biol Chem. 2007 Nov 30;282(48):35078-87.

Abstracts

John W Elrod, Rene Wong, Shikha Mishra, Ronald J Vagnozzi, Bhuvana Sakthievel, Jason Karch, John Farber, Thomas Force, Joan Heller Brown, Elizabeth Murphy and Jeffery D Molkentin. Ablation of Cyclophilin-D Blunts Mitochondrial Pore-Dependent

Calcium Release Resulting in a Loss of Metabolic Flexibility and Predisposition to Heart Failure. 2010 Basic Cardiovascular Sciences AHA, Palm Springs, CA July 2010

Shikha Mishra, Joan Heller Brown. Subcellular localization and activation of CaMKII delta splice variants 2010 Gordon Research Conference, New London, NH June 2010

Shikha Mishra, Tong Zhang, Joan Heller Brown. Subcellular localization and activation of CaMKII delta splice variants. 2010 Experimental Biology FASEB, Anaheim, CA April 2010

Shikha Mishra, Tong Zhang, Joan Heller Brown. Subcellular localization and activation of CaMKII delta splice variants. 2009 Basic Cardiovascular Sciences AHA, Las Vegas, NV July 2009

Shikha Mishra, Tong Zhang, Joan Heller Brown. Impact of CaMKII Localization on Function. 2008 Experimental Biology FASEB, San Diego, CA April 2008

Tong Zhang, Lars Maier, Shikha Mishra, Joan Heller Brown. Differential Role of Cytoplasmic and Nuclear Isoforms of CaMKII in the Heart. 2006 Keystone American Heart Association, Keystone, CO July 2006

Shikha Mishra, Tong Zhang, Tao Guo, Donald Bers and Joan Heller Brown. Phospholamban ablation rescues SR Ca^{2+} loading but not cardiac function in CaMKIIδ_C transgenic mice. 2006 Gordon Research Conference, New London, NH June 2006

Tong Zhang, Lars Maier, Shikha Mishra, Joan Heller Brown. Differential Role of Cytoplasmic and Nuclear Isoforms of CaMKII in the Heart. 2006 IUPHAR, Beijing, CHINA, July 2006

Shikha Mishra, Tong Zhang, Tao Guo, Donald Bers and Joan Heller Brown. Phospholamban ablation rescues SR Ca^{2+} loading but not cardiac function in CaMKIIδ_C transgenic mice. 2006 Experimental Biology FASEB, San Francisco, CA April 2006

Abstract of the Dissertation

Localization and activation of CaMKII delta isoforms and their involvement in heart failure

by

Shikha Mishra

Doctor of Philosophy in Biomedical Sciences

University of California San Diego, 2010

Professor Joan Heller Brown, Chair

Heart failure, the heart's inability to sufficiently deliver blood to meet the body's demand, is a leading cause of death in the U.S. As an adaptive response to stress, the heart undergoes structural remodeling resulting in enlargement known as cardiac hypertrophy. Although initially compensatory, chronic hypertrophy can lead to reduced contractility, often resulting in heart failure. The signaling mechanisms by which chronic hypertrophy transitions to heart failure are not well understood and are of great significance to advancing clinical treatment of heart failure. In cardiomyocytes, Ca^{2+} is a critical second messenger involved in many cardiac signaling pathways, and changes in Ca^{2+} handling are associated with hypertrophy and dysfunction leading to heart failure. Several proteins are involved in intracellular Ca^{2+} regulation, one being Ca^{2+}/calmodulin-

dependent protein kinase II, (CaMKII). This Ca^{2+}-sensitive protein kinase, which phosphorylates a number of known substrates, has emerged as a key molecule in hypertrophy and heart failure. CaMKII activity and expression are altered in heart failure patients and animal models of hypertrophy and heart failure. The predominant cardiac isoform is CaMKIIδ, and two splice variants (subtypes), δ_B and δ_C, differing only by a nuclear localization sequence, are present in the heart. Our lab has shown that overexpression of either subtype results in cardiac dysfunction, however whether the subtypes have differential roles is unclear. Studies presented in the first part of this dissertation extensively characterize the localization and activation of δ_B vs. δ_C, and reveal that subtype localization is nonspecific, and enzyme localization governs its activation and function. CaMKIIδ null mice overexpressing individual subtypes were generated and used throughout our studies to not only understand enzyme localization and activation, but also to provide an important perspective on whether δ_B and δ_C have differential roles. The second part provides an in-depth study of the mechanism by which CaMKII δ_C contributes to heart failure, studied by crossing δ_C transgenic mice with several genetically altered mouse models in an effort to rescue the heart failure phenotype. While attenuation of the heart failure phenotype was not achieved, our findings provide insight into the maladaptive mechanisms that contribute to cardiomyopathy, and underscore the multidimensional role of CaMKII in the heart.

I. Introduction

I.A. General introduction to dissertation

The work presented in this dissertation focuses on investigating the role of Ca^{2+}/Calmodulin dependent protein kinase II (CaMKII) in cardiac hypertrophy and heart failure. CaMKII activation is modulated by Ca^{2+} levels, and following initial activation, autophosphorylation leads to autonomous (Ca^{2+} independent) activity. CaMKII plays a critical role in the regulation of Ca^{2+} handling within the cardiomyocyte and human and animal models of heart failure exhibit increased enzyme activity and/or expression [1]. The major cardiac isoform of CaMKII is CaMKIIδ and two splice variants (subtypes), CaMKIIδ_B and δ_C, differ in whether they contain a nuclear localization sequence. Transgenic overexpression of either subtype has been shown to lead to pathological cardiac phenotypes [2, 3]. The mechanism by with CaMKIIδ contributes to the development of cardiac dysfunction has not been well defined, and thus far, the individual roles of the two subtypes has not been clearly established. The studies presented in this dissertation offer insight into the mechanism by which CaMKIIδ contributes to cardiac dysfunction, and demonstrate a novel perspective of CaMKII δ_B and δ_C localization and activation.

I.B. Introduction to cardiac hypertrophy and heart failure

Cardiac hypertrophy is defined as an increase in myocardial mass, and is the compensatory mechanism by which the heart responds to stress or injury in an effort to minimize cardiac wall stress and preserve cardiac function. There are two distinct

classifications of hypertrophy: physiologic and pathologic. Physiologic hypertrophy occurs during normal heart development associated with growth, as well as in response to athletic conditioning or pregnancy [4]. Physiologic hypertrophy is usually associated with enhanced cardiac function to accommodate the increase in the body's metabolic demands and is reversible in the cases of athletic conditioning and pregnancy. Pathologic hypertrophy occurs in response to stress associated with disease states such as pressure overload, disrupted hormonal stimulation or ischemic events [5]. Although initially compensatory, chronic hypertrophy can result in cardiac dysfunction and heart failure.

In order to increase myocardial mass, cardiomyocytes, which are terminally differentiated and therefore unable to divide, increase their individual cell size [4]. Hallmarks of this hypertrophic growth include increased cell volume, changes in protein synthesis, cardiac remodeling, myofilament reorganization and increased expression of fetal genes [4]. These characteristics of pathologic hypertrophy are irreversible and maladaptive, contributing to cardiomyocyte death which eventually leads to ventricular chamber dilation and loss of cardiac function [6].

Heart failure is simply defined as the inability of the heart to supply the body with enough blood to meet its metabolic demands and results from the inability of the heart to functionally maintain either the diastolic (filling) or systolic (contractile) phase. Heart failure is currently the leading cause of death in the United States and is the endpoint of several common disease states including dilated cardiomyopathy, coronary artery disease and hypertension.

I.C. Introduction to Ca^{2+} regulatory mechanisms within the cardiomyocyte

Ca^{2+} is a critical second messenger involved in the regulation of ventricular function and gene expression. On a beat to beat basis, ventricular contraction occurs via a complex signaling process that couples a Ca^{2+} transient to each ventricular contraction. This process is known as excitation contraction (E-C) coupling [7, 8]. The generation of the calcium transient begins with depolarization of the membrane causing activation of voltage sensitive L-type Ca^{2+} channels and allowing a small amount of Ca^{2+} into the cytosol triggering a much larger Ca^{2+} release from the intracellular Ca^{2+} storage unit, the sarcoplasmic reticulum (SR). This mechanism is termed Ca^{2+}-induced calcium release (CICR) and ultimately leads to contraction. Relaxation occurs when Ca^{2+} is removed from the cytosol by extrusion through the Na^{+}/Ca^{2+} exchanger, (NCX), or reuptake into the SR by SR Ca^{2+}-ATPase, (SERCA2a) [7, 8]. Whereas each Ca^{2+} transient elicits a ventricular contraction, sustained or chronic changes in Ca^{2+} signaling can affect transcription, a process known as excitation-transcription (E-T) coupling [9]

Disruption of Ca^{2+} handling not only disrupts cardiac function but is thought to contribute to cardiomyocyte cell loss, a major factor in the development of heart failure [6]. Ca^{2+} regulatory mechanisms within the myocyte are regulated by a variety of Ca^{2+} sensitive enzymes, and a critical sensor and modulator of Ca^{2+} levels within the cardiomyocyte is Ca^{2+}/Calmodulin-dependent protein kinase II (CaMKII).

I.D. Introduction to CaMKII

CaMKs are Serine/Threonine (Ser/Thr) kinases, and are regulated by the binding of the Ca^{2+}/Calmodulin (Ca^{2+}/CaM) complex, which leads to autophosphorylation and

subsequent Ca^{2+} independent activity [10]. The CaMK family consists of CaMK I, II and IV, of which monomeric CaMKI and IV are expressed at low levels in the heart [11]. CaMKII is a ubiquitous enzyme found in most tissues of the body. CaMKII has four isoforms, α, β, δ or γ, and structurally exists as a multimer of 6-12 subunits. Each isoform is encoded by a distinct gene, and splice variants of the individual isoforms exist, sometimes including a nuclear localization sequence (NLS) targeting it to the nucleus. CaMKII can form hetero- or homomultimers consisting of subunits of any of the four isoforms and their splice variants [10]. CaMKII α and β are found primarily in neuronal tissue, and CaMKII δ and γ subunits are found in most tissues including the heart [11]. CaMKII δ is the predominant cardiac CaMK, and has two splice variants, δ_B and δ_C, that differ by the inclusion of an 11 amino acid NLS in δ_B [12-14]. The highly conserved structure of CaMKII includes three distinct domains: the association, regulatory and catalytic domains. The association domain is responsible for the assembly of the multimer, and the catalytic domain is responsible for the kinase activity. The regulatory domain contains the Ca^{2+}/CaM binding site and an autoinhibitory domain that inhibits kinase activity when the enzyme is in its unphosphorylated state. Upon binding of Ca^{2+}/CaM, a conformational change occurs allowing autophosphorylation at Thr287. This leads to Ca^{2+}-independent, or autonomous activity, because the negatively charged phosphate group prevents reassociation of the catalytic domain to the autoinhibitory region [15]. A novel mechanism for CaMKII autonomous activation was recently discovered involving methionine oxidation. Following Ca^{2+}/CaM binding to CaMKII, conformational change exposes the regulatory domain, but instead of autophosphorylation, oxidation of M281/282 can lead to persistent enzyme activation [16].

Known substrates of CaMKII include proteins critical to cardiac excitation-contraction coupling, such as the voltage sensitive L-type Ca^{2+} channels [17], ryanodine receptors (RyR2) [18, 19], which are SR Ca^{2+} release channels, SERCA2a [20, 21] and phospholamban (PLN) [22, 23], which regulates SERCA2a function [8] (Fig 1). CaMKII δ can also affect gene transcription by phosphorylation of type II histone deacetylases (HDACs) and subsequent de-repression of hypertrophic transcription factor MEF2 [24,25] (Fig 2), or through regulation of other transcription factors such as AP-1 [26, 27], GATA4 [28].

I.E. Introduction to CaMKII mediated hypertrophy and heart failure

It has been established that perturbation of Ca^{2+} handling in cardiomyocytes contributes to heart failure development which is associated with significant changes in the expression levels of intracellular Ca^{2+} regulatory proteins including sarcoplasmic reticulum calcium ATPase2 (SERCA2), inositol phosphate receptor 2 (IP_3R2), the predominant cardiac IP_3 receptor, and the RyR2 [29, 30], all known targets of CaMKIIδ. Numerous reports have established that CaMKII is a critical mediator of the development of cardiac hypertrophy and heart failure [31]. In human patients suffering from heart failure, CaMKII activity and expression has been found to be increased and evidence from *in vitro* studies and results from animal models suggest an important role for CaMKII in cardiac pathophysiology [2, 32, 33]. Initial studies using neonatal rat ventricular myocytes (NRVMs) demonstrated that hypertrophy induced by treatment with various known hypertrophic agonists such as phenylephrine (PE), endothelin 1 (ET-1) and leukemia inhibitory factor (LIF) was attenuated by CaMKII inhibitors, KN-62 and KN-93, implicating CaMKII in hypertrophy development [34-37]. Characterization of cardiac

specific CaMKIIδ transgenic (δ TG) mice overexpressing either the δ_B or δ_C subtype demonstrated that both mouse models develop cardiac enlargement at 8 weeks of age and exhibit several hallmarks of pathologic hypertrophy that eventually decompensate to heart failure [2, 3, 38].

In two independent studies characterizing a CaMKIIδ knockout (δKO) mouse model, it was found that loss of CaMKIIδ attenuated cardiomyopathy associated with pressure overload. Characterization of CaMKIIδ KO mice in our lab revealed that CaMKII is not required for the development of hypertrophy, but is necessary for the transition to heart failure [39]. Following isoproteronol treatment and short term TAC, δ KO mice were protected from the expected changes in protein expression, target phosphorylation, Ca^{2+} leak and ventricular dysfunction seen in control WT mice. Studies from the Olson lab were largely consistent with our lab's finding that loss of CaMKIIδ was protective against heart failure development, however they found that in their model, CaMKIIδ ablation also attenuated hypertrophic response to pressure overload [40]. Taken together, analysis of both mouse models demonstrate the importance of CaMKIIδ in heart failure.

I.F. Introduction to CaMKII δ_B and δ_C

The two δ subtypes, δ_B and δ_C, differ only by the inclusion of an NLS on CaMKII δ_B and several studies have observed the presence of δ_B in the nucleus, while δ_C displays cytosolic localization [11, 35, 41]. This led to the hypothesis that δ_B plays a role in transcriptional regulation while CaMKII δ_C is involved in cytosolic Ca^{2+} handling.

Studies in NRVMs showed that transient expression of δ_B but not δ_C led to transcriptional activation of ANF gene expression which was attributed to enzyme localization in the nucleus [35]. Development and characterization of cardiac specific δ_B and δ_C TG showed that while both δ_B and δ_C TG mice develop cardiac hypertrophy which is ultimately maladaptive, the δ_C TG mice exhibit a more severe cardiac phenotype and display rapid progression to heart failure [2, 38].

This difference in phenotype was consistent with the hypothesis that δ_C is involved in intracellular Ca^{2+} handling and δ_B is more of a transcriptional regulator [38]. The heart failure phenotype observed in the δ_C TG mice was characterized by increased number, frequency and width of Ca^{2+} sparks resulting in a significant increase in SR calcium leak compared to wild type myocytes. This contributed to an overall decrease in SR Ca^{2+} content, and decreased Ca^{2+} transients [30]**.** Comparative studies of the δ_B and δ_C TG mice showed that the disruption of Ca^{2+} handling seen in the δ_C TG mice were not seen in the δ_B TG mice, and the severe cardiac phenotype seen in the CaMKII δ_C TG mice was largely attributed to this disruption in SR Ca^{2+} handling [2, 30, 38].

Within the duration of completion of this dissertation, several *in vitro* studies have begun to implicate δ_C as a pro-apoptotic signaling molecule, and evidence has emerged indicating a protective role for CaMKII δ_B [42, 43]. Our lab has shown that CaMKII δ_B TG mice do not transition to heart failure as rapidly as the δ_C TG mice, although following chronic hypertrophy, secondary changes in protein phosphatase activity affected SR Ca^{2+} uptake and contributed to ventricular dilation [3]. The δ_C TG mice displayed increased ventricular dilation and cardiomyocyte loss, consistent with data suggesting that CaMKII

δ_C is involved in pro-apoptotic signaling and sensitizes towards activation of mitochondrial death pathways [44].

I.G. Rationale and significance

Characterization of cardiac-specific CaMKIIδ TG mice and CaMKII δ KO mice have demonstrated that CaMKIIδ activation induces pathologic hypertrophy leading to heart failure, and predisposes to pressure-overload induced heart failure. Several studies from our lab and others including work presented here in this dissertation have been published demonstrating the central role that CaMKIIδ plays in ventricular dysfunction resulting from a multitude of cardiac insults and is a critical mediator of cardiomyocyte death.

The work presented here show that the hypothesis that δ_B acts exclusively in the nucleus because it contains an NLS and δ_C acts exclusively in cytosolic compartments is not entirely correct. However, differential effects of the two CaMKII subtypes, δ_B and δ_C, have been shown *in vitro* and *in vivo* and has led to a question of whether there is a unique role for the individual subtypes within the cardiomyocyte, or if there is a relationship between their localization, activation and subsequent target phosphorylation.

The studies completed in this dissertation were aimed towards understanding the mechanism by which CaMKIIδ contributes to cardiac dysfunction, and provide an in-depth characterization of the localization and activation of the individual subtypes in an effort to understand whether they play differential roles in signaling in the cardiomyocyte

and by manipulating the CaMKIIδ_C TG mouse model to gain insight into the mechanism by which δ_C is contributing to heart failure and is more maladaptive than δ_B.

This work will serve as a basis to continue investigation of the individual roles of the CaMKII subtypes, and how they contribute to the development of hypertrophy and heart failure. In order to consider CaMKII as a potential therapeutic target, it is important to fully understand the mechanisms by which CaMKII is activated, whether there is subtype specificity in enzyme activation, binding partners, and importantly, whether the localization of the enzyme is responsible for the deleterious vs. protective effects, issue critical for developing an effective therapeutic agent and minimizing secondary effects.

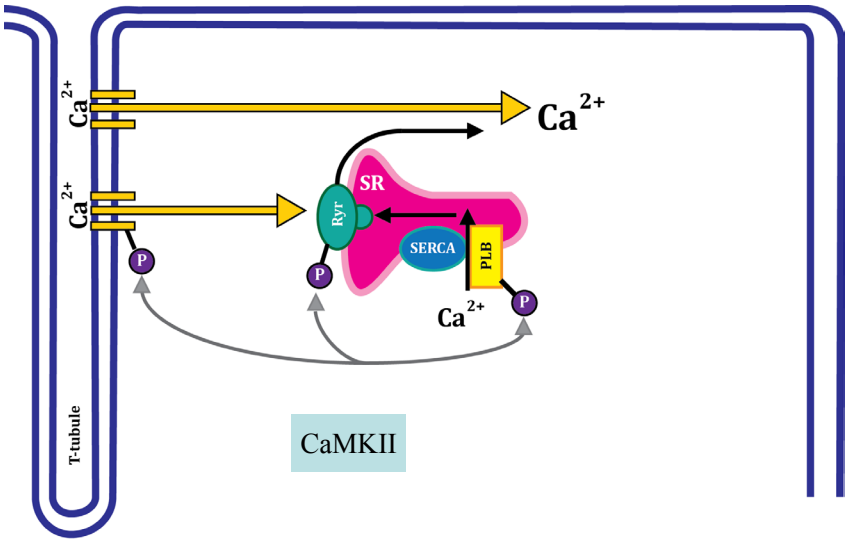

Figure 1. Cytosolic CaMKII targets. Several known CaMKII substrates include proteins critical to cardiac excitation-contraction coupling including L-type Ca^{2+} channels, ryanodine receptors (RyR2) SERCA2a and phospholamban (PLN).

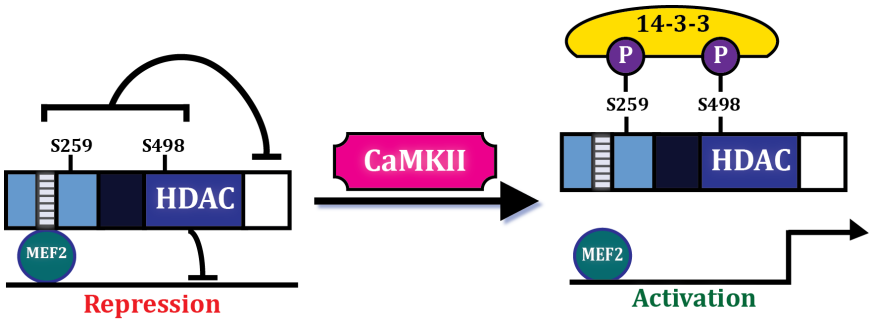

Figure 2. Nuclear CaMKII targets. CaMKII δ substrates also include type II histone deacetylases (HDACs), and can therefore affect gene transcription by phosphorylation of HDAC and subsequent de-repression of hypertrophic transcription factor MEF2.

II. Materials and Methods

II.A. Beta-galactosidase staining and activity assays

Hearts from CaMKIIδ_B or δ_C TG mice harboring MEF2-LacZ transgene or from mice expressing the MEF2-LacZ transgene but not CaMKII were collected and fixed in 4% paraformaldehyde buffered with PBS. Hearts were then immersed in Bluo-gal stain (3.1 mm ferricyanide, 3.1 mm ferrocyanide, 10 mm sodium phosphate, pH 7.2, 0.15 m sodium chloride, 1.0 mm magnesium chloride, 1 mg/ml Bluo-gal in dimethylformamide) overnight at room temperature. β-Galactosidase activity assays were performed on ventricular extracts using a β-galactosidase assay kit from Stratagene under conditions of linearity with respect to time and protein concentration.

II.B. Transgenic mice

Transgenic mice expressing either the cytoplasmic CaMKIIδ_C or the nuclear CaMKIIδ_B in the heart were generated as described previously [2, 3]. MEF2 indicator mice harboring a lacZ transgene controlled by the MEF2 binding site were developed and described previously [45]. CaMKII δ_B or δ_C TG mice were crossed with the MEF2 indicator mice and offspring of δ_C and δ_B TG mice harboring the MEF2-LacZ transgene were used for activity assay experiments. PLN KO mice were developed and described previously [29]. CaMKII δ_C TG mice were crossed with PLN KO mice and heterozygous PLN offspring carrying the CaMKII transgene were inbred with mice lacking the transgene. CaMKIIδ_C mice were crossed with the cyclophilin D (Ppif $^{-/-}$) mice [46] and SR-AIP mice [47] in a similar fashion. CaMKII δ KO mice lacking CaMKIIδ were generated as described

previously [39]. CaMKIIδ_B and δ_C TG mice were crossed with CaMKIIδ KO mice, and heterozygous offspring carrying the transgene were inbred with mice lacking the transgene. All mice used in the studies presented in this dissertation were of mixed gender and 5-6 weeks of age, unless otherwise noted. All procedures were performed in accordance with NIH Guide for the Care and Use of Laboratory Animals and approved by the Institutional Animal Care and Use Committee.

II.C. Preparation of heart tissue extract and cell lysate for western blot analysis

Mice were cervically dislocated and placed in supine position. An incision was made parallel to the diaphragm and the rib cage was separated by cutting parallel to the sternum to visualize the heart. The heart was excised and immediately rinsed in ice cold PBS to remove blood. Atria were removed and the ventricles were snap frozen in liquid nitrogen. Frozen hearts were pulverized and powder was homogenized using a tissue homogenizer (Tissuemiser, Fisher Scientific) in ice cold radio-immunoprecipitation assay (RIPA) buffer (150 mM/L sodium chloride, 50 mM/L Tris (pH7.4), 1% NP-40, 1 % of sodium deoxycholate,0.1 % of SDS, 0.2 mM/L EDTA) supplemented with protease and phosphatase inhibitors (100 μM sodium orthovanadate, 10 μg/ml leupeptin, 10 μg/ml aprotinin, 1 mM *p*-nitrophenyl phosphate, 1mM phenylmethylsulfonyl fluoride, 1 mM sodium sodium fluoride). Cardiomyocytes were washed 3 times in ice cold PBS and then harvested in the RIPA buffer formulation described above. Tissue and cell lysates nutated 4°C for 20 min, and lysates were clarified by centrifugation at 21.000 x g at 4°C. Protein concentration was measured using Bradford analysis.

II.D. Western blotting

Western blot analysis was carried out as described previously [38]. Lysates were mixed with Nupage LDS sample buffer and reducing agent, heated at 80°C for 10 minutes. Equal amounts of protein (10-40 μg), or equal volumes of fractions were loaded onto SDS-PAGE (invitrogen NuPage system), run, transferred to PVDF membranes (Millipore), blocked in 5% milk in TBS/Tween for 1 hour and the resulting blot probed using antibodies at a 1:1000 dilution in 3% BSA/TBS-tween. The antibodies used for immunoblotting were as following: rabbit CaMKIIδ antibody (a gift from Don Bers laboratory, University of California Davis, Davis, CA), mouse anti-phospholamban (Upstate Biotechnology), rabbit anti-phospho-phospholamban (Thr^{17}) (Cyclacel, Dundee, UK), rabbit Rho-GDI (Cell signaling technology), rabbit VDAC/porin (Calbiochem), mouse SERCA2a (Thermo/Affinity Bioreagents), mouse Lamin A/C (Cell Signaling Technology), mouse anti-phospho-CaMKII (Thermo/Affinity Bioreagents), and rabbit anti-phospho-HDAC5 Ser498 (Signalway Antibody). Following primary antibody incubation, blots were washed with TBS-tween (10 min x 3 times) and incubated with secondary antibodies (1:5000) in 5% milk/TBS-Tween for 30-60 minutes. Anti-rabbit or anti-mouse secondary antibody (Sigma) was used at 1:10,000 dilution.

II.E. Cell viability study in AMVMs

Ventricular myocytes were isolated as described previously [48]. After isolation, cells were plated for 1 hour on laminin-coated dishes in MEM-HBSS (minimum essential medium/Hanks balanced salt solutions) medium containing 5% serum. Cells were then washed, and serum-free medium added. As indicated, vehicle, 2 μmol/L KN-93, 100

nmol/L ryanodine, 5 μmol/L Ru-360, or 5 μmol/L cyclosporine A were added to medium. Using a grid marking system, 8 fields were chosen per dish and the number of rod shaped living cells was counted at various times over a 12-hour time course. At the 12-hour time point, living cells were quantitated by trypan blue exclusion.

II.F. Subcellular fractionation of ventricular tissue

Tissue was fractionated using differential centrifugation as described previously [49]. Briefly, flash frozen hearts were pulverized and homogenized using a Dounce glass tissue grinder. The homogenate was centrifuged for 10 min at 600 ×g, the pellet washed three times and then re-suspended in nuclear extract buffer (in mM: HEPES 20, 25% Glycerol, NaCl 420, $MgCl_2$ 1.5, EDTA 0.2). The resulting supernatant is the Nuclear Fraction. The supernatant from the first centrifugation was centrifuged at 5000 ×g (to remove mitochondria) and the resulting supernatant then centrifuged at 100.000 ×g. The supernatant is the Cytosolic Fraction and the pellet, after being washed 3 times and re-suspended in RIPA buffer (in mM: NaCl 150, Tris 20, 1% Triton X 100, 0.1% SDS), is the SR/membrane fraction.

II.G. SR purification

Freshly isolated myocytes from 4 mouse hearts were suspend in homogenization buffer and using a dounce homogenizer, cells were homogenized using 15-20 strokes on setting B. Cell lysates were spun at 10,600 x g to clarify lysates and pellets resuspended in homogenization buffer and homogenize for 10 strokes at setting B. Following a spin @ 10,600 x g for 8min, supernatant was collected and loaded onto a fresh sucrose gradient

consisting of 1ml of 20%, 2ml of 27%, 2 ml 30%, 2ml of 34%, 3ml of sup with 72% sucrose (1.5 ml +1.5ml 72%). Gradients were spun at 100,000x g for 24hrs @4C. SR fraction was harvested from the interface of the 27% and 30% gradient.

II.H. Adult mouse ventricular myocyte isolation

Adult mouse ventricular myocytes were isolated from adult WT and CaMKIIδ KO mice [48]. Hearts were removed, cannulated and perfused via the aorta at 37° C at a rate of 3ml/min. Hearts were first perfused with Ca^{2+} free buffer for 4 minutes, followed by perfusion with the buffer containing 0.25 mg/ml collagenase (Blendzyme 1, Roche) for 8-12 minutes. Atria were removed, and ventricle was dissociated by pipetting with increasingly smaller diameter transfer pipette tips. Following tissue digestion, collagenase was inactivated by addition of 10% bovine calf serum to tissue suspension. Calcium was gradually added back to a final concentration of 1mM/l. Cells were plated on laminin-coated dishes or chamber slides in minimal essential medium/Hanks' balanced salt solution containing 5% serum. After 1 hour, cells were washed and serum-free medium was added back. Prior to adenoviral infection, cells were serum starved for 4 hours.

II.I. Adenoviral infection and immunofluorescence measurements in AMVMs

Isolated AMVMs were infected with control vector (AdCMV), GFP-tagged CaMKIIδ_B or CaMKIIδ_C at 3000-5000 viral particles/cell and cultured in serum free media for 24 hours. The GFP- tagged CaMKIIδ_B and δ_C adenovirus were a gift from Don Bers laboratory, University of California Davis, CA. Cells were fixed using 4%

paraformaldehyde (20 min at room temperature), rinsed three times in PBS and then mounted with Vectashield with DAPI (Vector) immediately prior to confocal imaging. Metafluor© imaging software was used to generate the linescan quantification.

II.J. Langendorff perfusion of intact heart

Mice (4 weeks old, weighing 23–25 g) were heparinized (500 units/kg, intraperitoneally) and sacrificed by cervical dislocation. Hearts were rapidly excised, washed in ice-cold Krebs-Henseleit solution (118 mmol/L NaCl, 24 mmol/L $NaHCO_3$,4 mmol/L KCl, 1 mmol/L NaH_2PO_4, 2 mmol/L $CaCl_2$, 1.2 mmol/L $MgCl_2$, 12 mmol/L glucose and 10 mmol/L HEPES,pH7.4), and cannulated via the aorta on a 20-gauge stainless steel blunt needle. Hearts were perfused at 80 mm Hg on a Langendorff apparatus using Krebs-Henseleit solution at 37 °C. Hearts were perfused with oxygenated buffer for 12 min to allow for equilibration, followed by 15 minutes perfusion with 100nM phenylephrine or vehicle, or a bolus injection of 10mM caffeine or vehicle directly into the heart. The heart was removed following perfusion/treatment and immediately rinsed in ice cold buffer, atria removed, and then flash frozen in liquid nitrogen.

II.K. Culture and adenoviral infection of NRVMs

For adenoviral infection, cells were washed after overnight culture. Cells were infected with AdCMV, CaMKIIδ_B, and CaMKIIδ_C adenoviruses at 200-500 viral particles/cell for 3-4 h. Cells were subsequently washed and maintained in serum-free

medium with supplements. After an additional 24-36 h, cells were harvested for western blot or fractionation studies.

II.L. NRVM isolation

Hearts were excised from 1-2 day old Sprague-Dawley rat pups, atria removed and the remaining tissue was treated with trypsin overnight and rocked gently at 4°C. The following day, hearts were treated with collagenase for one hour at 37°C and then passed through a 70 μm strainer to remove undigested material. The cells were then pelleted using a clinical centrifuge and resuspended in medium 199 containing 15% fetal bovine serum a total of two times. The resulting myocytes were plated onto 6 cm dishes ($0.8x10_6$ cells per plate), or 10 cm dishes ($1.5x10_6$ cells per plate), coated with 1% gelatin prior to plating. Cells were plated overnight in medium 199 supplemented with 15% fetal bovine serum and antibiotics (100 units/ml penicillin and 100 μg/ml streptomycin), and then maintained in serum-free Dulbecco's modified Eagles medium (DMEM) for the duration of the experiments. This method of cell isolation results in a prep culture that is >95% myocytes at the outset.

II.M. Subcellular fractionation of NRVMs

Cells were harvested in PBS and pelleted by a 5 minute spin at 4^oC at 435 x g. Pellet was resuspended in 75uL of cytosolic lysis buffer (10mM HEPES pH 7.6, 10 mM NaCl, 1.5 mM $MgCl_2$, 10% glycerol) supplemented with protease and phosphatase inhibitors (100 μM sodium orthovanadate, 10 μg/ml leupeptin, 10 μg/ml aprotinin, 1 mM *p*-nitrophenyl phosphate, 1mM phenylmethylsulfonyl fluoride, 1 mM sodium sodium

fluoride) and incubated at 4^{o}C for 15 minutes. Nuclei were spun down at 4^{o}C centrifuge at 2,655 x g for 5 min and supernatant was transferred to a clean tube (Cytoplasmic fraction). The pellet was washed with cytosolic lysis buffer and nuclei were spun down at 4^{o}C at 2,655 x g for 5 min. supernatant was discarded, and nuclei were resuspended in 75µL of high salt RIPA lysis buffer (50mM Tris-HCL PH 7.4, 500mM NaCl, 1mM EDTA, 1% Triton-X, 1% Na deoxycholate, 0.1% SDS) with protease and phosphatase inhibitors listed above and incubated on ice for 15 minutes, vortexing every 5. Both cytosolic and nuclear fractions were clarified using a 15 minutes spin at 21,000 x g.

II.N. Transfection of NRVMs with siRNA

Pre-designed CaMKIIδ ON-TARGET*plus* small interfering ribonucleic acid (siRNA) for rat (catalog number; J-094929-09) and control siRNA (catalog number; D-001810-02) were purchased from Thermo Scientific. NRVMs were transfected with siRNA using DharmaFECT-I transfection reagent (Thermo Scientific) based on manufacture's instruction. Two µmol/L siRNA were transfected into 1x106 cells. siRNA and DharmaFECT-1 (4 µl and 12 µl for 1x106 cells in 6 cm dish, respectively) were individually incubated in conical tubes containing 0.5 ml OPTI-MEM media (GIBCO) at room temperature for 5 min, mixed and incubated at room temperature for 20 min. Media in culture dishes were replaced with fresh media (3 ml for 6 cm dish) and siRNA/DharmaFECT-I mixtures (1 ml/dish) were added to culture dishes. After overnight incubation, cells were washed and cultured for another 48 hrs in serum free media (DMEM including 100 units/ml penicillin and 100 µg/ml streptomycin).

II.O. TUNEL staining of ventricular sections

Transverse sections of mouse hearts isolated from WT, PLN KO, δ_C TG and KO/TG mice, were labeled with fluorescein-terminal deoxynucleotidyl transferase-mediated dUTP-biotin nick end labeling (TUNEL) using DeadEnd™ Fluorometric TUNEL System (Promega) according to manufacturer's instructions. Briefly, sections were deparaffined using xylene, re-hydrated and then permeabilized in 0.2% Triton X-100 for 10 minutes at room temperature. Sections were labeled with fluorescein-12-dUTP for 1 hour at room temperature to visualize apoptotic nuclei, and then mounted using Vectashield (vector) mounting media containing DAPI to identify nuclei. Wheat germ agglutinin was used to stain cell membranes and cardiomyocytes identified by their centrally located nuclei. Labeled nuclei were counted to determine the apoptotic index (number of labeled nuclei/10^5 total myocyte nuclei).

II.P. Mitochondrial isolation from whole heart tissue

Hearts were removed from adult mice (CharlesRiver, C57, male 2–4 months old) and perfused with PBS at room temperature for 5 min to remove blood. The ventricle was homogenized in isolation buffer containing 70mM sucrose, 190mM mannitol, 20mM Hepes and 0.2mM EDTA. For western blotting experiments, the isolation buffer also contained 1 mMNa_3VO_4, 10mg/ml aprotinin, 10 mg/ml leupeptin, 0.5mM PNPP and 1mM PMSF. The homogenate was centrifuged at 600 g for 10 min to remove nuclei and debris. The resulting supernatant was then centrifuged at 5000 g for 15 min. The resulting mitochondrial pellet was resuspended in 500 ml isolation buffer and centrifuged three times at 5000 g for 15 min, to wash the pellet. Liver was homogenized in buffer

containing 250mM sucrose, 10mM Tris (pH 7.4) and 1mM EGTA. The homogenate was centrifuged at 1000 g for 5 min and the resultant supernatant was centrifuged at 13 000 g for 10 min. The pellet was washed twice and resuspended.

II.Q. Mitochondrial swelling assay

Mitochondria were isolated from whole hearts as described above. Mitochondria were diluted to 1 μg/μl in isolation buffer. Changes in mitochondrial volume were assayed using spectrophotometer readings taken at 520nM of mitochondrial suspensions first under basal conditions and then over time following addition of 100μM Ca^{2+} to the mitochondrial suspension. Changes in light absorbance were normalized with respect to basal values.

II.R. Histological and morphometric analysis

Hearts from mice were collected and fixed in 4% paraformaldehyde buffered with PBS, dehydrated and paraffin embedded. Hearts were sections at 5mM and stained with hematoxylin and eosin and Masson's Trichrome or Connexin-43 was used to identify gap junction formation.

II.S. Echocardiography

Transthoracic echocardiography was performed in mice using an Agilent Technologies Sonos 5500 system with a 15 MHz transducer. Mice were anesthetized, and M-mode and Doppler tracings were recorded at a sweep speed of 150 mm/sec. Measurements were obtained by an examiner blinded to the genotype of the animals.

II.T. Measurements of mitochondrial respiration, Ca^{2+} fluxes, Ca^{2+} content and swelling in mitochondria

Respiration measurements were performed polarographically using a Hansatech "Oxyterm" respirometer; Ca^{2+} and swelling were measured optically in LS-50B spectrofluorometer (Perkin-Elmer). Mitochondrial protein concentration was 0.25 mg/ml. The experiments were completed within 2–3 h after the isolation procedure.

For respiration measurements, mitochondria were incubated at 37 °C in a basal saline medium (125 mM KCl, 20 mM HEPES/KOH, pH 7.4, and 2 mM phosphate) supplemented with 1 mM $MgCl_2$ and either complex I-linked substrates (a mixture of 5 mM glutamate and 5 mM malate) or a complex II substrate (5 mM succinate in the presence of 2 μM rotenone). To measure uncoupler-stimulated respiration (state 3u), sequential additions of the protonophore carbonyl cyanide *p*-(trifluoromethoxy)phenylhydrazone (FCCP) (200 nM) were made until the respiration rate reached maximum.

Extramitochondrial Ca^{2+} was monitored with the membrane-impermeable fluorescent dye Calcium Green 5N (0.5 μM). Mitochondrial Ca^{2+} uptake was detected as disappearance of the extramitochondrial fluorescent signal. Measurements were performed in the same medium as that used for respiration measurements supplemented with glutamate and malate but without $MgCl_2$. Energized mitochondria were challenged with a Ca^{2+} bolus (100 nmoles/mg protein) which lead to delayed Ca^{2+} release following the initial uptake. Mitochondrial Ca^{2+} content was determined in the same basal medium (above) supplemented with respiratory inhibitor (0.5 μM Antimycin A). The amount of Ca^{2+} released from mitochondria was calculated based upon calibration of the fluorescent

signal at the end of each experimental run by additions of known concentrations of $CaCl_2$ to the medium. Due to the presence of released Ca^{2+} this calibration deviates from a theoretical hyperbolic binding curve, however incrementing added Ca^{2+} levels by the amount of released Ca^{2+} restores the theoretical shape of the calibration curve. Therefore, the amount of released Ca^{2+} could be determined by regression analysis of the calibration curve.

Mitochondrial swelling was measured as a decrease in mitochondrial light scattering at 540 nm under the conditions of Ca^{2+} flux measurements.

II.U. Statistical analysis

All results are reported as mean ± S.E. All data was analyzed using Prism software. Statistical significance of differences between groups was determined using 1-way ANOVA with Tukey post hoc test. A probability value of <0.05 was considered statistically significant.

III. Subcellular localization of CaMKII δ subtypes governs its activation

III.A. Abstract

Differential effects of the CaMKIIδ_B and CaMKIIδ_C subtypes on cardiac Ca^{2+} handling and cell survival have been suggested to result from their respective nuclear vs. cytosolic localizations. However CaMKII subtype localization and its relationship to enzyme activation and subsequent target phosphorylation has not been systematically evaluated.

The studies presented in this chapter aim to determine whether CaMKII δ subtypes are restricted to a particular subcellular location within the cardiomyocyte and assess the relationship of localization to enzyme activation and function. We show that CaMKIIδ_B and δ_C subtypes are both expressed in ventricular tissue and myocytes isolated from wild type mice. Studies using subcellular fractionation demonstrate that most CaMKII δ is present in the SR/membrane and nuclear fractions. Surprisingly, quantification of individual subtypes reveals that the δ_B and δ_C subtypes are both present in most cellular compartments. Analysis of hearts from transgenic mice expressing CaMKII δ_B or δ_C in ventricle demonstrates that the overexpressed subtype is also distributed in all compartments of the cell. Furthermore this relatively nonselective subcellular distribution of δ_B and δ_C is maintained in hearts of mice generated to overexpress CaMKII δ_B or δ_C in a CaMKIIδ null background, providing, exclusive expression of only one of the two CaMKII δ subtypes. We also examined subtype distribution in a system where cell morphology was not disrupted; isolated myocytes

infected with GFP-tagged CaMKII δ_B or δ_C. These studies showed that while CaMKII δ_B was visually concentrated in the nucleus, significant levels of δ_B were outside of the nucleus. Conversely, while δ_C was highly expressed in the cytosol, a significant fraction was detected in the nucleus.

If the subtypes are not distinctly compartmentalized, both subtypes should be activated by the same interventions. This was tested using isolated perfused hearts from mice expressing either CaMKII δ_B or δ_C and treated with either phenylephrine (PE) or caffeine. Treatment with PE resulted in activation of either subtype of CaMKIIδ in nucleus but not SR, whereas caffeine treatment activated either CaMKIIδ subtype but only in the SR. Finally, to test whether there was a functional correlation between localized CaMKII activation and target phosphorylation, phosphorylation of HDAC5 or phospholamban was assessed. Treatment with PE resulted in increased HDAC5 phosphorylation, but did not induce PLN phosphorylation. On the other hand, treatment with caffeine resulted in increased PLN T-17 phosphorylation but not HDAC5 phosphorylation. These following studies demonstrate that CaMKII δ_B and δ_C are not restricted to the nucleus and cytosol respectively, and show that the subcellular localization of the enzyme rather than its subtype dictates its mode of activation by localized increases in Ca^{2+}.

III.B. Introduction

CaMKII is a multifunctional serine/threonine kinase critical for the regulation of Ca^{2+} signaling within the cardiomyocyte. Our work and that of others have implicated

CaMKII in the development of cardiac hypertrophy and heart failure. The expression of CaMKII is elevated in animal models of heart failure and human patients suffering from heart failure [1, 50]. Transgenic overexpression of the predominant cardiac isoform, CaMKII δ, elicits hypertrophy and heart failure phenotypes while genetic deletion of CaMKII δ prevents the development of heart failure following pressure overload [2, 3, 39]. Two splice variants, CaMKII δ_B and δ_C, which differ by the inclusion of a NLS have been shown to be present at the protein level in myocardium [11]. The δ_B and δ_C subtypes have been implicated in distinct cardiomyocyte functions, but whether or not the two subtypes subserve distinct compartmentalized functions, the mechanism by which the two are activated differs, and the relationship of enzyme localization to its activation has not been clearly defined.

CaMKII is activated by binding of the Ca^{2+}/CaM complex to the enzyme, and the resultant conformational change permits subsequent autophosphorylation of the enzyme to a Ca^{2+} independent activated form [15]. Downstream targets phosphorylated by CaMKII δ include proteins important for the modulation of Ca^{2+} handling such as PLN, RyR2 and voltage sensitive L-type Ca^{2+} channels [1, 50, 51]. CaMKII δ can also regulate gene transcription by phosphorylation of type II HDACs and de-repression of MEF2 [25], or through AP-1 [26, 27], GATA4 [28] and other transcription factors.

The δ_B and δ_C subtypes differ only by the presence of an 11 amino acid NLS in CaMKII δ_B [11, 41], and both the Schulman lab and subsequently our own studies demonstrated that heterologously expressed CaMKII δ_B primarily localizes to the nucleus, whereas δ_C is found primarily in the cytosol [11, 35, 41]. Accordingly, we suggested

different functions of the two subtypes: nuclear δ_B would be involved in hypertrophic gene regulation and cytosolic δ_C in the regulation of Ca^{2+} handling. This was supported by early findings using isolated neonatal rat ventricular myocytes [52-58] and by the differential phenotypes that we observed in the CaMKII δ_B and δ_C transgenic (TG) mice models [2, 3, 35]. The δ_B TG mice primarily develop cardiac hypertrophy whereas the δ_C TG mice develop hypertrophy that rapidly transitions to heart failure characterized by severely disrupted cytosolic Ca^{2+} handling [2, 3]. Subsequent work directly comparing the two lines showed that δ_B and δ_C both modulate MEF2 activity and gene expression, results attributed to the ability of CaMKIIδ to phosphorylate HDAC in either the cytosol or the nucleus [38]. In the studies presented here we extensively investigated the localization of the CaMKII δ_B and δ_C subtypes in the mouse heart ventricle and isolated cardiomyocytes and tested the hypothesis that enzyme location within the myocyte is crucial to its activation by virtue of its proximity to distinct Ca^{2+} pools. The findings reported here demonstrate that CaMKII δ_B is present in the nucleus, and CaMKII δ_C at the SR, but this localization is not exclusive, either for the endogenous or overexpressed enzyme. In addition, we demonstrate that the nature of the stimulus and presumed site of localized Ca^{2+} release determines where CaMKII is activated and is indiscriminate with regard to enzyme subtype. Finally, downstream target phosphorylation provides a functional readout of the consequences of activation of CaMKII at specific cellular locations.

III.C. Results

III.C.1. CaMKII δ_B and δ_C both regulate MEF2 activation *in vivo*

Histone deacetylases (HDACs) have been shown to associate with and repress hypertrophic transcription factor MEF2. Following phosphorylation, HDACs dissociate from MEF2, resulting in its activation [24]. Using CaMKIV TG mice, it was shown that MEF2 is a downstream target for CaMK [59]. Whether MEF2 is a target of CaMKIIδ, and whether CaMKII δ_B, which contains an NLS, selectively phosphorylates HDAC *in vivo*, compared to CaMKII δ_C, and thereby regulates hypertrophic gene expression was investigated using CaMKIIδ TG mice crossed with MEF2/β galactosidase indicator mice [45]. Activation of MEF2 was visualized using β-galactosidase staining of whole mouse hearts and quantified using an enzymatic assay for β-galactosidase activity in ventricular lysates isolated from WT, CaMKIIδ_B and CaMKIIδ_C TG mice expressing the MEF2-LacZ transgene. Hearts were isolated from mice that were 4-5 weeks old, and had not yet developed an overt cardiac phenotype to control for secondary effects in MEF2 activation. WT mice expressing the MEF2/β-galactosidase gene showed background β-galactosidase staining, reflecting basal MEF2 activity. Staining of mouse hearts isolated from the δ_B and δ_C TG mice showed a much higher level of staining compared to the WT mouse hearts, however, the finding that either δ_B or δ_C subtype was able to increase MEF2 activation was surprising (Fig 3) [38]. In order to quantify the level of MEF2 activation seen in the δ_B vs. the δ_C TG mice, β-galactosidase activity was measured in ventricular lysates. In both the δ_B and δ_C TG animals, there was a significant increase in

MEF2 activation compared to WT (7-fold increase), and consistent with the staining, the increase in activation seen in both models was equivalent (Fig 4) [38].

III.C.2. CaMKII δ_B and δ_C are both present in ventricular tissue and AMVMs isolated from WT mouse hearts

The finding that both δ_B and δ_C overexpression were able to elicit and increase in MEF2 activity was surprising, and was explained by the fact that cytosolic CaMKII can still phosphorylate HDAC, preventing it from returning to the nucleus and thereby regulating gene expression. However, it did raise the question about whether the two subtypes may in fact not be as distinctly localized as believed; the δ_C subtype may be present in the nucleus and contributing to the transcriptional regulation seen in the δ_C TG mice. In order to critically address this issue, we first looked at endogenous expression of the two subtypes.

Ventricular tissue and AMVMs were isolated from adult WT and δ KO mice and analyzed by western blotting using a CaMKII δ antibody that recognizes both the δ_B and δ_C subtypes. Two bands are clearly evident in the WT and absent in the CaMKII δ KO mouse heart and isolated cells (Fig 5). The difference in mobility of these bands is consistent with the inclusion of an 11 amino acid (2 kD) NLS in δ_B [11, 41]. Quantification of the individual bands indicates that CaMKII δ_B is the more predominant splice variant, with approximately 60% of the total endogenous CaMKII migrating as the δ_B splice variant, and just under 40% as δ_C (Fig 5).

III.C.3. Endogenous CaMKIIδ is most abundant in the SR/membrane and nuclear fractions.

After confirming the presence of the two subtypes, we wanted to determine the subcellular compartments in which endogenous CaMKII δ_B and δ_C are localized under basal conditions. Left ventricle isolated from WT mice was fractionated using a protocol that resulted in cytosolic, mitochondrial, sarcoplasmic reticular/membrane (SR/mem) and nuclear fractions all obtained from the same sample. The purity of these fractions was verified using Rho-GDI, VDAC, SERCA and Lamin A/C respectively (Fig 6).

Based on subcellular fractionation, the highest proportion of CaMKII δ was found to be at the SR/membrane and nuclear compartments of the cell (Fig 7), consistent with cellular localization of known CaMKII δ targets. Less than 20% of the total CaMKII δ is in the cytosolic fraction while a small but significant percent of the total CaMKII δ is associated with the mitochondrial fraction.

III.C.4. Endogenous CaMKII δ_B and δ_C are indiscriminately localized throughout the cell

We went on to analyze the percent of CaMKII δ_B vs. δ_C in each of the subcellular fractions. The 2kD molecular weight difference of δ_B and δ_C allowed for separation and quantification of the individual bands. CaMKII δ_B is more abundant in the nuclear compartment but also unexpectedly in the SR/mem fraction (Fig 8). Most strikingly, however, the endogenous δ_B and δ_C subtypes do not appear to be well segregated

amongst cellular compartments, with both subtypes present in all four of the isolated subcellular compartments.

III.C.5. Purification of SR from WT mouse ventricle reveals that endogenous δ_C is more abundant than CaMKII δ_B

Since the SR/mem fraction obtained using this protocol is heterogeneous thus including nuclear and sarcolemma as well as SR membrane, a more refined protocol was developed to isolate SR from whole ventricle using a sucrose gradient separation for increased purification from whole ventricle. Two distinct bands are clearly visible in the SR preparation, and CaMKII δ_C is in fact the more abundant subtype in the purified SR compartment (Fig 9).

III.C.6. Subcellular distribution of overexpressed CaMKII δ_B or δ_C *in vivo* is similar to endogenous CaMKII δ distribution

We have generated cardiac specific CaMKII δ_B and δ_C TG mice and extensively characterized these mice in numerous studies from our lab [2, 3, 30, 38]. We assumed that phenotypic differences observed in these TG lines reflected differential overexpression of δ_B and δ_C in the nuclear vs. SR compartments respectively.

To test this assumption in light of our new findings, we isolated and fractionated ventricular tissue from CaMKII δ_B or δ_C TG mouse hearts. Western blots were run with fractions prepared from CaMKII δ KO mice (to demonstrate the specificity of the band identified by the antibody) and from WT (to demonstrate the extent of overexpression of

the transgene which runs at a slightly higher molecular weight due to the presence of an HA tag). Remarkably, while CaMKII δ_B TG mice show a high concentration of CaMKII δ_B in cardiomyocyte nuclei based on immunofluorescence staining [38], the subcellular fractionation indicates that CaMKII δ_B is also present in the cytosolic and SR/membrane fractions (Fig 10). Conversely, in the CaMKII δ_C TG mice, visualization based on immunostaining suggested exclusion of δ_C from the nucleus [38], but a substantial amount of the δ_C transgene is found in the nuclear fraction (Fig 10). The percent of the total CaMKII δ transgene in each subcellular compartment was quantitated from a series of experiments and is graphed with the distribution pattern of endogenous CaMKII δ (light gray bars) for comparative purposes (Fig 11). Two conclusions emerge: distribution of the transgenes is not exclusive and despite overexpression, the pattern closely mirrors that of endogenous CaMKII.

III.C.7. CaMKII δ_C is not excluded from the nuclear compartment following siRNA knockdown of CaMKII δ in NRVMs

CaMKII δ is believed to exist largely as a multimer of 12 subunits [15]. Nuclear vs. cytosolic localization can be significantly affected by changing the expression ratio of δ_B and δ_C splice variants consistent with heteromultimerization of the subtypes [35, 60]. This led us to consider the possibility that the broad and relatively nonselective subcellular distribution of the CaMKII δ_B and δ_C subtypes could reflect such heteromultimerization. In the case of the CaMKII δ_B and δ_C transgenes, multimerization of overexpressed CaMKII δ_C with endogenous CaMKII δ_B could promote its localization in the nucleus,

whereas multimerization of CaMKII δ_B with endogenous CaMKII δ_C might lead to its exclusion from the nuclear compartment.

To test this, we used siRNA to knock-down endogenous CaMKIIδ, and then re-introduced individual subtypes back into the system using adenoviral overexpression. siRNA knockdown of CaMKIIδ in NRVMs was largely successful, decreasing protein expression by ~ 85% (Fig 12). Following siRNA knockdown, CaMKIIδ_C was reintroduced to the cells using adenoviral infection. Surprisingly, the ensuing subcellular fractionation to isolate nuclei showed the presence of CaMKII δ_C in the nucleus. The appearance of δ_C in the nuclear compartment could result from heteromultimerization with the small amount of endogenous CaMKIIδ that was not eliminated by the siRNA. We were unable to express CaMKII δ_B in the system because the virus background is identical to that of the siRNA, coupled to the fact that δ_B infection is not as efficient as the δ_C infection.

III.C.8. Overexpression of δ_B or δ_C in a CaMKII δ null background does not alter its distribution

The availability of CaMKIIδ KO mice in our lab presented the opportunity to generate a system where endogenous CaMKIIδ was completely ablated and individual subtypes could be overexpressed in the absence of the other. We reasoned that our heteromultimerization hypothesis could be tested by crossing the CaMKIIδ_B and δ_C TG mice with the CaMKIIδ KO mice. Progeny from these crosses expressing only a single splice variant of CaMKIIδ in the null background were selected and analyzed. To our

surprise, the subcellular distribution of CaMKII δ_C and δ_B in the CaMKII δ null background (Fig 13, black columns) was not significantly different from that observed in the δ_B and δ_C TG mice.

III.C.9. Adenoviral overexpression of CaMKII δ_B or CaMKII δ_C in WT and KO AMVMs reveals non preferential distribution throughout the cell

To examine the distribution of the δ_B and δ_C subtypes in a manner that does not require cell disruption we used adenoviral infection of AMVMs with GFP-tagged CaMKII δ_B and δ_C. Myocytes infected with CaMKII δ_B and visualized using confocal microscopy showed accumulation of the overexpressed protein in the nuclear compartment but a significant amount of CaMKII δ_B was also distributed in a striated pattern corresponding to T-tubule organization (Fig 14).

Line scan quantification of fluorescent intensity taken from a 1μM thick plane of several different cells indicated that the fluorescence intensity of δ_B in the nucleus was about 1.6 times higher than that in the cytosol (Fig 14). Experiments were also carried out using GFP-tagged CaMKII δ_C. This subtype showed localization coincident with the striated patterns of the cardiomyocyte but CaMKII was also detectable in the nuclear compartment (Fig 15). Quantification of fluorescence intensity in the nuclear compartment from several different cells infected with GFP-tagged δ_C shows that the intensity of the nuclear signal is approximately 40% of that in the cytosolic compartment.

III.C.10. Caffeine stimulation increases CaMKII activation at the SR and phenylephrine increases CaMKII activation at the nucleus

The studies above demonstrate that endogenous, transgenically overexpressed CaMKII subtypes in mouse ventricle and adenovirally expressed CaMKII in AMVMs are not confined to a single subcellular compartment. Thus it would seem mechanistically unlikely that there would be selectivity in activation of CaMKII δ_B vs. δ_C. To examine this further, we isolated hearts from δ_B and δ_C TG mice in the CaMKIIδ null background. These hearts, which express only CaMKII δ_B or only CaMKII δ_C were perfused in the Langendorff mode and treated with either a bolus injection of caffeine to release SR Ca^{2+} or 15 minutes of perfusion with phenylephrine to increase nuclear Ca^{2+} levels [61].

Hearts were then fractionated to obtain either a purified SR fraction or nuclear fractions and analyzed by western blot analysis. Phosphorylation of CaMKII Thr286, indicative of enzyme autophosphorylation, was used as a read-out for CaMKII activation. Perfusion with PE increased P-CaMKII by 2-3 fold in the nuclear fraction with only a 30% increase in the SR (Fig 16). In contrast, caffeine treatment increased P-CaMKII levels by more than 2 fold in the SR fraction but only by 25% in the nuclear fraction (Fig 16). Most remarkably, PE activated both the δ_B and δ_C subtype in the nucleus and caffeine activated both subtypes in the SR. Thus caffeine selectively activates whichever CaMKIIδ subtype is located at the SR, but not that located in the nucleus, whereas PE selectively increases the activation of either subtype of CaMKII if it is localized to the nucleus, consistent with the hypothesis that mobilization of different pools of Ca^{2+} can activate CaMKII δ localized in close proximity to that pool [61].

III.C.11. Although caffeine preferentially activates δ_C and ET-1 and PE preferentially activate δ_B in isolated AMVMs, activation is not subtype exclusive

Although δ_B and δ_C are expressed throughout the cell, the majority of the δ_C was located at the SR, and δ_B was highly concentrated in the nuclear region. Adult mouse ventricular myocytes were isolated from WT mice and δ_BTG and δ_CTG mice in the δ null background (δ TG/δKO) and treated with caffeine, endothelin 1 (ET-1) or phenylephrine (PE). When myocytes were treated with caffeine to release SR Ca^{2+}, there was a robust increase in P-CaMKII levels in the myocytes from δ_CTG/δKO mice (Fig 17A). Although it was not significant, there was a slight increase observed in the myocytes from the δ_BTG/δKO mice. When myocytes were treated with PE and ET-1, the P-CaMKII levels were significantly increased in the δ_BTG/δKO myocytes, with significant, but less robust activation in the δ_CTG/δKO myocytes (Fig 17B-C).

III.C.12. Caffeine preferentially increases phospholamban phosphorylation and PE preferentially increases HDAC5 phosphorylation in WT hearts

To examine functional consequences of compartmentalized CaMKII activation, the phosphorylation of two CaMKII targets, PLN and HDAC5, was measured in perfused hearts treated with PE or caffeine. Treatment with PE increased P-HDAC5 levels while caffeine did not (Fig 18). On the other hand, treatment with caffeine increased phosphorylation of PLN Thr17, the CaMKII phosphorylation site, while treatment with PE had no effect (Fig 18).

III.D. Discussion

CaMKIIδ_B and δ_C subtypes, which differ only by the inclusion of a NLS, are present in the mouse heart ventricle at similar protein levels. The seminal papers from the Schulman laboratory describing these two splice variants [11, 41], along with our early studies in which we expressed CaMKIIδ_B and δ_C in NRVMs [35], supported the notion that CaMKIIδ_B would be localized to and signal in the nucleus whereas δ_C would localize to and signal in the cytosol. These conclusions were based on studies in which CaMKIIδ was heterologously expressed in COS cells or NRVMs [34, 35, 59].

Subsequently we generated CaMKIIδ_B or δ_C TG mice and examined the HA-tagged protein by immunostaining of myocytes isolated from these mice [2, 3, 38]. Our findings confirmed the predominant localization of CaMKIIδ_B in the nucleus and δ_C in the cytosol [2, 3, 38]. The more extensive analysis presented in the current chapter was motivated by our observation that endogenous CaMKIIδ is present in SR/membrane and nuclear compartments isolated from mouse ventricle, and in both compartments, two CaMKIIδ immunoreactive bands are visible on SDS page. That these bands are absent in CaMKIIδ knockout mouse hearts indicates that they are both CaMKIIδ gene products and that they differ in mobility by 2 kD suggests that they represent δ_C and the 11 amino acid larger NLS containing δ_B [41].

The concept of nuclear and cytosolic splice variants/subtypes, promulgated through our early work and that of others, was largely consistent with the different phenotypes that we observed in our CaMKII δ_B and δ_C TG mice. We recognized that the pathological changes seen in the mouse models could be exaggerated by overexpression

(Fig 19), but reasoned that this highlighted the compartment specific effects of these subtypes: nuclear effects on gene expression leading to hypertrophy for CaMKIIδ_B, and effects on SR protein phosphorylation and Ca^{2+} handling leading to heart failure development for CaMKII δ_C. To our surprise, as reported here, the subcellular distribution profile for transgenically overexpressed CaMKIIδ subtypes is quite similar to that of the endogenous enzyme: the δ_C transgene is more highly represented in the SR and the δ_B transgene in the nuclear compartment, but both are also present in all of the subcellular compartments.

CaMKII isoforms and subtypes can form heteromultimers [15, 60], a property that could account for the ability of either subtype to be present in the nucleus (or SR) independent of whether it possessed an NLS. We further reasoned that the influence of heteromultimerization would be eliminated if one subtype was expressed in the absence of the other. To determine whether this would also alter subcellular localization, we crossed the CaMKIIδ_B and δ_C TG mice into the CaMKIIδ null background. Remarkably, expression of CaMKII δ_B in the absence of CaMKII δ_C did not restrict its localization to the nucleus nor was δ_C confined to the cytosolic/SR compartment when expressed alone. While these data indicate that heteromultimers of δ_B and δ_C is unlikely to account for their indiscriminate distribution, there are other minor cardiac CaMKII isoforms, including CaMKII γ and β, which could heteromultimerize with CaMKIIδ and contribute to its appearance in unexpected locations. This could be particularly important in explaining the widespread localization of endogenous CaMKII δ_B and δ_C subtypes. Regardless of the molecular mechanism, the conclusion from cell fractionation

experiments is that CaMKII δ_B is not restricted to the nuclear compartment, and δ_C is not excluded from the nuclear compartment.

Since subcellular fractionation does not yield pure fractions and can disrupt normal structure we supplemented these finding with experiments using intact AMVMs infected with GFP-tagged CaMKII δ_B or δ_C. Data obtained using confocal imaging clearly show an accumulation of GFP-tagged CaMKII δ_B in the nucleus, consistent with what we reported previously [38]. Notably however, quantitative analysis confirmed that δ_B is not wholly restricted to the nucleus, and that δ_B fluorescence outside of the nuclear compartment, which is approximately one third of that in the nucleus, appears to align with the typical sarcomeric organization seen in cardiomyocytes. Conversely, the distribution of GFP-tagged CaMKII δ_C was largely consistent with the earlier studies from our lab showing δ_C to be primarily excluded from the nucleus. Quantitative analysis showed that the fluorescence intensity inside the nuclear compartment was not zero, but was approximately one third of that in the cytosol.

The finding that both subtypes are present throughout the cell raised the question of whether localization or subtype would determine the mode of activation of the enzyme. In cardiomyocytes, the majority of IP_3R2s are located on the nuclear envelope and our previous studies demonstrated that ET-1 and PE increase Ca^{2+} release from nuclear IP_3 sensitive stores [61]. Treatment with caffeine would instead be expected to cause a large $[Ca]_i$ increase in the cleft region as a result of SR Ca^{2+} mobilization. We used hearts from the transgenic mice in the δKO background to facilitate analysis of the activation of individual subtypes. Treatment with PE increased phosphorylation of

nuclear CaMKII δ_B or δ_C, with little change in CaMKII activation at the SR; conversely caffeine activated both CaMKII δ_B and δ_C in the SR, with little change in CaMKII activation in the nuclear compartment. Thus we demonstrate for the first time that CaMKII is activated in different cellular compartments depending on the stimulus and that activation is independent of subtype.

Our original motivation for investigating subtype distribution and activation was the finding that the endogenous enzyme did not show preferential localization. Although our heterologous and transgenic overexpression systems facilitated our studies, we returned to studies of the endogenous enzyme to test the functional relevance of compartmentalized activation. The findings were consistent with the activation results: phosphorylation of the SR target, phospholamban, was increased following addition of caffeine and phosphorylation of the nuclear transcriptional regulator HDAC5 was increased following PE treatment. Thus CaMKII substrate phosphorylation occurs in localized compartments and in response to agonists predicted to selectively mobilize Ca^{2+} at those sites.

We previously demonstrated differential roles of the δ_B vs. δ_C subtypes in regulating hypertrophy and Ca^{2+} handling, both *ex vivo* and *in vivo*. The most important effect of δ_C appears to be RyR2 phosphorylation and enhancement of SR Ca^{2+} sparks, but expression of δ_C can also affect nuclear function, regulating HDAC/MEF2 and hypertrophic gene expression [2, 3, 30, 35, 38]. These data are consistent with what we show here to be the predominant localization of CaMKII δ_C in the SR, but its clear presence and ability to be activated in the nucleus. CaMKII δ_B has predominant effects on

hypertrophic gene expression with little direct effect on Ca^{2+} handling [38]. However as we show here, there is δ_B is in the SR and it can be activated by caffeine. The absence of increased RyR2 and PLN phosphorylation and Ca^{2+} handling changes in the δ_B TG mice [38] may reflect the fact that the amount of CaMKII δ_B in the SR of the δ_B TG mice is 10-15% of the amount of CaMKII δ_C in the SR of CaMKII δ_C TG mice (Fig 20). Our data would suggest, however, that further upregulation or activation of δ_B could in fact elicit SR responses, just as δ_C can elicit nuclear responses. There is also the intriguing possibility that there may be subtype specificity in binding partners and substrates at the SR such that δ_C but not δ_B is poised to elicit RyR2 phosphorylation.

In conclusion, we show for the first time CaMKIIδ_B and δ_C subtypes are not exclusively localized. Both subtypes can be activated at the same cellular locations and the activation is agonist, not subtype dependent. Phosphorylation of different substrates is also dependent upon agonist. The evidence for nonpreferential CaMKII localization is particularly interesting and challenging with regards to understanding mechanisms by which δ_B would have a protective role, and δ_C a more deleterious role in heart disease [43, 44, 62].

III.E. Acknowledgment

The text and figures in this chapter are, in part, a reprint of material as it appears in:

Mishra S., Bers D.M., Brown J.H. Location matters: Clarifying the concept of nuclear and cytosolic CaMKII subtypes *Circ Res* Submitted November 2010

Zhang T, Kohlhaas M, Backs J, Mishra S, Phillips W, Dybkova N, Chang S, Ling H, Bers DM, Maier LS, Olson EN, Brown JH CaMKIIdelta isoforms differentially affect calcium handling but similarly regulate HDAC/MEF2 transcriptional responses. *J Biol Chem.* 2007 Nov 30;282(48):35078-87.

The dissertation author was the primary researcher and author of the manuscript entitled "Location matters: Clarifying the concept of nuclear and cytosolic CaMKII subtypes". All experiments presented in this chapter were carried out by the dissertation author. Dr. Joan Heller Brown directed and supervised the research which forms the basis for this chapter.

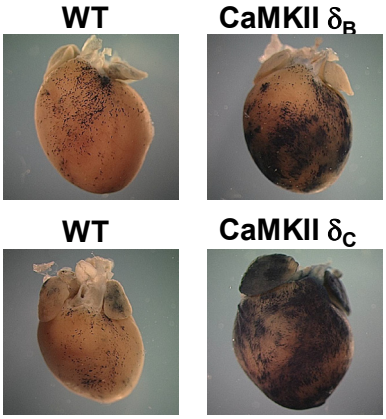

Figure 3. MEF2 can be activated by either CaMKIIδ_B or δ_C *in vivo*. A. CaMKIIδ_B or δ_C TG mice were crossed with MEF2/β-galactosidase indicator mice. β-Galactosidase staining of mouse hearts expressing either CaMKIIδ_B or δ_C isoforms with the MEF2-LacZ transgene showed markedly increased staining compared with WT mice harboring the MEF2-LacZ transgene.

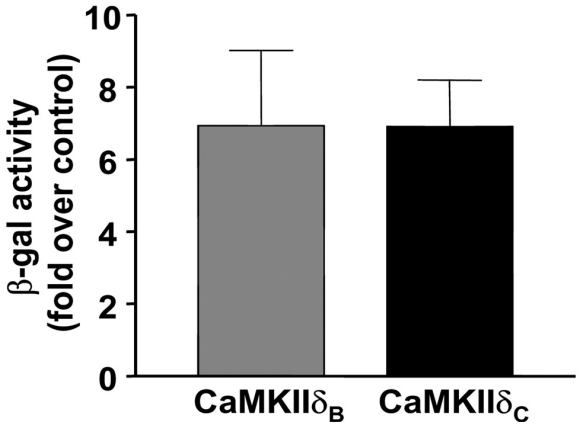

Figure 4. Quantitative analysis shows equivalent activation of MEF2 by either CaMKIIδ_B or δ_C *in vivo* β-galactosidase activity was measured in ventricular extracts from WT, CaMKIIδ_B and δ_C TG mice harboring the MEF2-LacZ transgene. Equivalent increases (~ 7-fold over WT) were seen in both CaMKIIδ_B and CaMKIIδ_C expressing MEF2 reporter mice (n = 4 for each group).

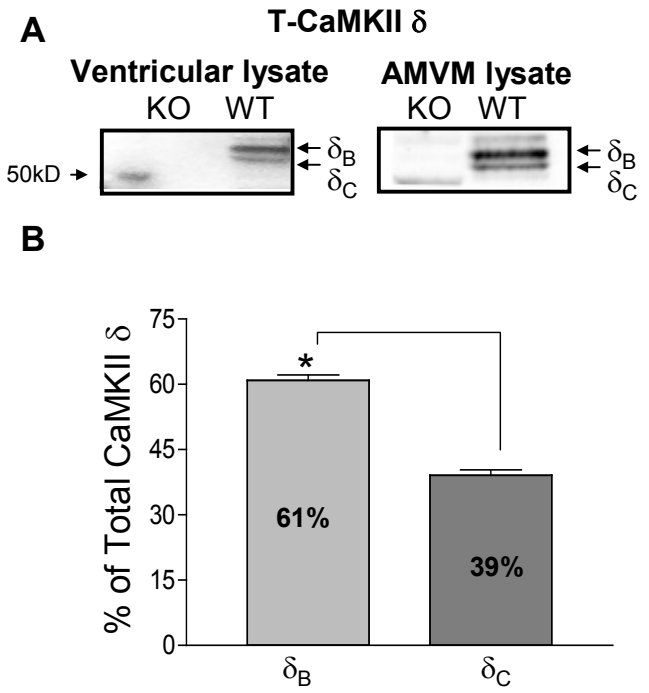

Figure 5. Expression of CaMKII δ in mouse ventricular tissue and AMVM lysate shows expression of both subtypes and higher CaMKII δ_B levels compared to CaMKII δ_C. Ventricular tissue and AMVMs isolated from wild type (WT) and CaMKII δ knockout (KO) mice were harvested and subjected to Western blotting. A. Representative blot of CaMKIIδ expression in whole ventricular tissue homogenate and AMVM lysate. B. Quantitative analysis of endogenous CaMKII δ_B and δ_C expression from isolated WT ventricular tissue (n=8). * $p<0.01$

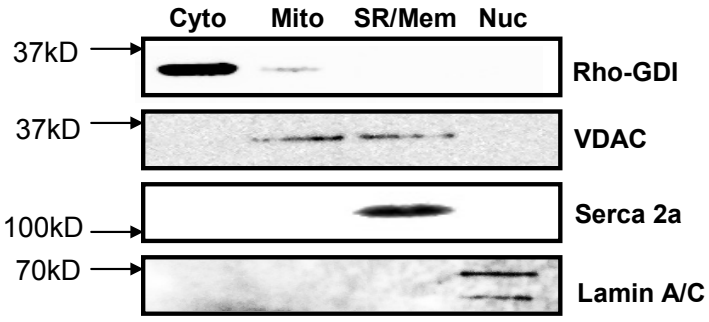

Figure 6. Subcellular Fractionation of whole heart tissue. Whole heart tissue from WT mice was fractionated into cytosol, mitochondria, SR/membrane and nuclei. The protocol use for subcellular fractionation of whole heart tissue yields relatively pure fractions assessed by western blotting and probing for cellular markers: Rho-GDI, cytosol; VDAC, Mitochondria; Serca 2a, SR; Lamin A/C, nucleus

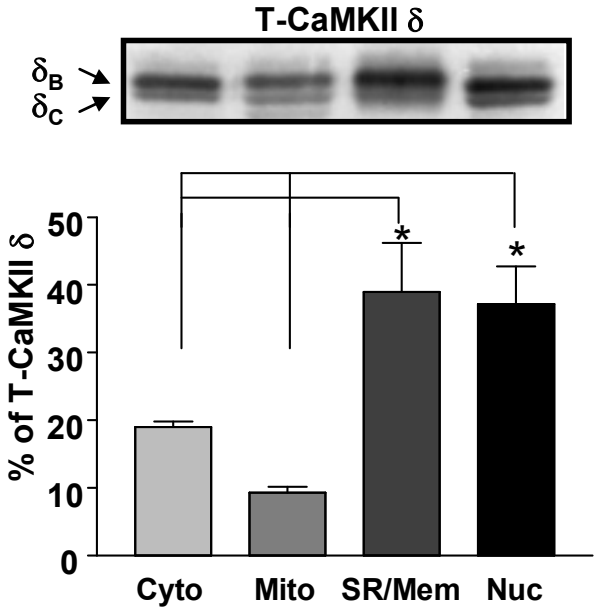

Figure 7. Endogenous CaMKII is primarily located at the SR/Mem and nuclear compartments. Ventricular tissue isolated from WT mice was fractionated using the protocol for whole tissue. Fractions were resuspended in equal volumes, and loaded onto SDS-PAGE to compared relative amounts of CaMKII expression between compartments. Representative western blot shows total CaMKII δ distribution. Quantification of endogenous CaMKIIδ distribution is graphed below. (n=8) $p < 0.01$

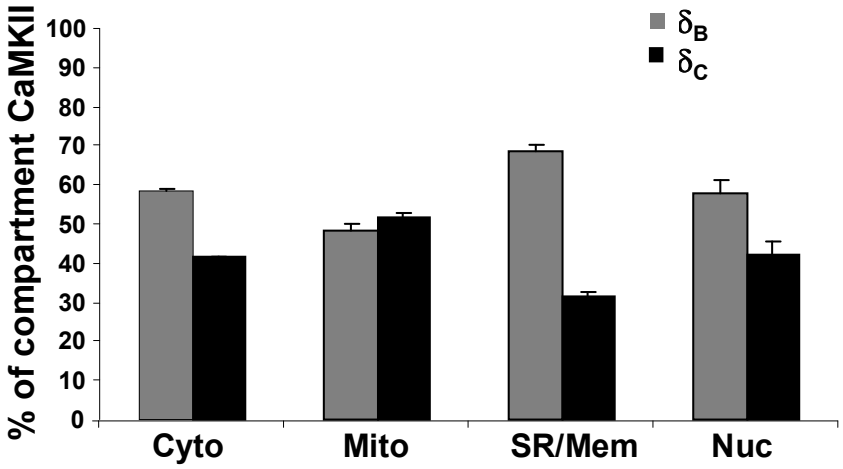

Figure 8. CaMKII δ_B and δ_C subtypes are both distributed throughout the cell. Quantification of δ_B vs. δ_C in each subcellular compartment. The two bands seen when blotting for CaMKIIδ were added together and considered the total, and the top band was considered to be δ_B and the bottom band δ_C. (n=4)

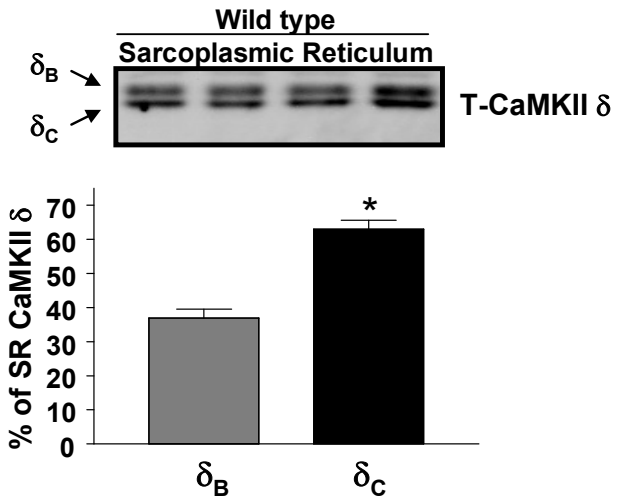

Figure 9. CaMKII δ_C is the more predominant subtype at the SR. A protocol to extract a more purified SR fraction was developed to reduce contamination from other membranes. SR was made from fresh ventricular tissue isolated from WT mice. Western blotting for T-CaMKIIδ shows both bands clearly present at this compartment. Quantification of the individual bands, identified as δ_B and δ_C is shown below, and indicates that δ_C is the more predominant endogenous subtype at the SR. (n=8) * $p<0.01$

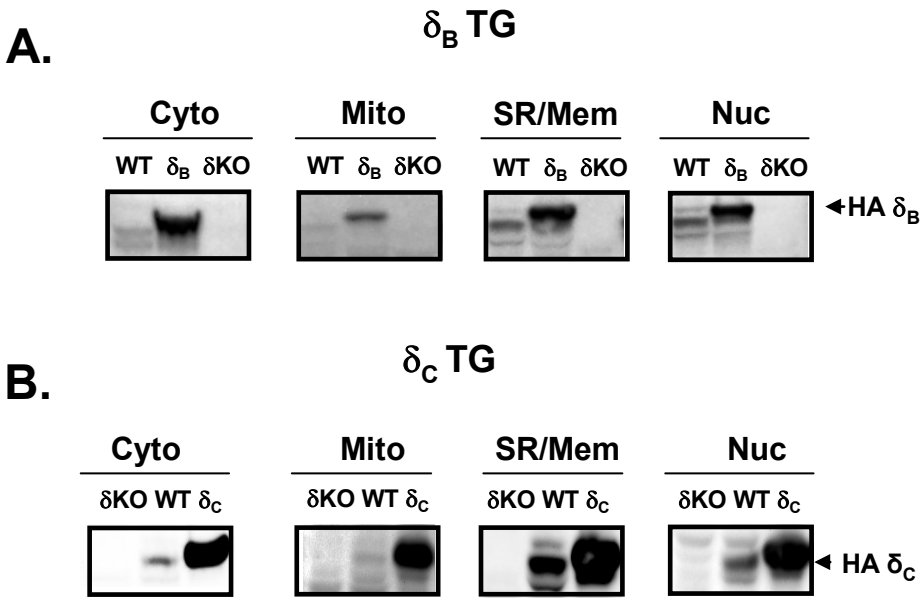

Figure 10. Subcellular distribution of CaMKIIδ in δ_B and δ_C TG mice is not significantly altered compared to endogenous distribution. Ventricular tissue isolated from WT, KO, δ_B TG and δ_C TG mice was harvested and fractionated into cytosolic, mitochondrial, SR/membrane and nuclear fractions and subjected to Western blotting. A. Representative blots of CaMKIIδ expression in δ_BTG mice compared to WT and KO mice. B. Representative blots of CaMKIIδ expression in δ_C TG mice compared to WT and KO mice.

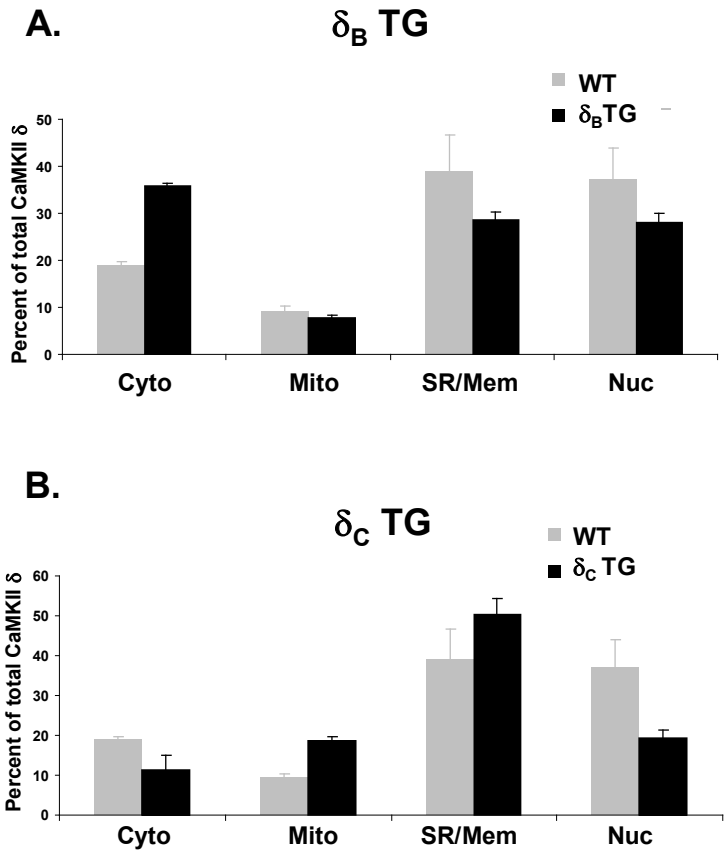

Figure 11. Subcellular distribution of overexpressed transgene shows no significant difference from endogenous CaMKII distribution. A. Quantitative analysis of overexpressed CaMKII δ_B distribution compared to WT. (n=4). B. Quantitative analysis of overexpression CaMKII δ_C distribution compared to WT. (n=4).

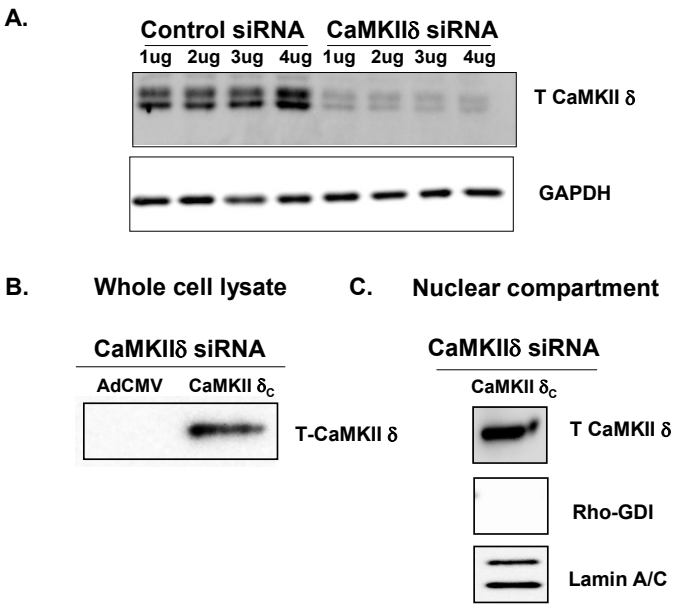

Figure 12. siRNA knockdown of CaMKII δ in NRVMs. A. Significant knockdown of CaMKII δ expression is achieved following siRNA transfection in NRVMs. B. CaMKIIδ expression in NRVM whole cell lysate following transfection with CaMKIId siRNA and adenoviral reintroduction of CaMKII δ_C. (Adenoviral add-back of δ_B was not successful in the presence of the siRNA) C. Subcellular fractionation was used to isolate the nuclear compartment from NRVMS following siRNA knockdown of CaMKII δ and adenoviral reintroduction of CaMKII δ_C and western blotting shows presence of δ_C in the nucleus.

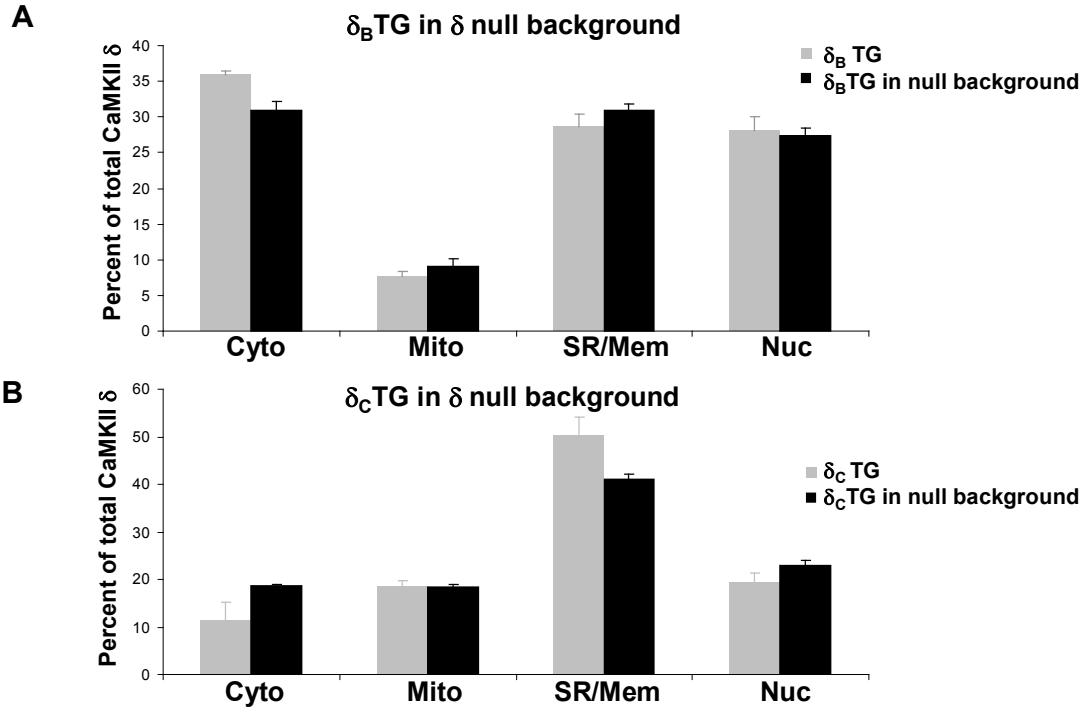

Figure 13. Transgenic overexpression in CaMKII δ null background does not alter CaMKII localization. Ventricular tissue isolated from WT, KO, and δ_B and δ_C TG mice in the δ null background was harvested and fractionated into cytosolic, mitochondrial, SR/membrane and nuclear fractions and subjected to Western blotting. A. Quantitative analysis of overexpressed CaMKII δ_B distribution in the CaMKII δ null background compared to the δ_B TG mice (n=4). B. Quantitative analysis of overexpressed CaMKII δ_C distribution in the CaMKIIδ null background compared to δ_C TG mice (n=4).

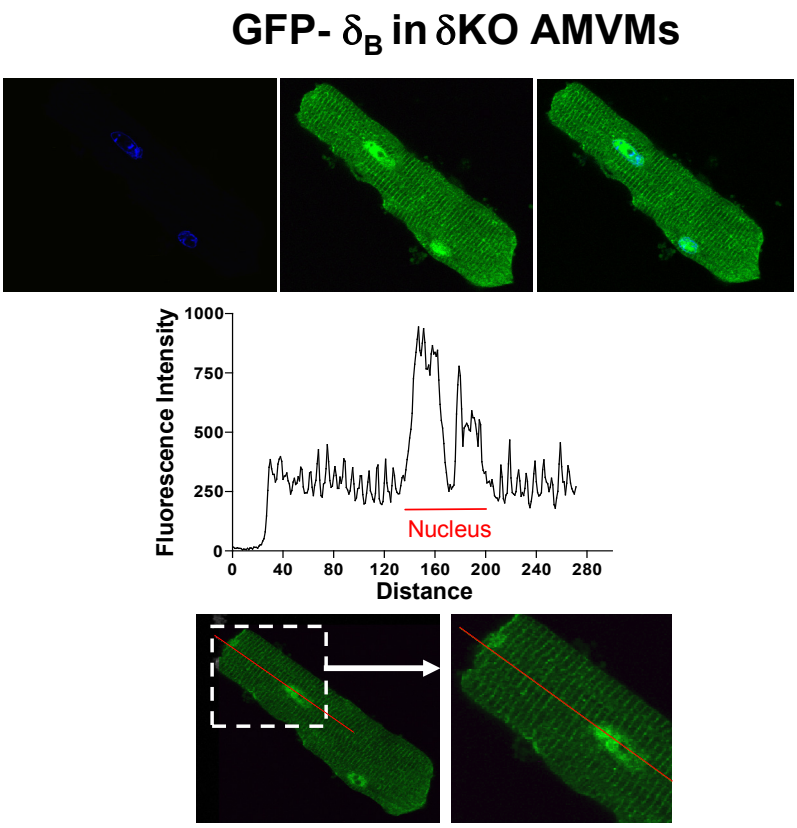

Figure 14. GFP-tagged CaMKII δ_B expressed in AMVMs isolated from δKO mice show δ_B presence outside of the nuclear compartment. Adenoviral infection of AMVMs isolated from δKO mice with GFP-tagged δ_B were imaged using confocal microscopy. DAPI co-stain was used to identify nuclei. Line scan quantification of fluorescence intensity was used to measure distribution.

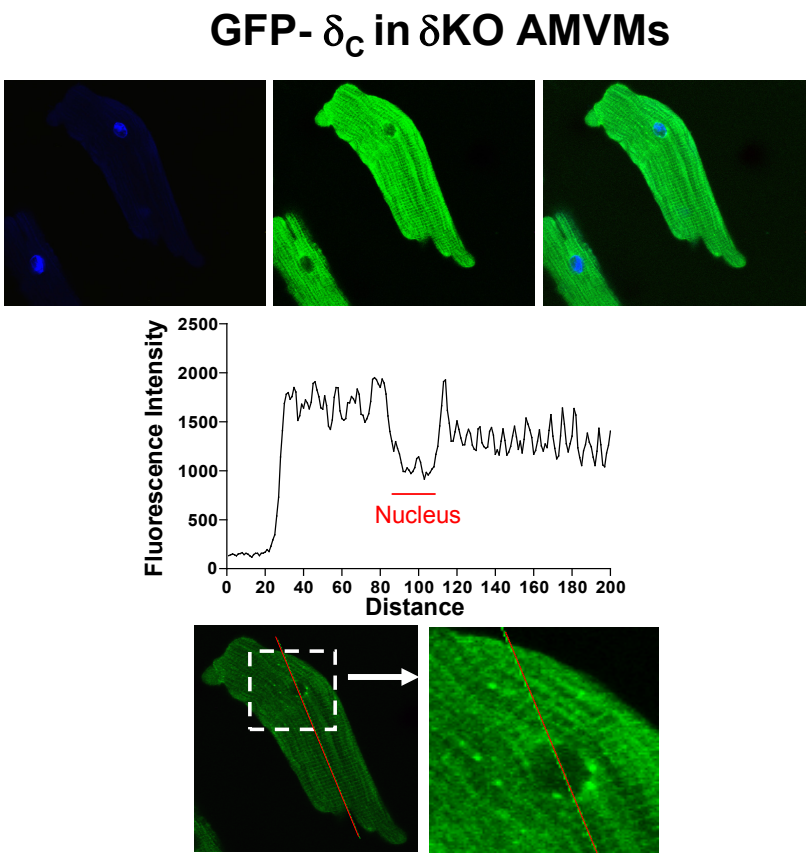

Figure 15. GFP-tagged CaMKII δ_C expressed in AMVMs isolated from δKO mice shows δ_C in the nuclear compartment. Adenoviral infection of AMVMs isolated from δKO mice with GFP-tagged δ_C were imaged using confocal microscopy. DAPI co-stain was used to identify nuclei. Line scan quantification of fluorescence intensity was used to measure distribution.

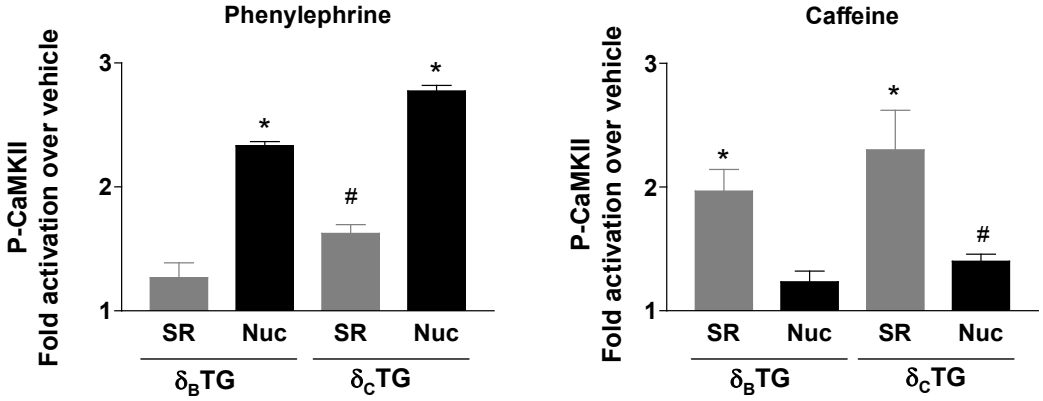

Figure 16. Caffeine stimulation increases CaMKII activation at the SR and phenylephrine increases CaMKII activation at the nucleus. Sarcoplasmic reticulum or nuclei were isolated from ventricular tissue isolated from mice overexpressing δ_B or δ_CTG in the CaMKII δ null background following perfusion with drug. P-CaMKII levels were measured using western blotting and quantified following **A.** 15 minutes of perfusion with 100nM PE or **B.** bolus injection of 10mM caffeine. (n=4) * $p< 0.01$ # $p< 0.05$

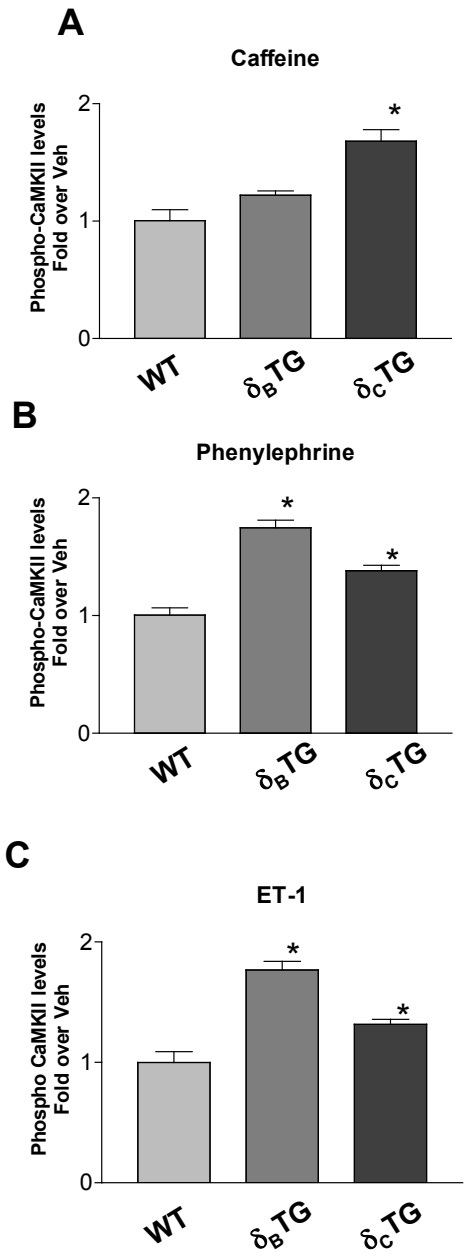

Figure 17. Caffeine preferentially activates δ_C and ET-1 and PE preferentially activate δ_B in isolated adult mouse ventricular myocytes. AMVMs were isolated from WT, δ_B TG and δ_CTG mice in the δ null background and treated with A.10mM Caffeine B. 100nM phenylephrine or C. 100nM Endothelin-1. Whole cell lysate was subjected to western blotting. Quantitative analysis for P-CaMKII levels is shown. (n=4) * $p<0.01$

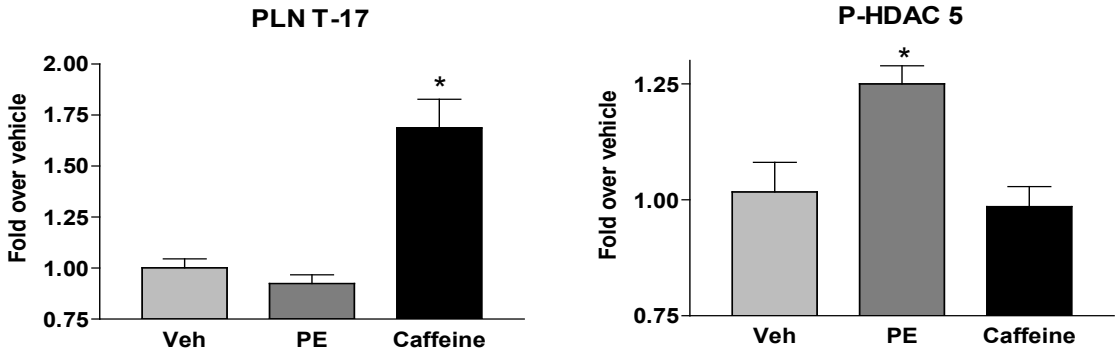

Figure 18. Caffeine preferentially increases phospholamban phosphorylation and PE preferentially increases HDAC5 phosphorylation in WT hearts. Ventricular tissue was isolated from WT mice and treated with 10mM Caffeine or 100nM phenylephrine. Lysates were subjected to western blotting and quantitative analysis for **A.** PLN phosphorylation at T-17 and **B.** HDAC5 phosphorylation is shown. (n=4) * $p<0.01$

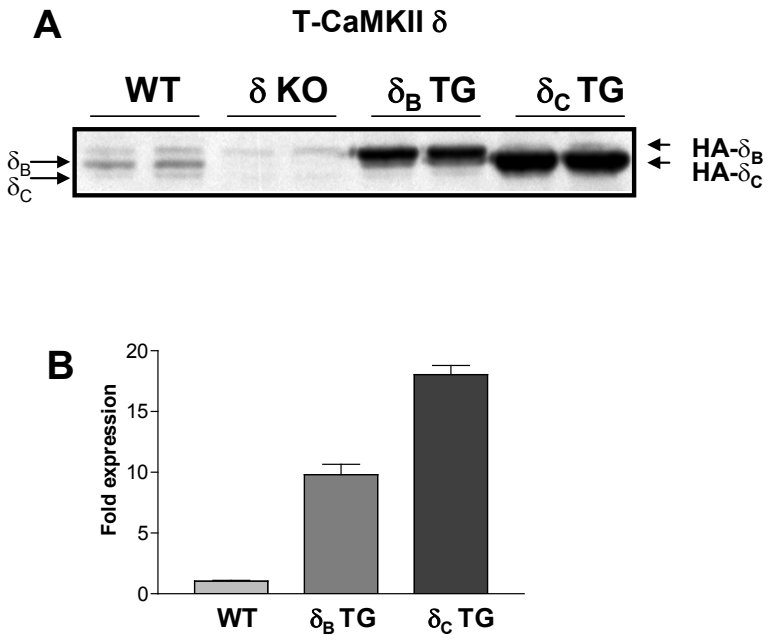

Figure 19. Expression of CaMKII δ_B and δ_C transgenes. A. Relative expression of CaMKII δ in ventricular tissue isolated from WT, δ KO, δ_B and δ_C TG mice. B. Quantification of transgene expression of δ_B and δ_C compared to WT. (n=4)

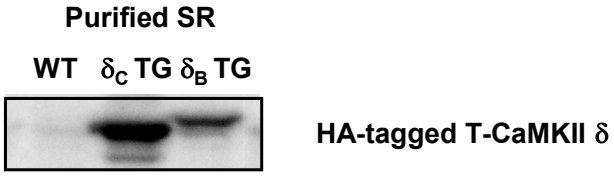

Figure 20. The δ_C transgene is more highly expressed than the δ_B transgene at the SR. SR was extracted from ventricular tissue isolated from WT, δ_B and δ_C TG mice. Western blotting for HA-tagged protein shows greater amount of δ_C than δ_B at the SR.

IV. Role of CaMKII δ_C in the development of heart failure

IV.A. Abstract

CaMKII activity and expression are altered in animal models of hypertrophy and heart failure, as well as in patients suffering from dilated cardiomyopathy. Cardiac overexpression of CaMKIIδ_C, a splice variant of the predominant cardiac CaMKII isoform, results in cardiac dysfunction in mice. These studies test the hypotheses that activation of CaMKIIδ_C is critical for the transition from hypertrophy to heart failure by contributing to increased myocyte death through altered Ca^{2+} signaling. The exact mechanism by which the δ_C TG mice developed heart failure has not yet been established. In order to better understand the mechanism by which CaMKII δ_C induces heart failure, specifically whether it is through Ca^{2+} handling changes or mitochondrial dependent cell death, several *in vivo* experimental systems were generated and characterized. CaMKII δ_C TG mice were crossbred to mice i) lacking a key regulator of Ca^{2+} handling, ii) lacking cyclophilin D, a protein critical for PT pore formation, and iii) with SR CaMKII inhibition achieved by overexpressing SR targeted AIP.

IV.B. Introduction

Intracellular Ca^{2+} is a ubiquitous second messenger involved in many cardiac signaling pathways and is critical for regulating cardiac contractility. In cardiomyocytes, changes in Ca^{2+} handling have been associated with the development of cardiac hypertrophy and dysfunction, leading to heart failure. Development of heart failure in the δ_C TG mice was associated with increased RyR2 phosphorylation (P-RyR2) leading to

SR Ca^{2+} load depletion. The Kranias' lab developed a mouse model with a genetic deletion of PLN that had enhanced contractile function and augmented Ca^{2+} transients resulting from increased SERCA function [63]. We hypothesized that rescuing SR Ca^{2+} content might rescue the heart failure phenotype and accordingly crossed the δ_C TG mice with the PLN KO mice. Surprisingly, mice showed exaggerated heart failure associated with increased SR Ca^{2+} leak and characterization suggests that the combined changes in Ca^{2+} handling affect the mitochondria and mediate cell death [63]. An important role for mitochondrial cell death pathways in cardiomyopathy and heart failure has been demonstrated [64]. A mouse model lacking the *Ppif* gene which encodes the protein cyclophilin D was generated by the Molkentin lab, and characterization showed that the mice were resistant to Ca^{2+} and oxidative damage induced cell death [65]. Ablation of cyclophilin D has also been shown to rescue several maladaptive phenotypes in a number of disease models, including heart failure [66-68]. We crossed the cyclophilin D knockout mice with our δ_C TG mice (δ_C TG/ Ppif $^{-/-}$) to determine if mitochondrial PT-pore involvement is important in cell death and heart failure development induced by CaMKII δ_C [69]. In the last study of this chapter, SR-AIP mice, which have been shown to directly inhibit CaMKII dependent activation of SR Ca^{2+} uptake, SR Ca^{2+} release and I_{Ca} by CaMKII [70], were crossed with CaMKIIδ_C TG mice. The increased RyR2 phosphorylation and SR Ca^{2+} leak was thought to be critical to the development of the δ_C TG mice heart failure phenotype. In collaboration with Bers lab, the CaMKII δ_C TG mice were crossed with SR targeted CaMKII inhibitor mice (SR-AIP) [47].

IV.C. Results

IV.C.1. Phospholamban ablation in CaMKII δ_C TG mice exacerbates heart failure

IV.C.1.i. Abstract

Our lab previously demonstrated that cardiac specific transgenic overexpression of CaMKII δ_C results in dilated cardiomyopathy characterized by increased phosphorylation of critical Ca^{2+} handling proteins, increased Ca^{2+} leak from the SR and decreased SR Ca^{2+} load which correlated with a decrease in the Ca^{2+} transient. The basis for the following study was the hypothesis that recovering the decrease in Ca^{2+} load would attenuate the decrease in ventricular activity and development of heart failure that was seen in the CaMKIIδ_C TG mice.

The model system developed to carry out our experiments was generated by crossing CaMKIIδ_C TG mice with phospholamban knockout (PLN KO) mice to generate PLN KO x δ_C TG (KO/TG) mice. Experiments done in collaboration with Bers lab indicated that the decreased SR Ca^{2+} load was normalized in KO/TG. What was surprising, however, was that the heart failure phenotype observed in the CaMKIIδ_C TG mice was not improved, but was actually exacerbated. The mice exhibited higher mortality, and displayed a more rapid development of heart failure characterized by increased left ventricular dilation, decreased ventricular function and an increase in apoptosis [63]. No significant changes in Ca^{2+} handling protein levels or phosphorylation were observed. Mitochondrial Ca^{2+} load was found to be increased in cardiomyocytes from KO/TG versus WT or CaMKIIδ_C TG mice. AMVMs from KO/TG showed poor

viability that was dependent upon CaMKII activity, and improved by inhibiting SR Ca^{2+} release or mitochondrial Ca^{2+} loading [63].

Taken together, these data suggested that the increased Ca^{2+} load resulting from PLN deletion, coupled with CaMKII δ_C overexpression and hyperphosphorylation state of the RyR2 resulted in an increased level of Ca^{2+} leak, which in turn increased mitochondrial Ca^{2+} load, increased cell death, and exacerbated the heart failure phenotype.

IV.C.1.ii. Introduction

Our lab generated cardiac specific CaMKII δ_C TG mice that exhibited a heart failure phenotype characterized by increased mortality, decreased ventricular function and ventricular dilation [2]. Characterization of the δ_C TG mice revealed that Ca^{2+} handling was dysregulated in these mice largely due to increased phosphorylation of the cardiac ryanodine receptor (RyR2) at the CaMKII site accompanied by an increase in SR Ca^{2+} sparks and increased diastolic SR Ca^{2+} leak. The SR Ca^{2+} leak resulted in profound depletion of the SR Ca^{2+} load coupled with decreased Ca^{2+} transients [2, 30]. Echocardiography showed a decrease in contractility and ventricular function, as well as ventricular dilation. We hypothesized that the defect in contractility cardiac dysfunction could be a result of the decrease in SR Ca^{2+} load.

Uptake of Ca^{2+} into the SR is governed by SR Ca^{2+}ATPase (SERCA2a) activity, which is regulated via association with phospholamban [71]. PLN KO mice generated in the Kranias lab show enhanced myocardial contractility [29] resulting from increased SERCA2a activity and a concomitant increase in SR Ca^{2+} load [72]. We hypothesized that

the depletion of SR Ca^{2+} and severe cardiac dysfunction seen in the CaMKII δ_C TG mice would be attenuated if SR Ca^{2+} was recovered by PLN ablation. The experiments presented here examine the result of the PLN KO x CaMKII δ_C TG cross.

IV.C.1.iii. Results

IV.C.1.iii.1. Expression and Phosphorylation of Ca^{2+} regulatory proteins are unchanged in the KO/TG mice compared to δ_C TG mice.

Western blot analyses were performed on ventricular homogenates from δ_CTG and KO/TG mice to evaluate the expression level of calsequestrin, SERCA2a and NCX, proteins important for Ca^{2+} handling. Previous studies on the δ_C TG mice had found that SERCA2a expression was reduced and NCX expression was increased and there was no change in CsQ expression compared to WT mice. There were no significant differences in expression levels of these proteins in the KO/TG mice compared to the δ_C TG mice (Fig 21). The level of activated CaMKII, measured using a P-CaMKII antibody was also unchanged in the δ_C TG vs. KO/TG mice.

Phosphorylation of RyR2 measured using an antibody specific for the CaMKII phosphorylation site, Ser2814 was increased in CaMKIIδ_C expressing lines(Fig 22), but there was no difference in phosphorylation between the δ_C TG and the KO/TG mice. No difference in phosphorylation of RyR2 at Ser2809, the PKA site, was seen between the δ_C TG and the KO/TG mice. Thus, the exaggerated phenotype does not result from changes in the expression or activation of major Ca^{2+} handling proteins.

IV.C.1.iii.2. Gap junction organization is unchanged in the KO/TG mice compared to the δ_C TG mice.

In a separate study attempting to rescue heart failure the McTiernan lab crossed mice overexpressing TNF alpha with the PLN KO mice, and found that PLN ablation did not improve survival, cardiac function, or limit cardiac chamber dilation and hypertrophy. However, contractile function and Ca_i^{2+} transients (amplitude and kinetics) of isolated TKO cardiomyocytes were markedly enhanced. They concluded that this discordance between unimproved cardiac function, and enhanced Ca_i^{2+} cycling and cardiomyocyte contractile parameters arose from decreased expression of gap junction proteins (connexin 43). Cell-to-cell electric coupling of cardiomyocytes is mediated by gap junctions that form between the cells. The main gap junction protein is connexin 43 (Cx43) [73]. In order to assess gap junction formation, we stained paraffin sections from δ_C TG mice, KO/TG and WT mice for Connexin 43. While there was significant disruption of gap junction formation in the CaMKII δ_C TG mice compared to WT mice, which was expected due to the heart failure phenotype of the δ_C TG mice, we did not see greater disruption in the KO/TG hearts compared to the δ_C TG sections (Fig 23). Quantification of staining showed no increase or decrease in Cx43 in the KO/TG compared to the δ_C TG mice.

IV.C.1.iii.3. Increased apoptosis is observed in heart tissue sections from KO/TG mice compared to δ_C TG mice.

Apoptosis has been demonstrated to be a causal factor in cardiomyocyte loss that is a hallmark of heart failure [64]. Accordingly we determined whether increased cardiomyocyte death was associated with the reduced cardiac function, ventricular wall thinning and exaggerated phenotype of the KO/TG mice. Apoptosis was assessed by TUNEL staining was performed on paraffin sections prepared from WT, PLN KO, δ_C TG and KO/TG mice. To confirm that the TUNEL positive nuclei were actually cardiomyocytes and not fibroblasts, DAPI was used to stain for nuclei, and wheat germ agglutinin (WGA) was used to stain the cell membrane. Transversally sectioned myocytes can be identified by centrally located nuclei using the WGA stain, distinguishing them from fibroblasts and epithelial cells [74]. TUNEL positive cardiomyocytes were counted and reported as number of positive nuclei per 10^5 cardiomyocytes. There was a highly significant increase in TUNEL positive nuclei was seen in the KO/TG compared with the WT and CaMKII δ_C TG mice (Fig 24).

IV.C.1.iii.4. Inhibition of CaMKII or SR Ca^{2+} leak rescues cell viability

The increased in apoptotic nuclei observed in the KO/TG mice compared to the δ_C TG mice implied a difference in cardiomyocyte viability. In order to address this more directly and determine mechanism, we isolated AMVMs from the four lines and examined viability by trypan blue exclusion and cellular morphology changes over a 12 hour time course. Experiments were performed using a variety of pharmacological treatments to determine if cell viability could be altered by inhibiting various pathways.

To determine whether CaMKII activity or SR Ca^{2+} release were directly responsible for decreased cell viability, cells were treated with either 2 μmol/L KN-93 (to inhibit CaMKII) or 100 nmol/L ryanodine (to deplete SR Ca^{2+} and prevent Ca^{2+} sparks). AMVMs isolated from WT myocytes remained viable over the 12 hour time course study, and there was no significant alteration following treatment with either KN-93 or ryanodine indicating low toxicity of the concentrations used (Fig 25). Survival of AMVMs from both δ_C TG and KO/TG mice were significantly reduced compared to WT over the 12 hours time course. Inhibiting either CaMKII or SR Ca^{2+} leak improved cell viability in AMVMs from both δ_C expressing lines. These findings implicate CaMKII as a causal factor in the decrease in viability, and suggest that SR Ca^{2+} leak contributes significantly to the decrease in myocyte survival (Fig 25) [63].

IV.C.1.iii.5. Inhibition of mitochondrial Ca^{2+} overload or PT pore formation rescues AMVM viability

To establish a link between increased Ca^{2+} sparks and mitochondrial Ca^{2+} overload, we carried out a second set of cell survival studies. In these studies, AMVMs were treated with either 5 μmol/L Ru-360, a selective inhibitor of the mitochondrial Ca^{2+} uniporter to inhibit mitochondrial Ca^{2+} overloading, or mitochondrial permeability transition (PT) pore inhibitor, cyclosporine A (5 μmol/L). Both drugs significantly attenuated myocyte death in the KO/TG myocytes indicating that the overloading of the mitochondrial Ca^{2+} levels and permeability transition was contributing to loss of cell viability (Fig 26). Neither treatment had significant effects on the survival of the δ_C TG AMVMs suggesting that the overloading of mitochondrial Ca^{2+} was most critical to the

decreased viability seen in the KO/TG mice [63]. This does not mean that mitochondrial Ca^{2+} overloading is not a contributing factor to the phenotype of the δ_C TG mice as will be demonstrated in a later section.

IV.C.1.iv. Discussion

A hallmark of heart failure in both animal models and human patients is a decrease in contractility resulting from a decreased Ca^{2+} transient from the SR. This can be explained by decreases in SR Ca^{2+} content making less Ca^{2+} available for release [75]. Re-uptake of Ca^{2+} into the SR is modulated by PLN, an inhibitor of SERCA2a, the activity of which depends upon its phosphorylation state. Inhibition of PLN has been suggested as a potential heart failure treatment strategy, and evidence from several studies have indicated the importance of SR Ca^{2+} load regulation via PLN [76-82]. However, we show here that recovery of cardiomyocyte Ca^{2+} stores and twitch Ca^{2+} transients does not translate into recovery of overall cardiac function and attenuation of heart failure. The KO/TG mouse model provided an opportunity to study why restoration of SR Ca^{2+} load might fail to rescue heart failure development.

SR Ca^{2+} sparks were increased and contributed to the decrease in SR Ca^{2+} load in the CaMKII δ_C TG mice, most likely due to the increased phosphorylation of RyR2 [2, 30]. In the KO/TG mice, the combination of increased RyR2 phosphorylation and associated SR Ca^{2+} leak, with an increase in SR Ca^{2+} load due to PLN deletion, served to increase the SR Ca^{2+} sparks dramatically (7.5 fold over WT and 2.5 fold over δ_C TG) compared to the other two models.

The downstream effect of this more pronounced SR Ca^{2+} dysregulation appeared to translate to mitochondrial dysfunction. Numerous studies have shown that mitochondrial Ca^{2+} overload results in permeability transition leading to cell death [83-86]. Apoptosis and necrosis have both been implicated as major contributors to cardiomyocyte loss in heart failure [87-89]. More relevant is the growing evidence for the close interaction between the SR and mitochondria, where Ca^{2+} from the SR is taken up by mitochondria via a Ca^{2+}-uniporter [90, 91 92].

Based on the findings from our studies, we find that the rescue of SR Ca^{2+} load causes exaggeration of the already increased SR Ca^{2+} leak, contributing to increased mitochondrial Ca^{2+} loading and potentiating downstream consequences ultimately leading to increased cell death and contributing to cardiac dysfunction.

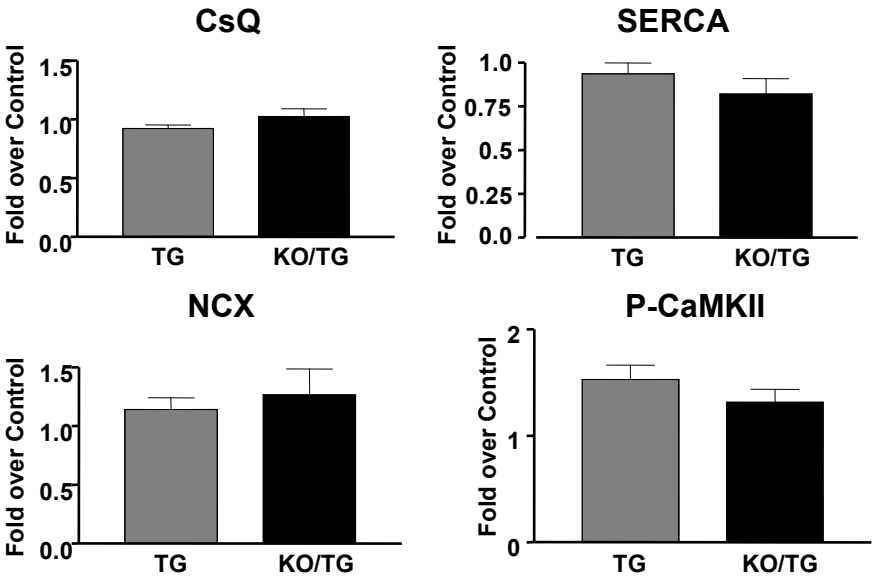

Figure 21. Quantitative immunoblotting of major Ca^{2+} handling proteins and CaMKII activation in mouse ventricular homogenate. A. Expression levels of calsequestrin (CsQ), SERCA, and NCX did not change and P-CaMKII levels were also similar in ventricular tissue homogenates obtained from both δc TG and KO/TG mice at 8 week old. (n=4) *p<0.05 vs. WT

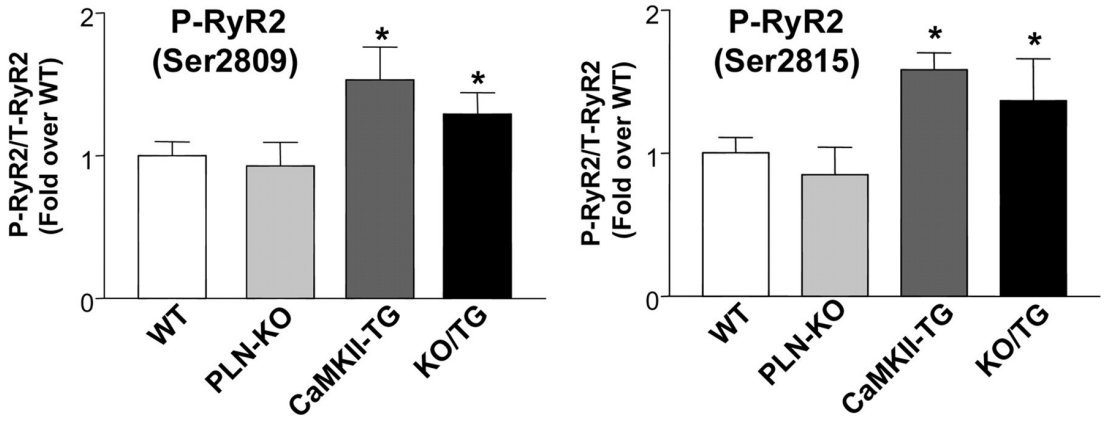

Figure 22. Phosphorylation of RyR is not changed in the δ_C TG mice following PLN ablation. Western blot analysis of Ryanodine Receptor phosphorylation at the PKA (Ser2809) and CaMKII (Ser 2815) sites (normalized to total RyR2) in ventricular tissue homogenates obtained from both the TG and DM at 8 weeks old showed significant but not differential increase in CaMKIIδc TG and KO/TG mice. (n=4) * $p<0.01$

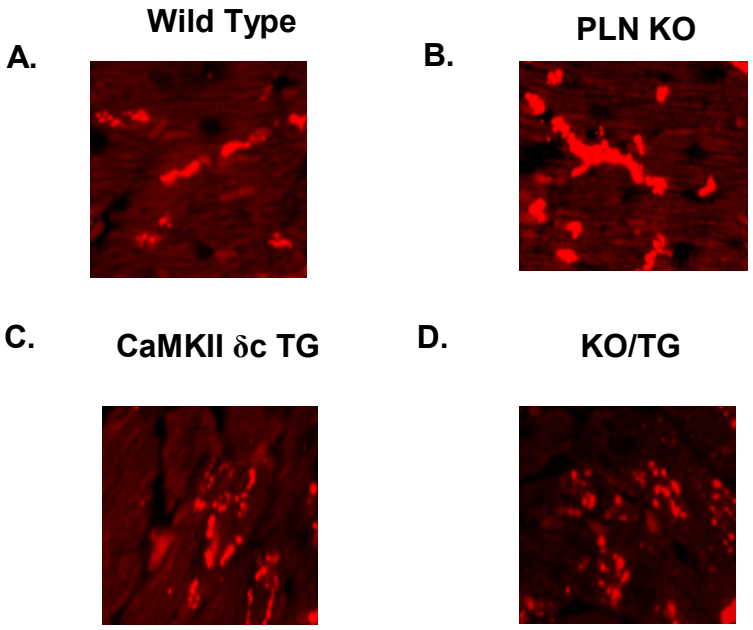

Figure 23. Gap junction formation. Heart sections taken from 8 week old mice were stained for Cx-43 expression and show that while there is significant disruption in the KO/TG mice, it is not different from the disruption seen in the δ_C TG mice.

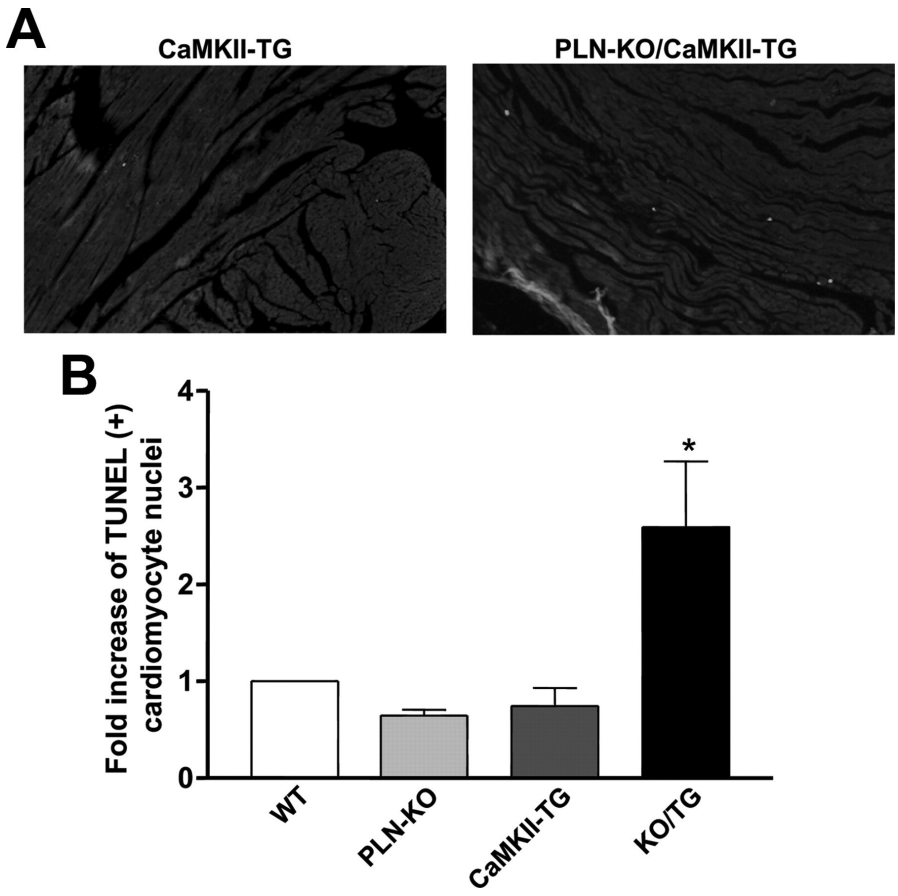

Figure 24. Apoptosis is greater in PLN KO/CaMKIIδ_C TG myocytes than in CaMKIIδ_C TG myocytes. A. Representative TUNEL staining in heart sections from 8 week old δ_C TG and KO/TG mice. **B**. Quantification of average TUNEL (+) nuclei for 105 total cardiac myocytes vs. WT. Data were normalized to WT; the average number from all experiments was ≈75 TUNEL-positive nuclei/10^5 myocytes in the KO/TG group. (n=4 mice) * $p<0.01$

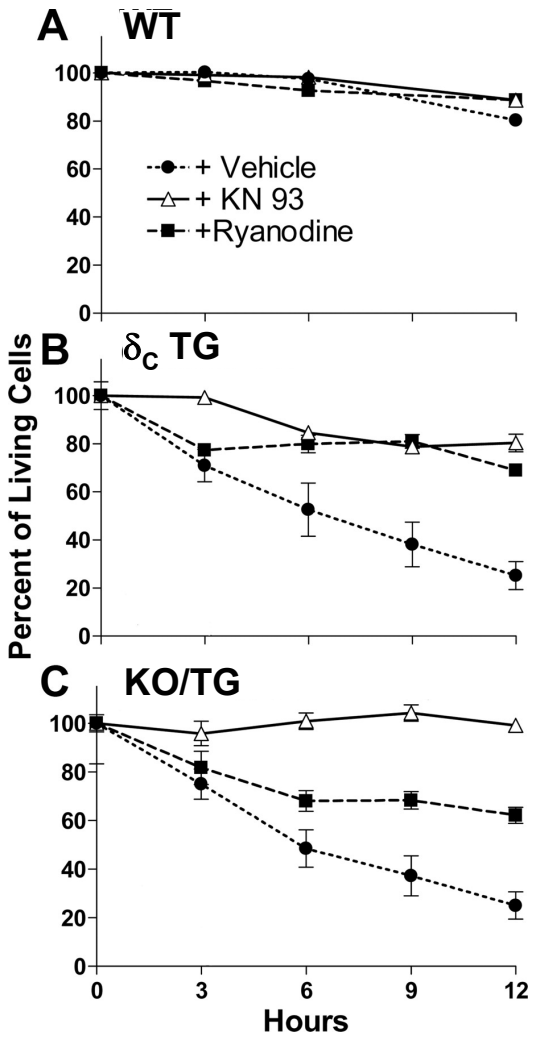

Figure 25. Inhibition of SR Ca^{2+} leak by KN-93 or ryanodine decreases the rate of death in isolated cardiomyocytes from KO/TG mice. Isolated cardiomyocytes were plated and incubated in the presence and absence of inhibitors, and cell viability was assessed at various times using morphology and at 12 hours by trypan blue exclusion. A. WT myocytes showed only slight decreases in viability over 12 hours after plating. B and C. The percent of living myocytes from both δ_C TG and KO/TG mice decreased dramatically over 12 hours. Inhibition of CaMKII with 2 μmol/L KN-93 or of SR Ca^{2+} leak with 100 nmol/L ryanodine decreased the rate of myocyte death in both δ_C TG and KO/ TG mice. (n=4)

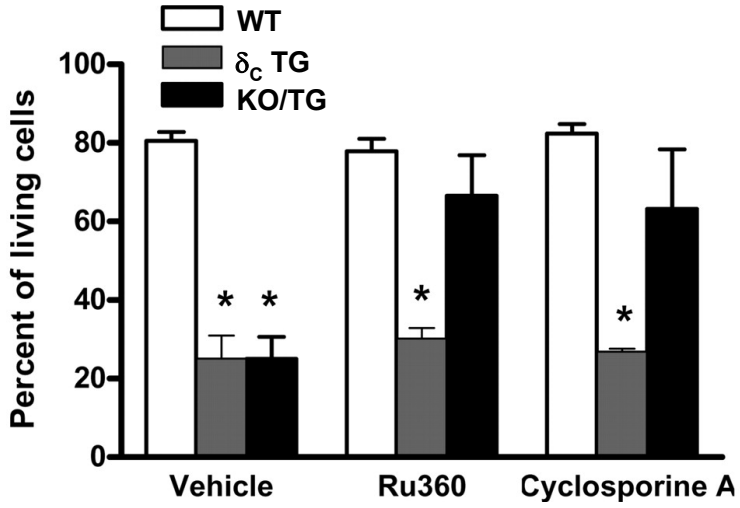

Figure 26. Inhibition of mitochondrial Ca^{2+} loading by Ru-360 or PT-pore formation using cyclosporine A decreases the rate of death in isolated cardiomyocytes from KO/ TG mice. Isolated cardiomyocytes were plated and incubated in the presence and absence of inhibitors, and cell viability was assessed at 12 hours by trypan blue exclusion. Inhibition of the mitochondrial uniporter by 5 μmol/L Ru-360 or inhibition of the mitochondrial permeability transition pore by 5 μmol/L cyclosporine A decreased the rate of death in isolated cardiomyocytes from PLN-KO/CaMKII-TG mice at 12 hours. (n=4) *P<0.05 vs. WT.

IV.C.2. Loss of cyclophilin D contributes to heart failure development

IV.C.2.i. Abstract

Changes in mitochondrial permeability transition (mPT) can lead to mitochondrial swelling, outer membrane rupture and cytochrome c release, all associated with cell death. Modulation of mitochondrial permeability transition occurs via several components, one being cyclophilin D, a mitochondrial matrix peptidyl-prolyl isomerase. Loss of cyclophilin D by Ppif $^{-/-}$ deletion is associated with resistance to *in vitro* mitochondrial swelling and permeability transition in mitochondria isolated from hearts of these mice, and cells from these mice are largely protected from Ca^{2+} overload [65]. A key inducer of PT-pore opening is increased mitochondrial Ca^{2+} loading and we hypothesized that inhibition of PT pore formation in the CaMKII δ_C TG mice via ablation of cyclophilin D might rescue the heart failure phenotype. To test this, we crossed δ_C TG mice with cyclophilin D knockout mice, (Ppif $^{-/-}$) mice. Mitochondria isolated from the hearts of the δ_CTG/Ppif $^{-/-}$ mice were protected from Ca^{2+} induced swelling. Remarkably however, loss of cyclophilin D in the δ_C TG mice exaggerated the heart failure phenotype as indicated by decreased survival, cardiac enlargement (HW/BW) and congestive heart failure (LW/BW) [69].

IV.C.2.ii. Introduction

In heart failure, decreased cardiac function and ventricular dilation are associated with loss of ventricular myocytes. Understanding the mechanisms causing myocyte death is critical for preventing cell loss. Within the cardiomyocyte, mitochondria are important regulators of both necrotic and apoptotic cell death pathways. In response to

insult, changes in mitochondrial membrane permeability can occur, mediated by the opening of the mitochondrial permeability transition pore (mPTP) and leading to a loss of ionic homeostasis. Induction of mPT results in mitochondrial swelling, outer membrane rupture and cytochrome c release which are associated with cell death. The mPTP is composed of multiple components (ANT, VDAC, cyclophilin D), but geneteic deletion of ANT and VDAC has shown them not to be critical for mPT [46, 93]. Induction of the mPT is associated with both necrotic and apoptotic cell death, and a key inducer of mPTP opening is increased mitochondrial Ca^{2+}.

CaMKII inhibition has been shown to protect against apoptosis in cardiac and other cell types. [44, 94-96] As mentioned previously, CaMKII δ_C TG mice developed heart failure preceded by dilation and thinning of the ventricular wall. Although this is associated with increased apoptosis the mechanism causing the marked loss of cardiomyocytes has yet to be determined, we hypothesize that increased SR Ca^{2+} leak contributes to the loss of cells. Results from the δ_C TG mouse model in which phospholamban was deleted implied that Ca^{2+} changes affect the mitochondria, and mediate cell death.

A mouse model lacking the Ppif gene which encodes cyclophilin D was generated by the Molkentin lab, and characterization of the mouse model demonstrated the critical role of cycophilin D in PT pore opening, as mitochondria from these mice were resistant to Ca^{2+} and oxidative damage induced cell death [65]. We crossed cyclophilin D KO mice with our δ_C TG mice to determine if mPTP is important in heart failure development and cell death induced by CaMKII δ_C.

IV.C.2.iii. Results

IV.C.2.iii.1. Mitochondria from δ_C TG/Ppif $^{-/-}$ mice are protected against Ca^{2+} overload induced swelling.

The initial studies characterizing the Ppif $^{-/-}$ mice showed that mitochondria lacking the Ppif $^{-/-}$ gene product were protected from Ca^{2+} induced swelling [65]. We wanted to confirm that this was also the case in the Ppif $^{-/-}$ null mice crossed with the δ_C TG mice. Mitochondria were isolated from the four mouse lines (WT, Ppif $^{-/-}$, δ_C TG and δ_CTG/Ppif$^{-/-}$) and challenged with Ca^{2+} to determine their susceptibility to Ca^{2+} induced PT pore opening. Swelling studies showed that the mPT elicited by addition of high Ca^{2+} was fully evident in the WT and δ_C TG mice, but was inhibited by genetic loss of Ppif, in the absence or presence of the CaMKIIδ_C transgene (Fig 27).

IV.C.2.iii.2. Cyclophilin D ablation in δ_C TG mice is lethal

Inhibition of mPTP opening is expected to decrease cell death associated with heart failure development and since mitochondrial protection was preserved in the Ppif $^{-/-}$ mice crossed with CaMKIIδ_C, we expected to see attenuation of the CaMKII induced heart failure phenotype.

Previous characterization of the δ_C TG mice showed decreased survival, with half of the animals dying by 16 weeks of age [2]. Unexpectedly, δ_C TG mice crossed into the Ppif $^{-/-}$ (δ_C TG/Ppif $^{-/-}$) background showed worsened lethality compared to the δ_C TG mice, with 50% of the δ_CTG/Ppif $^{-/-}$ mice dying at 8 weeks of age, and none of the mice able to survive past 14 weeks of age (Fig 28).

IV.C.2.iii.3. Cyclophilin D ablation in δ_C TG mice exaggerates cardiomyopathy.

The decreased survival of the δ_CTG/Ppif $^{-/-}$ mice led us to investigate how quickly heart failure developed in the δ_C TG/Ppif $^{-/-}$ mice compared to the δ_C TG mice. Heart weight measurements were initially determined at 8 weeks of age, but since half the δ_C TG/Ppif $^{-/-}$ mice died by that time, an earlier time point of 4 weeks of age was examined. Even at this time point, a significant increase in hypertrophy was seen in δ_C TG mice in the Ppif $^{-/-}$ background compared to δ_C TG or WT mice (Fig 29). δ_C TG/Ppif $^{-/-}$ mice also displayed pulmonary congestion, a symptom of heart failure, measured by an increase in lung/body weight ratio compared to δ_C TG mice (Fig 30). Even heterozygous mice (Ppif +/-) expressing the δ_C transgene also showed increased lethality and hypertrophy, indicating that partial loss of cyclophilin D is sufficient to exaggerate the CaMKIIδ_C cardiomyopathy (data not shown).

IV.C.2.iii.4. Distribution of overexpressed δ_C is not altered following cyclophilin D ablation.

The severe phenotype of the δ_C TG/Ppif $^{-/-}$ mice was initially surprising because we had hypothesized that then increased SR Ca^{2+} leak in the δ_C TG mice leads to mitochondrial Ca^{2+} overload and subsequent cell death. Accordingly we had expected cyclophilin D ablation to inhibit cell death. In an effort to understand why the mice developed the unexpected phenotype, we determined whether expression of CaMKII δ_C at the mitochondria or other cellular locations was changed by cyclophilin D ablation. Subcellular fractionation of ventricular tissue isolated from WT, Ppif $^{-/-}$, δ_C TG and δ_C

TG/Ppif $^{-/-}$ mice was performed and fractions were probed for CaMKIIδ_C transgene expression. No significant changes in CaMKIIδ_C distribution were seen in any of the subcellular compartments (Fig 31).

To determine whether there were changes in activation of CaMKIIδ at the mitochondria, P-CaMKII was measured by western blot in mitochondria isolated from the δ_C TG/Ppif $^{-/-}$ mice and compared to δ_C TG mice. P-CaMKII levels were in fact increased in the mitochondrial fraction of the δ_C TG/Ppif $^{-/-}$ mice compared to the δ_C TG mice. P- Ser/Thr levels were also measured using western blot (Fig 32) and showed an increase in the intensity of a band present at 55kD, the molecular weight of CaMKIIδ (Fig 32). The reason that this occurs and its functional implications have not been determined, but it is provocative to consider that local Ca^{2+} at the mitochondria may be regulating CaMKII activation and that CaMKII may have direct actions at the mitochondria.

IV.C.2.iii.5. CaMKII δ_C overexpression affects mitochondrial Ca^{2+} handling

Genetic loss of cyclophilin D results in mitochondria with elevated resting Ca^{2+} levels compared to WT, and attribute this to the maladaptive phenotype observed following aging, stress or exercise [65].

There is growing evidence that CaMKIIδ_C predisposes to cell death through mitochondrial cell death signaling pathways. [44, 94-96] Subcellular fractionation of δ_C TG mouse hearts revealed a high level of transgenic CaMKII δ_C at the mitochondria and the unexpected exaggeration of heart failure in the δ_C TG mice following cyclophilin D

ablation motivated further understanding of the role of δ_C at the mitochondria. That loss of cyclophilin D in the δ_C TG mice causes mitochondrial Ca^{2+} dysregulation led us to perform experiments (in collaboration with Drs Anne Murphy and Aleksander Andreyev) comparing Ca^{2+} sensitivity of mitochondria isolated from WT and δ_CTG mouse hearts. Our results suggest that CaMKIIδ_C mitochondria are unable to sequester as much Ca^{2+} before mPTP opening occurs (Fig 33A). Interestingly, when mitochondria from the δ_C TG mice were isolated in a manner designed to preserve their Ca^{2+} level, [97, 98] measurement of endogenous Ca^{2+} levels in mitochondria from δ_C TG mice were shown to have higher mitochondrial Ca^{2+} loading than WT controls (Fig 33C). Lastly, we see that oxidative phosphorylation appears to be altered by CaMKIIδ_C overexpression (Fig 33D), as measured by changes to mitochondrial respiration rate which may indicate disruption of Ca^{2+} sensitive metabolic processes as was observed in the Ppif $^{-/-}$ mice [65].

IV.C.2.iv. Discussion

Following the initial characterization of the Ppif $^{-/-}$ mice, the Molkentin lab discovered that the mice did not have as normal a phenotype as they believed, noting that aging or stress (pressure overload or exercise) resulted in heart failure compared to WT mice [69].

Mitochondrial Ca^{2+} load is affected by increases in cardiac contractility which is associated with increased Ca^{2+} cycling rates in myocytes, and at these higher rates, Ca^{2+} accumulates in the mitochondria until the PT pore opens allowing Ca^{2+} levels to normalize. Recent work has provided evidence linking MPTP-mediated Ca^{2+} efflux to

global changes in metabolic substrate utilization, a mechanism that appears crucial to the heart's ability to maintain contractility in response to increased workload [99]. Increased mitochondrial Ca^{2+} loading leads to activation of mitochondrial dehydrogenases important in substrate utilization and oxidative metabolism, thereby increasing energy supply during increased workloads [100]. A correlation between increased mitochondrial Ca^{2+} load and ATP production has been reported, and inhibition of Ca^{2+} influx via the Ca^{2+} uniporter reduces the activity of mitochondrial dehydrogenases. [101, 102] Enhanced enzymatic activity of key mitochondrial dehydrogenases was found in Ppif $^{-/-}$ hearts consistent with constitutively higher intramitochondrial Ca^{2+} of the Ppif -/- mice. Ultimately, this would render the heart more sensitive to decompensation with stress provocation such as increasing CaMKIIδ_C activity [69].

The inability to adjust mitochondrial function in accordance with increased metabolic demand due to loss of cyclophilin D and inhibition of PT pore formation results in severe cardiac dysfunction and emphasizes its importance in regulating Ca^{2+} homeostasis [69]. The inability of mitochondria from the Ppif $^{-/-}$ mice to adapt to disease states (following δ_C overexpression as described above) or increased workload (exercise, aging and pressure overload) is most likely the explanation as to why these mice are more susceptible to cardiac dysfunction [69]. These findings suggest a physiologic role for the PT-pore, specifically that the PT pore may play a housekeeping role important for regulating mitochondrial Ca^{2+} levels.

Overexpression of CaMKII δ_C in the Ppif -/- mice emphasized the importance of the PT pore in regulating intramitochondrial Ca^{2+} in a disease state. This model also served to highlight that mitochondrial dysfunction may be an important factor in how

CaMKIIδ_C contributes to heart failure development and motivated our findings that mitochondrial Ca^{2+} load is increased in δ_C TG mitochondria compared to WT mitochondria and δ_C TG mitochondria are unable to take up as much Ca^{2+} compared to WT mice. These results, along with the alterations in mitochondrial respiration in the δ_C TG mice are consistent with the model for heart failure development described in the Ppif $^{-/-}$ studies [69], and will be taken into consideration in future studies of mitochondrial function in δ_C TG mice.

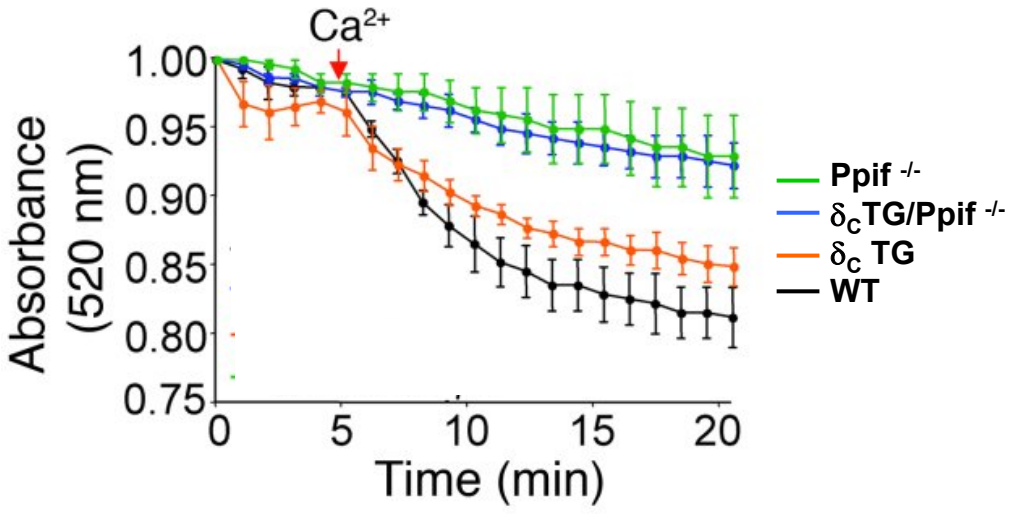

Figure 27. Cyclophilin D ablation inhibits mitochondrial permeability transition in δ_C TG mice. Mitochondria were isolated from WT, Ppif $^{-/-}$, δ_C TG, and δ_C TG x Ppif $^{-/-}$ mice. Absorbance was measured in the mitochondrial suspension to monitor changes in mitochondrial volume at various times following addition of Ca^{2+}. Cyclophilin D ablation (Ppif $^{-/-}$) in the δ_C TG mice protects mitochondria from swelling. (n=4)

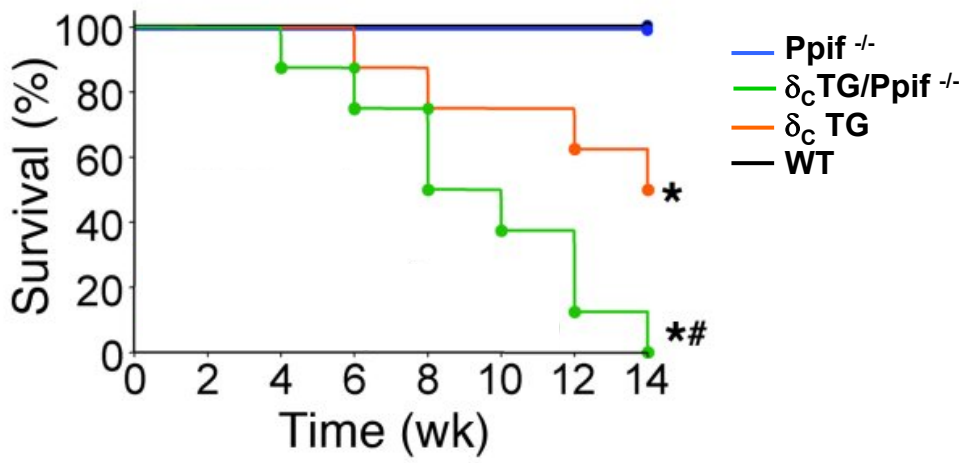

Figure 28. Cyclophilin D ablation is lethal in CaMKIIδ$_C$ TG mice. Survival curves for WT, Ppif $^{-/-}$, CaMKIIδ$_C$ TG and CaMKIIδ$_C$ TG x Ppif $^{-/-}$ mice. Cyclophilin D ablation accentuates premature death in CaMKIIδ$_C$ TG mice, and results in 100% lethality by 14 weeks of age. (n=12 per group) $P<0.01$ * vs. WT and # vs. CaMKIIδ$_C$ TG.

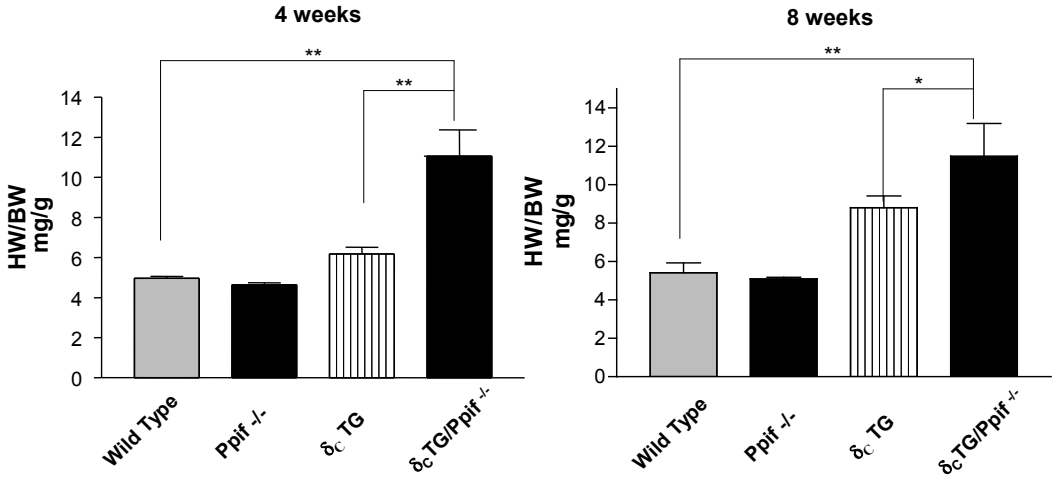

Figure 29. Cyclophilin D ablation in CaMKIIδc TG mice exaggerates cardiac enlargement. Ventricular tissue was isolated from mice at 4 weeks of age. Heart weight/body weight (HW/BW) ratio shows significant increase compared to WT and δ_C TG mice. (n=8) * $p<0.01$ vs. WT # $p<0.01$ vs. δ_C TG

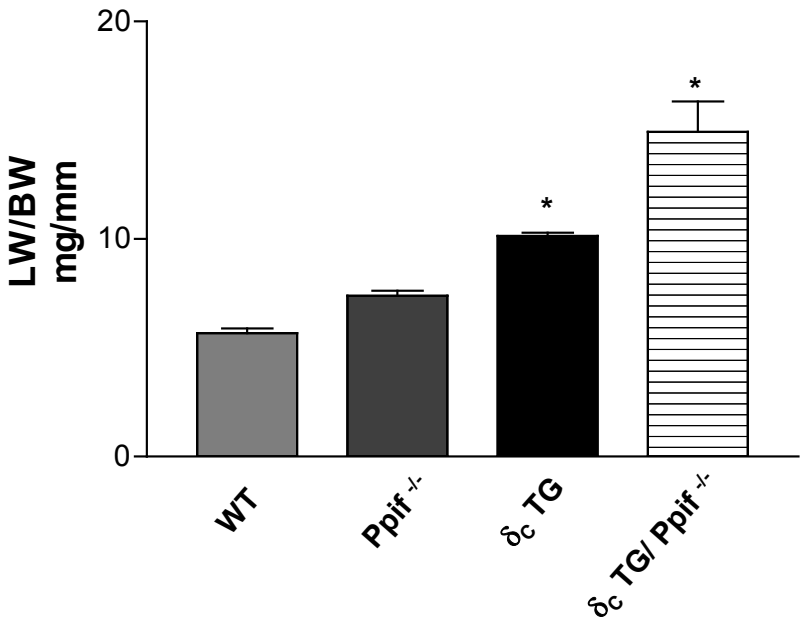

Figure 30. Cyclophilin D ablation in CaMKIIδ_C TG mice exaggerates the heart failure phenotype. Following removal of the heart from 4 week old mice and lungs were dissected and lung weight/body weight (LW/BW) ratio was measured. Results show a significant increase compared to WT and δ_C TG mice. (n=6) * $p<0.01$ vs. WT

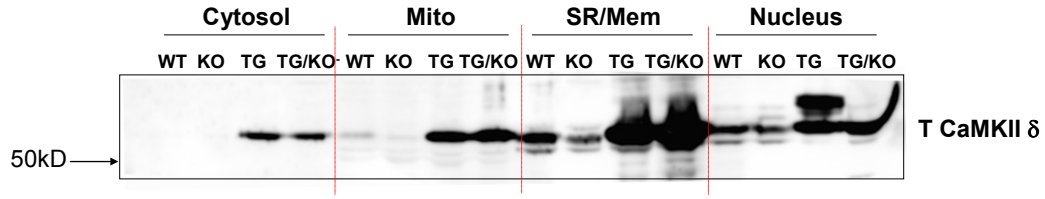

Figure 31. Cyclophilin D ablation does not alter CaMKIIδ_C subcellular expression. Subcellular fractionation of ventricular tissue isolated from 4 week old mice and subjected to western blotting shows not significant change in CaMKIIδ_C distribution between the δ_C TG (TG) and the δ_C TG/ Ppif $^{-/-}$ (TG/KO) null mice.

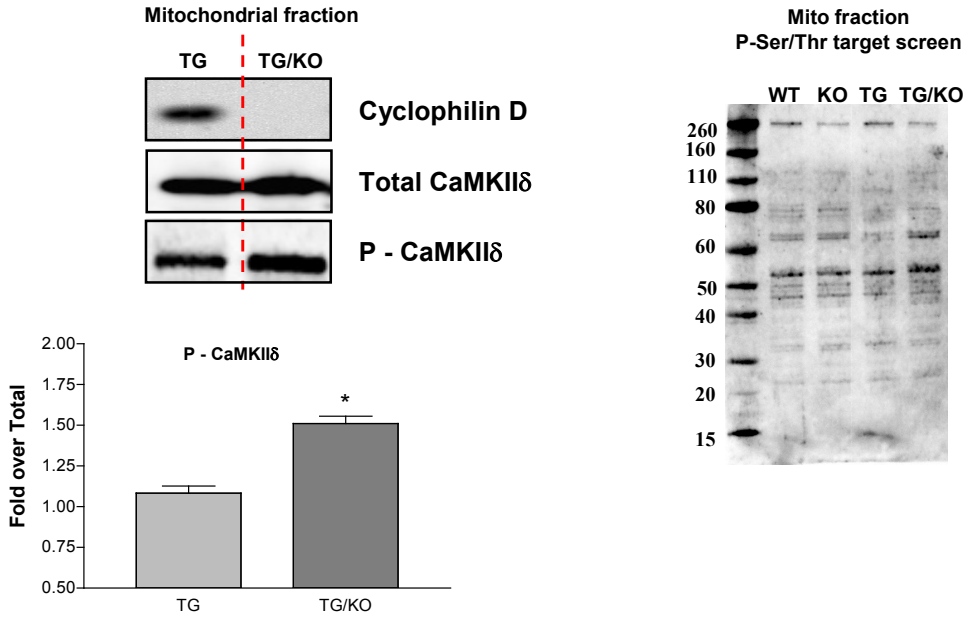

Figure 32. Cyclophilin D ablation in the δ_C TG mice increases CaMKII activation at the mitochondria. Mitochondria were isolated from fresh ventricular tissue harvested from WT, Ppif $^{-/-}$ (KO), δ_C TG (TG) and δ_C TG/Ppif $^{-/-}$ (TG/KO) mice. Western blotting for cyclophilin D shows loss of expression in the TG/KO null mice compared to the TG mice. Western blotting for total CaMKIIδ expression shows no change in expression level, but western blotting with a P-CaMKII antibody show an increase in band intensity in the Ppif $^{-/-}$ background. Quantification of CaMKII phosphorylation shows a significant increase in CaMKII activation (n=4). Western blotting using a P-Ser/Thr antibody also shows a band at approximately 55kD that is increased in the TG/KO mice compared to the TG mice, corresponding to the data obtained using the P-CaMKII antibody. (n=4) $p<0.01$

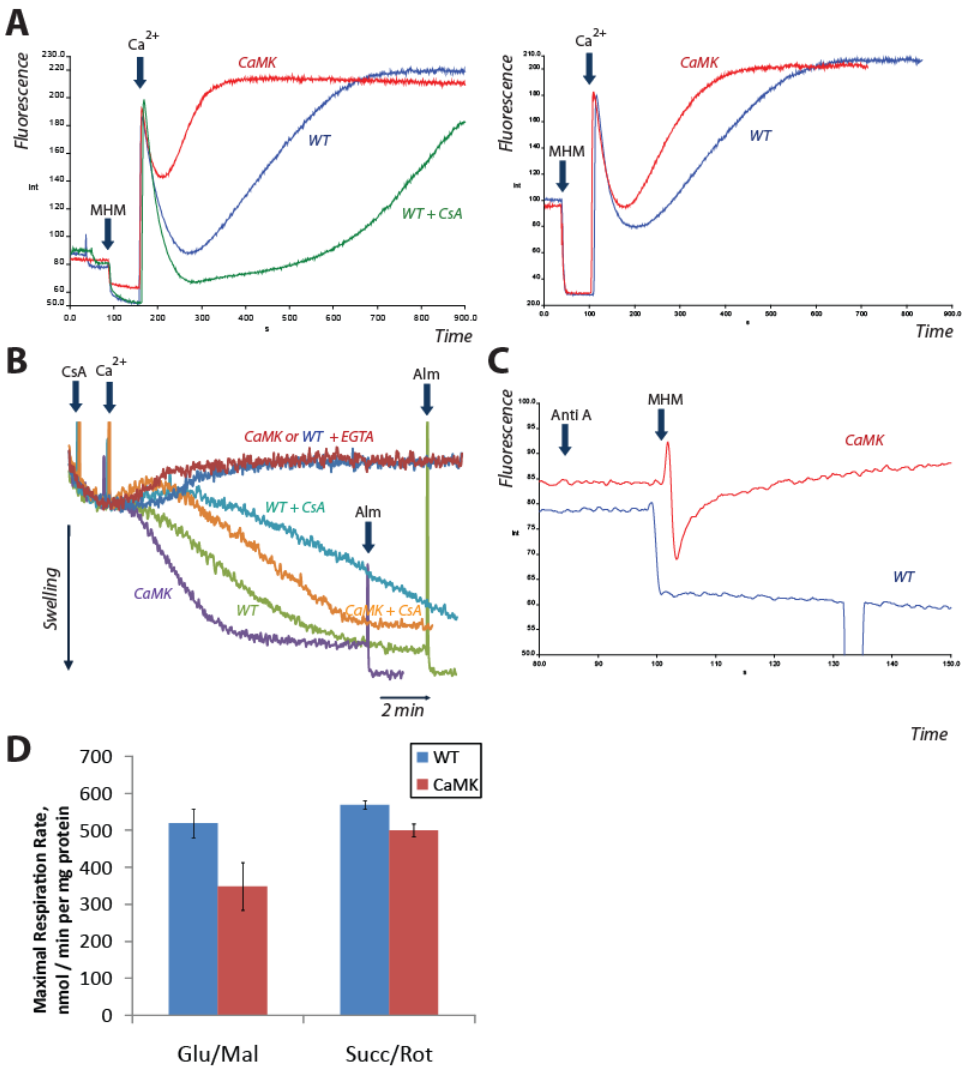

Figure 33. CaMKII-mediated mitochondrial dysregulation. A. Ca uptake and release in isolated cardiac mitochondria from WT and δ_CTG mice. B. Mitochondrial swelling in response to Ca^{2+} (100 nmoles/mg protein) addition. C. Measurement of endogenous mitochondrial Ca. Additions: MHM, 0.25 mg/ml mouse heart mitochondria D. Maximal (FCCP-stimulated) respiration rate in presence of Glu/Mal or succinate and rotenone (Succ/Rot). Mitochondria were energized by NAD+-linked substrates: glutamate and malate (Glu/Mal) (average of 2 experiments). Data are mean ±SE (n=4) for Glu/Mal or mean of duplicates for Succ/Rot.; Ca, 100 nmoles/mg protein; CsA, 1 mM cyclosporine A; Anti A, 0.5 mM antimycin A. Extramitochondrial Ca^{2+} was measured using 0.5 mM Calcium Green-5N.

IV.C.3. Inhibition of CaMKII at the SR improves Ca^{2+} handling, but exacerbates heart failure in CaMKII δ_C TG mice

IV.C.3.i. Abstract

The alterations in SR Ca^{2+} handling observed in cardiomyocytes from δ_C TG mice is believed to be a major factor contributing to the decreased contractile function and heart failure development observed in these mice. A particularly marked change was the hyperphosphorylation of the RyR2 and the increased diastolic SR Ca^{2+} leak. This was functionally important because of the resultant decrease in SR Ca^{2+} load and decreased twitch Ca^{2+} transient. In an effort to rescue the heart failure phenotype of the δ_C TG mice, animals were crossed with mice expressing AIP, a CaMKII inhibitor, targeted to the SR. We hypothesized that targeted inhibition of CaMKII at the SR would result in decreased RyR2 phosphorylation resulting in a decrease in SR Ca^{2+} leak and normalization of the decreased SR Ca^{2+} load and Ca^{2+} transient seen in the δ_C TG mice. Characterization of these mice indicated that CaMKII activation at the SR/mem was decreased while that in the cytosolic and nuclear fractions was not. Analysis of SR Ca^{2+} sparks and SR Ca^{2+} leak showed both to be significantly decreased by SR-AIP expression in the δ_C TG mice and this was accompanied by an increase in SR Ca^{2+} load. Interestingly, heart failure in the δ_C TG mice was not rescued, indeed hypertrophy and heart failure development appeared to be more severe in the δ_C TG/SR-AIP mice.

IV.C.3.ii. Introduction

Heart failure in the δ_C TG mice was associated with defects in Ca^{2+} handling resulting in disruption of normal E-C coupling and compromised cardiac function [2, 30]. The most prominent effects of CaMKII δ_C overexpression involved the SR. Increased CaMKIIδ_C expression led to increased RyR2 phosphorylation and increased diastolic SR Ca^{2+} leak associated with increases in SR Ca^{2+} spark frequency and a decrease in SR Ca^{2+} load [2, 30]. Inhibition of CAMKII using KN-93 blocked enhanced Ca^{2+} spark frequency in myocytes from δ_C TG mice, demonstrating the direct role of CaMKII [30]. Treatment with KN-93 also completely rescued the decreased cardiomyocyte viability of δ_C TG AMVMs [63].

We hypothesized that inhibition of CaMKIIδ_C activity at the SR would reduce the hyperphosphorylation of the RyR2, and subsequently inhibit the SR Ca^{2+} leak and reduced Ca^{2+} transient. Mice overexpressing SR-targeted CaMKII inhibitor (SR-AIP) were generated and characterized extensively [70, 103, 104]. To directly test the importance of CaMKIIδ_C at the SR, the δ_C TG mice were crossed with SR-targeted AIP mice. Crosses were carried out in the laboratory of our collaborators Don Bers and Sabine Huke, and isolated heart tissue was analyzed in our lab.

IV.C.3.iii. Results

IV.C.3.iii.1. CaMKII activation following SR-AIP overexpression in δ_C TG mice

To determine whether SR targeted inhibition of CaMKII δ_C reduced CaMKII activity specifically in the SR compartment, subcellular fractionation was used to isolate

the SR containing fraction from δ_C TG mice overexpressing SR-AIP. Consistent with the inhibitory effect of AIP on CaMKIIδ, CaMKII autophosphorylation at Thr287 (indicative of activation) was reduced to about 68% of the level in the CaMKIIδ_C TG mice at the SR (Fig 34). At the time these experiments were done, the purified SR fractionation described in earlier chapters was not yet developed. Thus, although the reported level of CaMKIIδ inhibition is significantly reduced, this value is likely an underestimate of the extent of inhibition of SR localized CaMKIIδ_C because the SR/mem fraction also includes membrane fragments other than the SR. Inhibition of CaMKII δ_C activation was selective for the SR/membrane compartment since analysis of other fractions (cytosolic and nuclear) from the δ_C TG/SR-AIP mouse hearts showed no changes in P-CaMKII levels compared to the δ_C TG mice (Fig 35). Accompanying the reduction in SR CaMKIIδ_C activation levels was a reduction in SR Ca^{2+} leak and enhanced SR load and twitch Ca^{2+} transient. [47] However, most striking was the fact that heart failure in the δ_C TG/SR-AIP mice was worsened.

IV.C.3.iii.2. Ca^{2+} handling in the δ_C TG mice following SR-AIP overexpression

The attenuation of Ca^{2+} handling disruption in the δ_CTG/SR-AIP mice led us to question whether there were alterations in proteins responsible for regulating cytosolic diastolic Ca^{2+} levels. In the δ_C TG mice, NCX expression and activity was seen to be upregulated, most likely to increase Ca^{2+} extrusion from the cell [105]. Measurement of NCX function in the δ_CTG/SR-AIP mice showed no change compared to the δ_C TG mice

and NCX expression was also unchanged in the δ_C TG/SR-AIP mice compared to the δ_C TG (Fig 36). SERCA expression was also unchanged between the two groups, suggesting that the recovery of the Ca^{2+} load was due to the reduction in SR Ca^{2+} leak that was attenuated by inhibition of CaMKIIδ_C at the SR.

IV.C.3.iv. Discussion

Hallmarks of heart failure include alterations in Ca^{2+} regulatory mechanisms within the cardiomyocyte which translate into compromised pump function. CaMKII expression and activity are increased in heart failure [106-109], and studies have shown that CaMKII regulates RyR2 phosphorylation at Ser2814/2815 [110], which in turn affects Ca^{2+} sparks in AMVMs [30, 111]. During heart failure, increased activity of CaMKII is believed to play a critical role in the regulation of RyR2 phosphorylation state and SR Ca^{2+} leak [105].

The main pathophysiological effects of cardiac specific overexpression of CaMKII δ_C are due to its role at the SR. Ablation of CaMKIIδ protects from the heart failure development, and this is accompanied by dimished TAC induced increases in SR Ca^{2+} leak and RyR2 phosphorylation [39, 40]. It has also been shown that protection against maladaptive cardiac remodeling occurs in response to chronic beta adrenergic stimulation occurs following global inhibition of CaMKII activity via overexpression of the inhibitor peptide AC3I [112]. These and additional studies reinforce the hypothesis that CaMKII is a critical mediator of the RyR2 and SR dysfunction associated with cardiomyopathy.

Our previous attempt to rescue the decreased Ca^{2+} load by PLN ablation in hopes of recovering the Ca^{2+} transient and ventricular function resulted in an exaggerated heart failure phenotype in the δ_C TG mice as described earlier in this chapter [63]. The recovered SR load accentuated the increased Ca^{2+} spark frequency and SR Ca^{2+} leak which we postulated led to downstream mitochondrial Ca^{2+} loading and increased death. It seemed rational to also test the hypothesis that inhibition of CaMKIIδ_C at the SR in the δ_C TG mice would decrease RyR2 phosphorylation and the Ca^{2+} leak. SR-AIP overexpression did in fact reduce CaMKII activation at the SR and as hypothesized, attenuated the decreased SR Ca^{2+} load and Ca^{2+} transient seen in the δ_C TG mice. Most striking was the fact that the heart failure phenotype was also worsened [47]. While several models have now shown the importance of CaMKIIδ on SR Ca^{2+} handling, we hypothesize that CaMKII activity in other parts of the cell may still be maladaptive and can contribute to the development of cardiomyopathy.

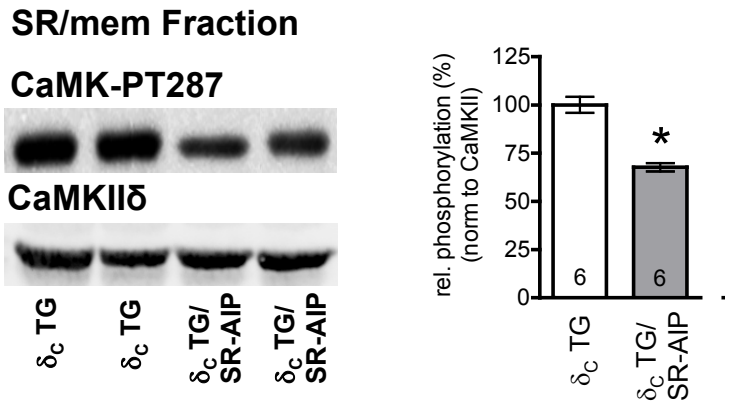

Figure 34. SR targeted AIP overexpression reduces CaMKII activation at the SR. SR/mem was isolated from ventricular tissue harvested from CaMKIIδ_C TG and CaMKIIδ_C TG/SR-AIP mice. Western blotting using P-CaMKII and CaMKIIδ antibodies show a decrease in P-CaMKII levels, and no change in CaMKIIδ expression at the SR/mem. Quantification of P-CaMKII levels (normalized to total CaMKIIδ expression) shows a significant decrease in P-CaMKII. (n=4) * $p \leq 0.05$ vs. CaMK

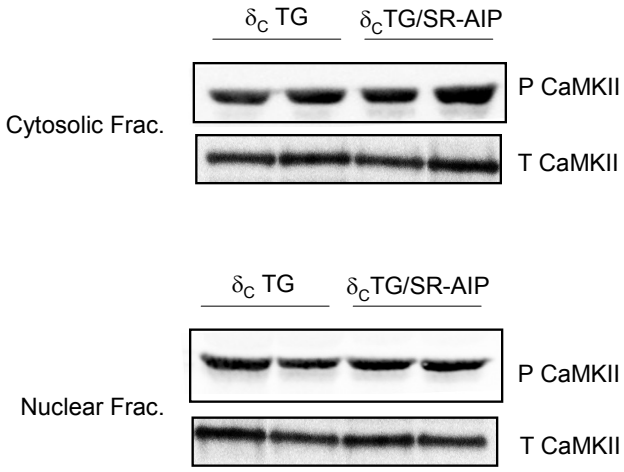

Figure 35. SR targeted AIP overexpression does not change CaMKII activation in cytosolic and nuclear fractions. Cytosolic and nuclear fractions were isolated from ventricular tissue, and western blotting for P-CaMKII and T-CaMKII shows no change in CaMKIIδ expression or activation following expression of SR-AIP in the δ_C TG mice.

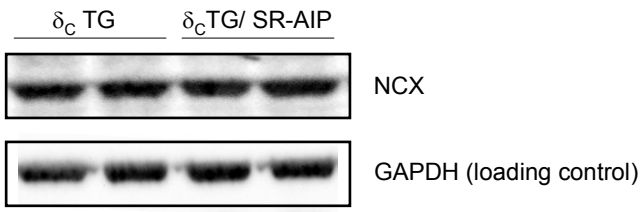

Figure 36. NCX expression is not changed following SR-AIP expression. Western blotting of ventricular homogenate from δ_C TG and δ_C TG/SR-AIP mice show no change in NCX expression. GAPDH is used as a loading control.

IV.D. Discussion

The motivation underlying the three collaborative studies presented in this chapter was to determine the mechanism by which CaMKII δ_C TG mice develop heart failure by interfering with key components of the molecular pathways on which it acts. The initial characterization of the cardiomyopathy seen in the δ_C TG mice showed increased phosphorylation of RyR2 accompanied by increased SR Ca^{2+} leak and decreased twitch Ca^{2+} transient. In order to determine whether the effects of CaMKII on SR Ca^{2+} release and concomitant store depletion were causal factors in the rapid transition of hypertrophy to heart failure, CaMKII inhibition at the SR and PLN ablation were studied in the δ_C TG mice. Neither mouse model was able to rescue the heart failure phenotype providing further insight into the complexity of CaMKII signaling.

The first attempt to rescue the δ_C TG mice focused on SR Ca^{2+} load recovery and was successful in that regard. What was not fully appreciated was the profound effect of CaMKIIδ_C mediated RyR phosphorylation in the face of a higher SR Ca^{2+} content and provided insight into CaMKII signaling effects at other sites of action, such as at the mitochondria [63]. Cyclophilin D ablation failed to correct the downstream effects of the altered Ca^{2+} handling on the mitochondria, and it was only subsequently recognized that removing a mitochondrial housekeeping function imposed significant stress and exaggerated the effects of increased CaMKII activity at the mitochondria [69]. The failure of the third strategy, aimed at blocking what we believed to be the primary target of CaMKIIδ_C (SR Ca^{2+} release), highlighted that CaMKIIδ_C is multifunctional, and inhibition of the kinase in one place may not be sufficient to affect the systemic effects of

this pleiotropic protein kinase. It also served to add a functional component to the data presented in chapter III indicating that CaMKIIδ_C is present, can be activated and functions at multiple subcellular sites.

These mouse models have provided a direct example illustrating the syngeristic balance between cellular processes and how their disruption has complex downstream effects that can not be simply reversed by addressing only one aspect of the downstream changes. The exaggerated phenotype of all of all three mouse models serves to further our understanding about the additive nature of cardiac insult, and suggests not only that increased CaMKII activation and expression have negative effects on cardiomyocyte health, but enhance sensitivity to secondary insults which can lead to severe loss of function and cell death.

IV.E. Acknowledgement

The text and figures in this chapter are, in part, a reprint of material as it appears in:

Zhang T, Guo T, Mishra S, Dalton ND, Kranias EG, Peterson KL, Bers DM, Brown JH. Phospholamban ablation rescues sarcoplasmic reticulum Ca(2+) handling but exacerbates cardiac dysfunction in CaMKIIdelta(C) transgenic mice. *Circ Res*. 2010 Feb 5;106(2):354-62.

Elrod J, Wong R, Mishra S, Vagnozzi RJ, Sakthievel, B, Karch J, Gabel S, Farber J, Force T, Brown JH, Murphy E, Molkentin JD Cyclophilin-D controls mitochondrial pore-dependent Ca^{2+} exchange, metabolic flexibility and predisposition to heart failure. *J Clin Invest*. 2010 Oct 1;120(10):3680-7

Huke S, DeSantiago J, Kaetzel MA, Mishra S, Brown JH, Dedman JR and Bers DM SR-targeted CaMKII inhibition improves SR Ca handling, but accelerates cardiac remodeling in mice overexpressing CaMKIIδ_C J Mol Cell Cardiol. 2010 Oct 21

The dissertation author was responsible for all of the experimental data presented in this chapter. Dr. Joan Heller Brown directed and supervised the research which forms the basis for this chapter.

V. Differential roles of δ_B and δ_C in cardiomyopathy *in vivo*

V.A. Abstract

Cardiac specific transgenic overexpression of CaMKIIδ_C and of CaMKIIδ_B in mice leads to distinct cardiac phenotypes. CaMKII δ_C TG mice develop hypertrophy that rapidly transitions to heart failure, and CaMKII δ_B TG mice develop chronic sustained hypertrophy. Recent *in vitro* evidence has indicated that exogenous expression of CaMKIIδ_C has a deleterious effect in the cardiomyocyte, whereas δ_B offers protection against cardiac insult. The results presented earlier indicate that both CaMKII δ subtypes are ubiquitously present at various subcellular localizations within the myocyte, and data from characterization of the distribution of endogenous CaMKIIδ subtype suggests that heteromultimerization could play a role in CaMKII distribution. Whether there are actual differences in the signaling pathways downstream of CaMKIIδ_B and δ_C has not been clearly established. In order to study the individual subtypes *in vivo*, and in a manner where only one was present at a time, we generated CaMKII δ_B and δ_C TG mice in a CaMKIIδ null background. Results presented earlier showed that the transgene is fully expressed in the null background and that its subcellular distribution is unchanged. On the other hand, we noted that the δ_C TG mouse in the δ null background (δKO/δ_CTG) appeared to be considerably more compromised. Further analysis showed increased ventricular dilation, decreased ventricular function and decreased survival. In addition, AMVMs isolated from δ_C mice in the null background appeared more susceptible to cell death induced by H_2O_2 while δ_B TG AMVMs were more resistant. We plan to further

characterize these mice to determine the extent to which the two subtypes differ from each other in their signaling properties, binding partners, and contribution to development of cardiac hypertrophy and the transition to heart failure.

V.B. Introduction

Little is currently known about the individual roles of the δ_B and δ_C subtypes *in vivo.* Initial discovery of the two subtypes indicated that they were splice variants differing only by an NLS, and it was hypothesized that due to the targeting sequence, the two subtypes would have differential localization and thus serve different functions. Over the past decade, several papers from our lab and others have demonstrated that CaMKIIδ is an integral component of the Ca^{2+} regulatory machinery of the cardiomyocyte, and our transgenic mouse models overexpressing the individual subtypes clearly demonstrate that overexpression of the two cause distinct cardiomyopathic phenotypes. There is evidence that CaMKII expression and activation is increased in human heart failure patients but whether there are differences or specificity of the individual subtype expression or activation has not been determined in any system. Recent studies using overexpression of CaMKII δ_B and δ_C in cells have begun to suggest that the two play differential roles in the cardiomyocyte.

To better understand the physiological and pathophysiological roles of the individual subtypes, the localization and activation of which was discussed in chapter III, we have begun to develop systems where we can study the individual subtypes *in vivo.* Ultimately, we plan to generate subtype specific KO mice however, as a more easily achievable approach, we crossed CaMKII δ_B and δ_C TG mice into the CaMKIIδ null

background using the CaMKIIδ KO mice recently generated in our lab [39]. Although the system is still a transgenic overexpression model, only one of the subtypes is present, and all of the endogenous CaMKIIδ is gone. Accordingly this provides a system where we can directly study how overexpression of the individual subtypes affects cell survival, protects against H_2O_2 insult, and affects phenotype.

V.C. Results

V.C.1. CaMKII δ_B is protective against H_2O_2 induced death

Adult mouse ventricular myocytes were isolated from WT, δKO, and δKO/δ_B TG and δKO/δ_C TG mice and subsequently treated with 25uM of H_2O_2 to induce cell death. Following 15 minutes of treatment, cell viability was assessed using cell morphology and trypan blue exclusion assay. The δKO myocytes, lacking both δ_B and δ_C had significantly enhanced protection compared to WT myocytes following H_2O_2 treatment. Overexpression of δ_C in the δ null background (δKO/δ_C TG) significantly decreased cell viability compared to δKO myocytes. Conversely, δKO/δ_B TG myocytes were protected against H_2O_2 induced cell death as seen by the significant increase in myocyte viability compared to both δKO and WT myocytes (Fig 37).

V.C.2. Loss of CaMKII δ_B decreases survival in CaMKII δ_C TG mice

The δ_C TG mice in the δ null background were initially generated to determine whether the distribution of the δ_C transgene was changed in the absence of endogenous δ_B. While no difference was found (Chapter III), it was immediately apparent that the δ_C

TG mice in the δ null background were sicker than the δ_C TG mice. Survival was impaired relative to δ_C TG mice, with 50% of the δKO/δ_C TG mice not able to survive past 12 weeks of age (Fig 38). There were no evident changes in survival of δKO/δ_B TG compared to WT or δ KO mice.

V.C.3. Loss of CaMKII δ_B causes exaggerated cardiac enlargement in CaMKII δ_C TG mice

To quantitatively compare the hypertrophic phenotype in δKO/δ_C TG mice versus δ_C TG mice, we determined heart weight to body weight of the mice. Initial studies were performed at 8 weeks of age, by which time hearts from δKO/δ_CTG mice were grossly enlarged (Fig 39). An earlier time point, 4 weeks of age, was chosen to better assess hypertrophy development. Compared to all other groups, CaMKII δ_C TG mice in the null background had significantly increased heart weight to body weight ratio at just 4 weeks of age suggesting rapid development of heart failure in the δKO/δ_C TG mice (Fig 39).

V.C.4. Loss of CaMKII δ_B accelerates development of ventricular dysfunction and dilation in CaMKII δ_C TG mice

The observation of exaggerated cardiac enlargement lead us to quantitatively assess cardiac function and ventricular dilation in the δKO/δ_C TG mice and compare the phenotype with the δ_C TG mice. Echocardiographic studies were performed on 5 week old mice to measure ventricular dimension and ventricular function. A significant increase in left ventricular internal diameter (LVID), indicative of ventricular dilation,

was observed in the δKO/δ_C TG mice compared to δ_C TG mice (Fig 40). Ventricular function was assessed by determining fractional shortening and demonstrated significant loss of function in the δKO/δ_C TG mice compared to δ_C TG mice (Fig 41).

V.D. Discussion

Our original characterization of CaMKII δ_B and δ_C TG mice revealed differential phenotypes [2, 3]. This, and other *in vitro* data, lead us to propose distinct signaling pathways in which CaMKII δ_C regulated Ca^{2+} handling and transcription from the cytosol, and δ_B had a transcriptional role in the nucleus. The analysis in chapter III revealed a lack of specificity in the actual distribution of δ_B and δ_C, and raised questions regarding the importance of localization of the kinase. Generation of CaMKIIδ KO mice served to underscore the important role that CaMKII δ plays in the development of heart failure without using overexpression techniques. However, the heteromultimeric structure of CaMKII poses a question of how specific the roles of the individual isoforms and subtypes are in cellular processes. The generation of the δ_B and δ_C TG mice in the δ null background afforded us an opportunity to study the effects of the individual subtypes and characterization of the phenotypes of the animals offers insight into the individual roles of the subtypes.

What is most interesting was that loss of the endogenous δ_B exacerbates the heart failure phenotype of the δ_C TG mice. Several animals models have been described above that were generated in an attempt to rescue the δ_C TG mice and involved deleting major regulatory proteins or overexpressing inhibitors. While these models proved to be

valuable tools in understanding how δ_C contributes to heart failure, it was extremely fascinating to find that deletion of endogenous δ_B could also exacerbate the heart failure phenotype. Our results provide promising evidence that δ_B does in fact play a protective role in heart failure development, and characterization of the δKO/δ_B TG mice following stress or cardiac insult will help determine whether loss of δ_C and overexpression of the δ_B offers protection.

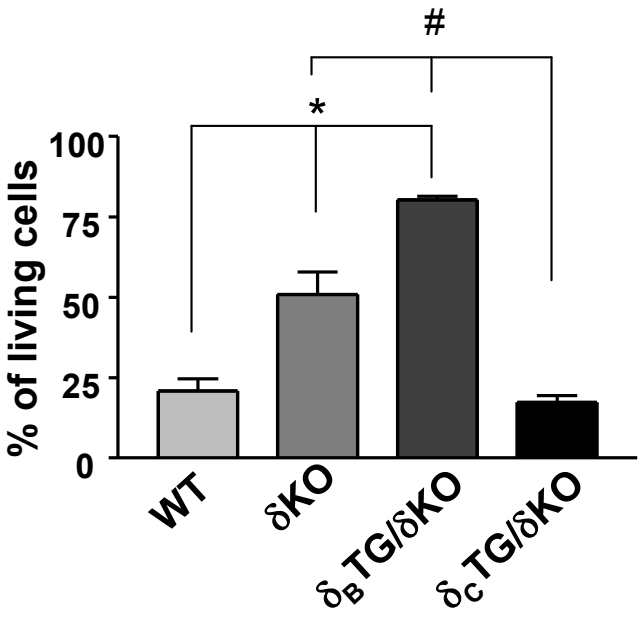

Figure 37. Survival of AMVMs is differentially affected by CaMKII δ_B and δ_C overexpression. AMVMs were isolated from WT, δKO, δ_BTG/δKO and δ_CTG/δKO mice and treated with H_2O_2 [25mM] for 30 minutes; myocyte survival was assessed using morphological changes and trypan blue staining. (n=8) * $p<0.01$ vs. WT # $p<0.01$ vs. δKO

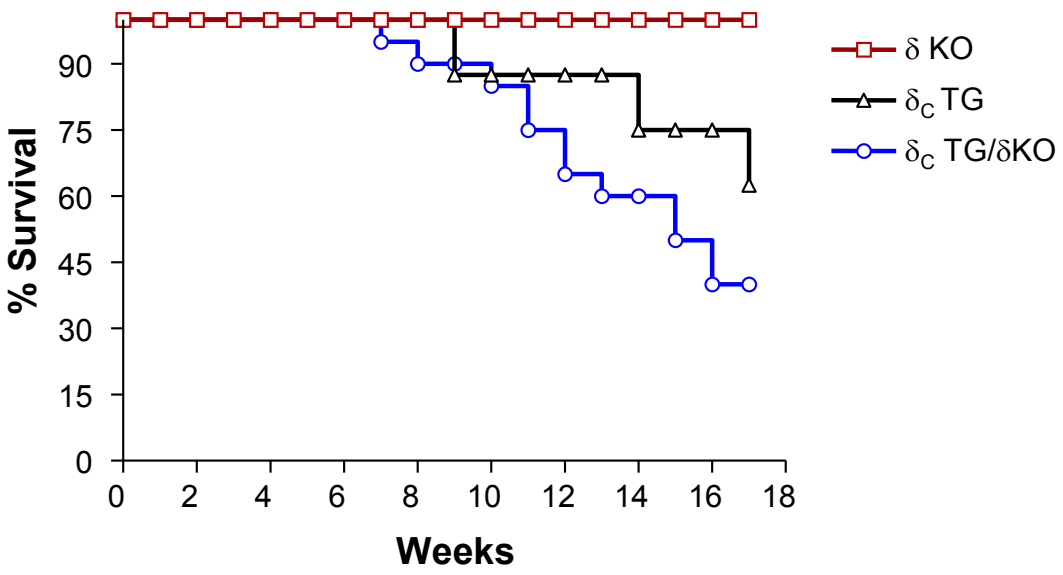

Figure 38. Ablation of endogenous CaMKIIδ leads to decreased survival of δ_C TG mice. Survival curves for CaMKII δ KO, δ_C TG and CaMKII δ_C TG in the CaMKII δ null background (δ_C TG/δKO). Loss of endogenous CaMKII δ_B accentuates premature death in CaMKII δ_C TG mice. (n=16 per group)

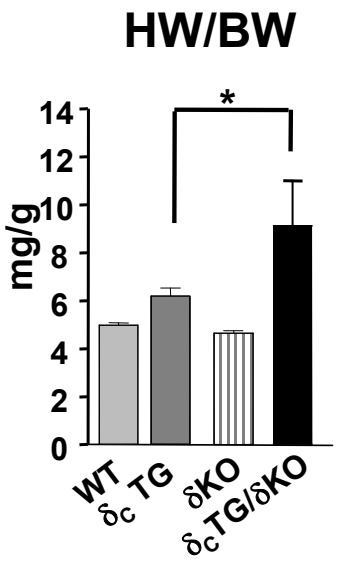

Figure 39. δ_CTG/δKO mice exhibit a significant increase in cardiac enlargement compared to the δ_C TG mice. Heart weight to body weight measurements were taken from WT, δ_C TG, δKO, δ_C TG/δKO. There was a significant increase in HW/BW in the δ_C TG mice in the δ null background compared to δ_CTG mice. (n=6) * $p<0.01$

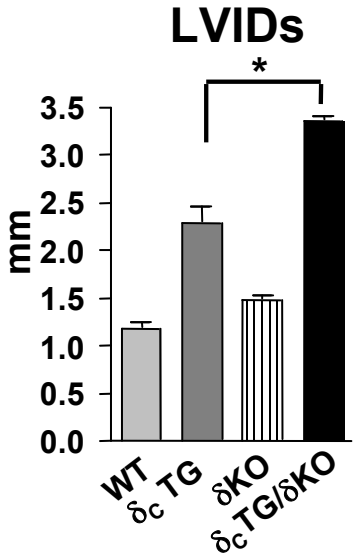

Figure 40. δ_CTG/δKO mice exhibit increased ventricular dilation compared to the δ_C TG mice Echocardiographic analysis of 5 week old mice revealed a significant increase in chamber dimension in the δ_C TG mice in the δ null background compared to δ_C TG mice. (n=6) *$p<0.01$ vs δ_C TG

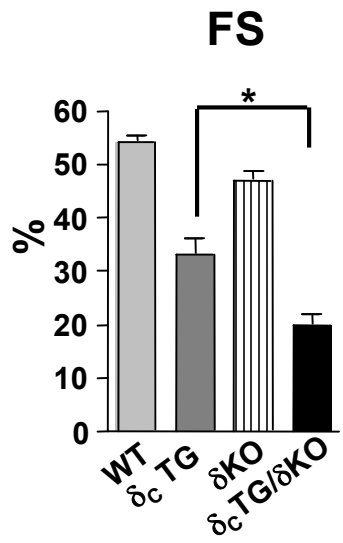

Figure 41. δ_CTG/δKO mice exhibit decreased ventricular function compared to the δ_C TG mice Echocardiographic analysis showed significant reduction in ventricular function in the δ_C TG mice in the null background compared to δ_C TG mice at 5.5 weeks of age. (n=6) *$p<0.01$ vs δ_CTG

VI. Conclusions and future directions

Since the initial 1994 discovery by Howard Schulman's laboratory that CaMKIIδ is the predominant CaMKII isoform in mouse and human heart, and that it is expressed as either of two splice variants, δ_B and δ_C, considerable progress has been made towards understanding the physiologic function of this Ca^{2+} sensitive kinase [11, 41]. Our lab and others have established that CaMKIIδ signaling leads to altered Ca^{2+} handling and cardiac hypertrophic gene expression [1]. Our studies using NRVMs reported that overexpression of δ_B induces ANF expression and other signs of hypertrophy whereas expression of δ_C has no effect on ANF [35]. We also showed that co-expression of δ_C reduced the amount δ_B present in the nucleus, thereby preventing the occurrence of hypertrophic responses following δ_B overexpression [35].

More important insights into the role of CaMKIIδ were achieved by studying its role *in vivo*. Increased activation and expression of the kinase was observed following pressure overload. Furthermore, evident cardiac phenotypes resulted from cardiac specific overexpression of CaMKII δ_B and δ_C, indicating that CaMKIIδ activation was sufficient to induce development of hypertrophy and heart failure. Most recently our laboratory showed that deletion of CaMKII protected against the transition from hypertrophy to heart failure following pressure overload suggesting that CaMKIIδ plays a critical role in the development of heart failure.

Prior to the studies presented in this dissertation, there was very little information regarding the individual roles of the CaMKII δ_B and δ_C subtypes. Early in the course of

my research I contributed to the studies which demonstrated that both δ_B and δ_C could regulate activation of the hypertrophic transcription factor MEF2. My subsequent studies have been aimed at understanding the differential roles of these individual subtypes, and elucidating the mechanism by which CaMKIIδ_C activity promotes development of heart failure.

The studies in this dissertation are the first to show that endogenous CaMKIIδ_B and δ_C, which were widely considered to be differentially localized, are in fact both present throughout the cell, as assessed by subcellular fractionation. The transgenically overexpressed subtypes recapitulate the distribution profile of endogenous CaMKII, and deletion of endogenous CaMKIIδ_B and δ_C does not affect the distribution of overexpressed CaMKIIδ_B or δ_C.

Generation of the transgenic mice lacking endogenous CaMKIIδ provided us with a system to characterize activation of individual subtypes. Using stimuli that mobilized Ca^{2+} from different stores within the cell (caffeine and phenylephrine), we show for the first time that the location of CaMKII relative to the site of Ca^{2+} release rather than subtype determines its activation. The functional relevance of activation at particular sites was illustrated by increased phosphorylation of SR target phospholamban, following SR Ca^{2+} release, with no change in phosphorylation of the nuclear target HDAC5; conversely, increased phosphorylation of HDAC5 resulted from nuclear Ca^{2+} increases, with no effect on the SR localized CaMKII target.

Although CaMKIIδ_B and δ_C are encoded by the same gene, differential regulation of expression of the two subtypes has been suggested in an *in vitro* system [43]. We showed

that CaMKIIδ is present throughout the cell, however, we also indicated that δ_B is the predominant nuclear subtype and that δ_C is the predominant SR subtype. While the CaMKII multimer composition is not well understood and could include varying amounts of δ_B and δ_C subunits, studies have shown that increasing δ_C in the presence of δ_B decreases the presence of nuclear CaMKIIδ [35]. If expression of one subtype were to increase while the other remained the same or was reduced, this could potentially result in redistribution of the enzyme, disrupting normal cellular processes, but could also exaggerate effects of CaMKII at particular subcellular compartments, as seen with increased CaMKIIδ expression at the SR in δ_C TG mice and the subsequent disruption in SR Ca^{2+} handling.

An important question that has emerged is why differential phenotypes were observed in the δ_B and δ_C TG mice. Whether the two subtypes interact with different binding partners is a possibility that might contribute to the observed phenotypic differences. The δKO/δTG mice used in the localization and activation study also provided us with a system where we could study the individual effects of the subtypes *in vivo*. Characterization of the δKO/δTG mouse models is the first *in vivo* evidence that CaMKIIδ_B may have protective effects against heart failure development as shown by the rapid development of heart failure in the δ_C TG mice in the δ null background.

Further studies and experiments using the mouse models developed in this thesis will allow us to study δ_B and δ_C binding partners, and we have begun to study this by making use of the HA tag on the transgene to extract the overexpressed protein and study other proteins associating with CaMKII. Preliminary analysis of differences in gene

transcription between the δ_B TG and δ_C TG mice was carried out using affymetrix microarray screening. Remarkably, results show minimal overlap between identified transcriptional targets of δ_B vs. δ_C, and will require extensive analysis in the future.

While beyond the scope of this thesis, my contribution in generating and performing the initial studies characterizing the phenotypes of the CaMKIIδ_B and δ_C TG mice in the δ null background will serve as the foundation for future experiments and will help us to understand how δ_B and δ_C differentially function in the cardiomyocyte. Finally, to extrapolate from the animal models of heart failure studied in this dissertation, it will be of considerable interest to examine changes in CaMKIIδ subtype expression, localization and activity in human heart failure patients.

As a final point, in the pursuit of CaMKII as a therapeutic target for the treatment of heart failure, much more remains to be understood about CaMKIIδ signaling in the heart. The matter of whether it is truly the location of the enzyme that governs its function is critical to developing drugs that can target CaMKII at specific cellular compartments without altering others, especially if enzyme action at some locations is deleterious while that at others is protective in nature. The studies presented in the second half of the thesis provide us with examples of the multidimensional nature of cardiac signaling processes involving CaMKIIδ. The regulatory mechanisms involved in Ca^{2+} handling within the cardiomyocyte are closely regulated, and targeting one specific aspect, such as SR Ca^{2+} load recovery, does not appear to be a viable approach to treating cardiomyopathy induced by CaMKIIδ_C upregulation. [63] Lastly, if CaMKII δ_B and δ_C have opposing roles and differentially signal within the cardiomyocyte, global CaMKIIδ

inhibition as a therapeutic approach may actually be deleterious. Identification of whether there are δ_B and δ_C specific signaling pathways and inhibition of the individual subtypes, or if that is not feasible, inhibition of targets specific to the individual subtypes is paramount to considering CaMKIIδ as a potential treatment of heart failure.

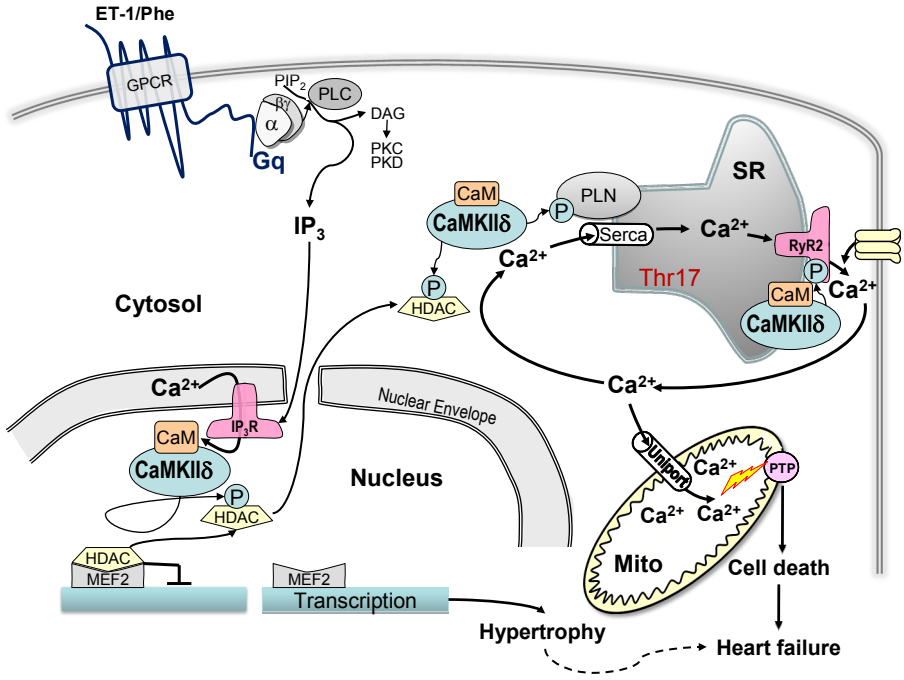

Figure 42. CaMKIIδ localization, activation and function. CaMKIIδ_B and δ_C have non-selective subcellular distribution, and subtype localization governs activation. Mechanistic studies suggest a potential role for CaMKII at the mitochondria that may be contributing to the deleterious phenotype observed in the δ_C TG mice.

Appendix I. *In vitro* subcellular distribution of overexpressed CaMKII δ_B and δ_C

In order to study CaMKII distribution in a system where CaMKIIδ_B and δ_C could be overexpressed either individually or simultaneously, and at different levels of expression, NRVMs were infected with CaMKII δ_B and δ_C adenovirus. Following infection, cells were harvested at varying time points (6 hours, 24 hours and 48 hours) to study protein distribution in an expression-dependent manner. A protocol to fractionate cardiomyocytes was developed which separates the cells into two fractions: the cytosolic and nuclear (Fig A1). Due to the lower protein level of cell lysates compared to whole heart tissue, mitochondrial and SR/mem fractions were not made using this protocol.

Consistent with our *in vivo* subcellular fractionation results, overexpressed CaMKII δ_C was predominantly located in the cytosolic compartment, but a significant fraction of the protein was found in the nuclear fraction. The presence of CaMKII δ_C in the nucleus did not appear to be a result of overloading of the system, demonstrated by the δ_C presence in the nuclei at lower expression levels (earlier times) (Fig A2). Results from CaMKII δ_B overexpression were also similar to our transgenic animal experiments, with δ_B present in both the cytosolic and nuclear fractions, seen at all timepoints (Fig A3).

Although a useful tool for studying nuclear protein levels, the cytosolic fraction in this protocol was dilute and mitochondria and SR were not able to be extracted using this preparation. The protocols used within the thesis were developed following development and optimization of this protocol.

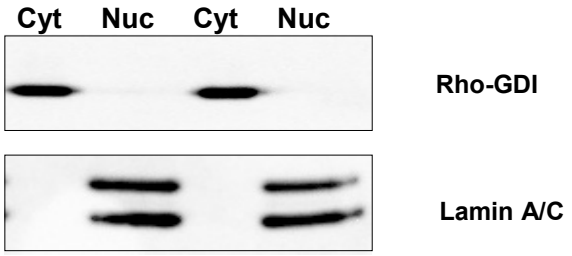

Figure A1. Purity of subcellular fractionation of NRVMs. Western blotting for Rho-GDI in cytosol and Lamin A/C in nucleus shows little contamination of the two compartments.

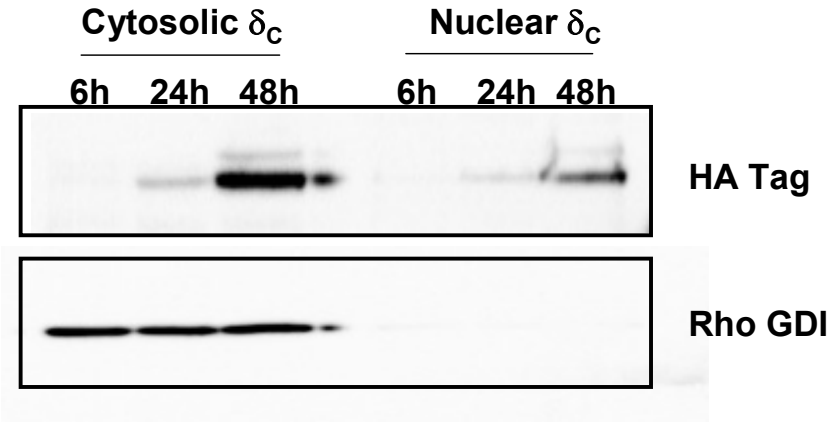

Figure A2. CaMKIIδ_C is present in the nucleus following *in vitro* overexpression. NRVMs were infected with CaMKII δ_C adenovirus, and fractionated into cytosolic and nuclear compartments. Western blotting for HA-tagged protein, indicative of overexpressed CaMKIIδ_C, and cellular marker Rho-GDI show purity of fraction are shown.

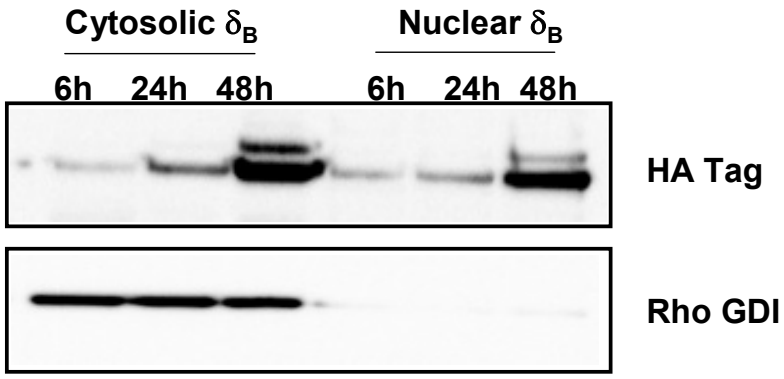

Figure A3. CaMKIIδ_B is present in the cytosol following *in vitro* overexpression. NRVMs were infected with CaMKII δ_B adenovirus, and fractionated into cytosolic and nuclear compartments. Western blotting for HA-tagged protein, indicative of overexpressed CaMKIIδ_B, and cellular marker Rho-GDI show purity of fraction are shown.

Appendix II. CaMKII kinase activity reporter (CAMKAR)

Signal transduction pathways involving kinases are modulated by the level of phosphorylation of a target, as well as the length of the phosphorylation state. The location within the cell of the site of phosphorylation is also a critical piece of information in learning about how kinases function within living cells.

Ca^{2+} is necessary for the activation of CaMKII δ but the signals and source of Ca^{2+} that activate the individual CaMKII isoforms are not known. The differential location and function of CaMKII δ_C and CaMKII δ_B, suggests different mechanisms of activation. A tool that can be used to study all of the spatial and temporal dynamics of kinase activity is a genetically encoded fluorescent kinase activity reporter (KAR) [113]. A series of kinase specific KARs have been generated, included ones for PKA [113], PKC [114], PKD [115] and PKB [116]. These reporters consist of a pair of fluorescent proteins fused together with a phosphoamino acid binding domain and a substrate sequence specific to the kinase of interest attached by a flexible linker [113].

Phosphorylation of the reporter's substrate sequence by the protein of interest causes the phosphoamino acid binding domain to bind the phosphate group, changing the conformation of the reporter and altering the spatial proximity of the fluorophores allowing for realtime imaging of kinase activity. This causes a change in the fluorescence resonance energy transfer (FRET) between the two fluorophores, which can be measured via fluorescent imaging techniques and allows the visualization of kinase activity in live cells.

Development of the CaMKIIδ Activity Reporter (CaMKAR) construct has been ongoing. A substrate sequence highly specific to CaMKII δ activity was generated by Dr. Ben Turk at Yale, using a phosphopeptide binding array assay (Fig A4) and considering other kinase consensus sequences similar to CaMKII (Fig A5). In collaboration with the Alexandra Newton's lab and Jin Zhang's lab at the Johns Hopkins University, we constructed a reporter using the AKAR2 backbone [117] (Fig A6).

An initial *in vitro* spectral scan of the reporter showed presence of both peaks at the appropriate excitation wavelength indicating that both fluorophores were present and excitable (Fig A7). Scans were taken in the presence of ATP, CaM and Ca^{2+} added consecutively, however although the curve was shifted (most likely due to changes in molarity following addition or stimuli), most important was that no change in FRET ratio was observed. Following this experiment, a spectral scan was performed in intact cells, either in the presence or absence of Ca^{2+}, and in intact vs. permeabilized cells (Fig A8), and no change in FRET ratio was detected.

Although the initial experiments were not successful in detecting CaMKII activity, we performed a series of experiments using a variety of experimental conditions to ensure that CaMKII was present along with CaMKAR. To do this, cardiomyocytes expressing CaMKAR with or without adenoviral overexpression of WT CaMKII were used. Intact cells were harvested and an initial control measurement was taken over the time course to be used for subsequent experiments to account for any decreases in fluorescence. A series of experiments were then performed with and without ATP, and following addition of Ca^{2+} and then CaM or CaM and then Ca^{2+}. Each addition was consecutive, and after each addition, a measurement was taken and represented by a time

point in the graphs in an effort to determine whether we could elicit a response from our reporter. (Fig A9). We were unable to elicit and measure a change in FRET and hypothesized that basal phosphorylation of the construct may be the reason as to why we were unable to measure any kinase activity. Pretreatment with KN-93 did not change CaMKAR activity in the absence or presence of Ca^{2+}, suggesting that the phosphorylation state of the CaMKAR construct at basal conditions was not CaMKII dependent. Most interesting was that following treatment with kinase inhibitor staurosporine, a decrease in FRET ratio was observed, suggesting that the reporter is activated by kinases other than CaMKII, and therefore unable to sense changes in CaMKII activity (Fig A10).

The most probable explanation of the inability to elicit a response from this reporter is the lack of specificity of the substrate sequence to CaMKII resulting in non-specific phosphorylation and activation of the reporter, rendering it unable to sense CaMKII activity.

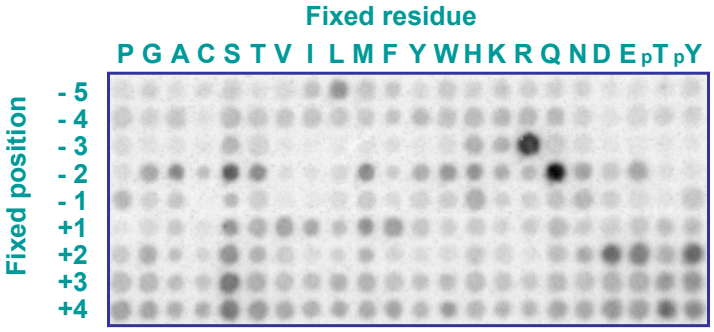

Figure A4.CaMKII phosphorylation motif. A positional scanning peptide library consisting of 198 distinct peptide mixtures was used to determine the ideal phosphorylation motif for CaMKII. Each condition contains one of the 20 naturally occurring proteogenic amino acids fixed at each of 9 positions surrounding a central serine/threonine residue, with the remaining positions degenerate The entire set of peptide mixtures was phosphorylated with radiolabeled ATP in parallel reactions by CaMKII and then quantified as shown above. (Courtesy of Ben Turk, Yale University)

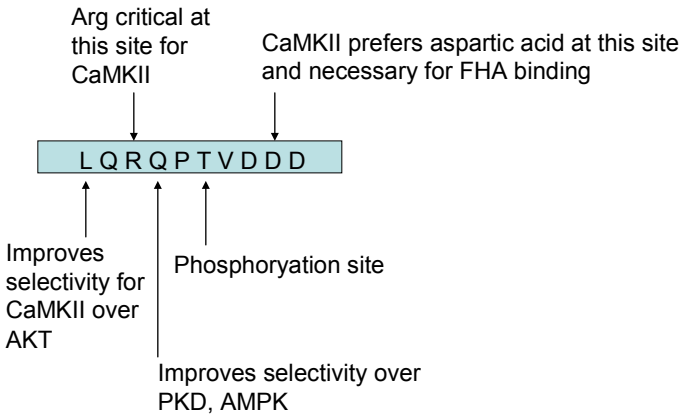

Figure A5. CaMKAR substrate sequence. Analysis of the phosphopeptide binding assay identified ideal residues for each position, and along with the results, particular residues were chosen that would increase specificity of the consensus sequence to CaMKII.

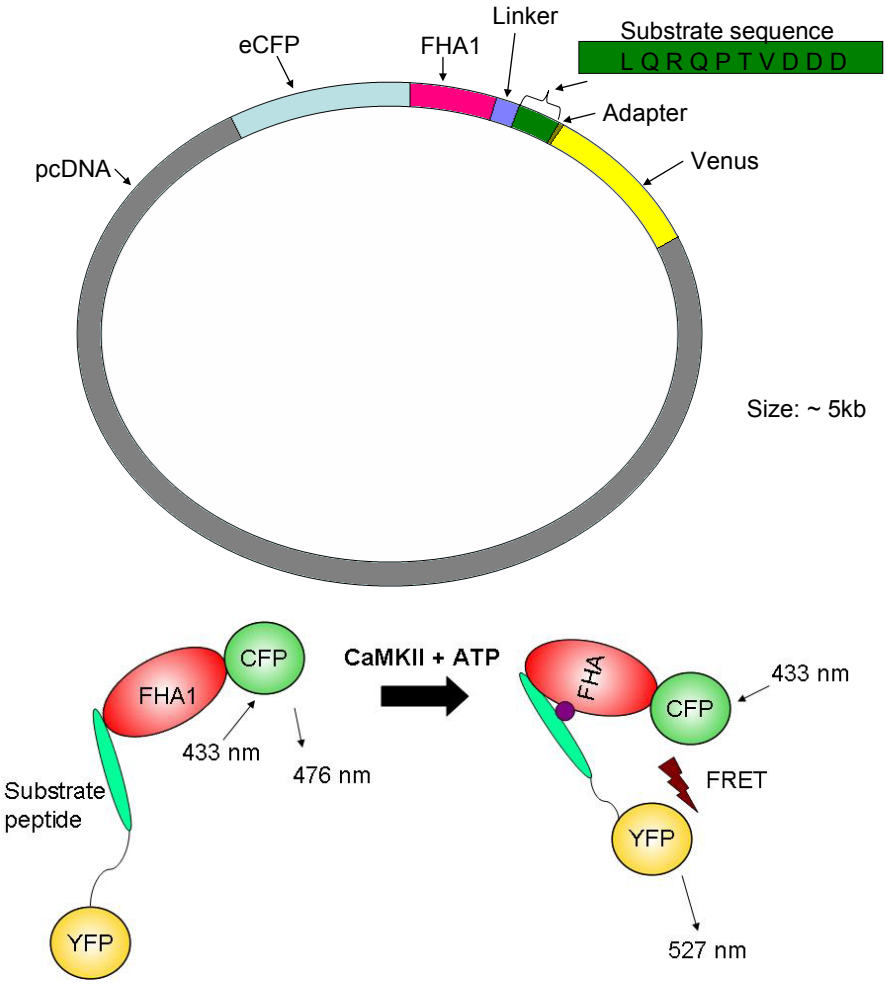

Figure A6. CaMKAR construct. Schematic illustration of the CaMKII construct plasmid, and pictoral illustration of CaMKAR function. FRET fluorophore pair CFP and eYFP (venus) were used along with phosphopeptide binding domain FHA1, and the newly generated substrate sequence. A decrease in observed FRET ratio of the reporter will indicate phosphorylation of the substrate sequence, reflecting CaMKII δ activity.

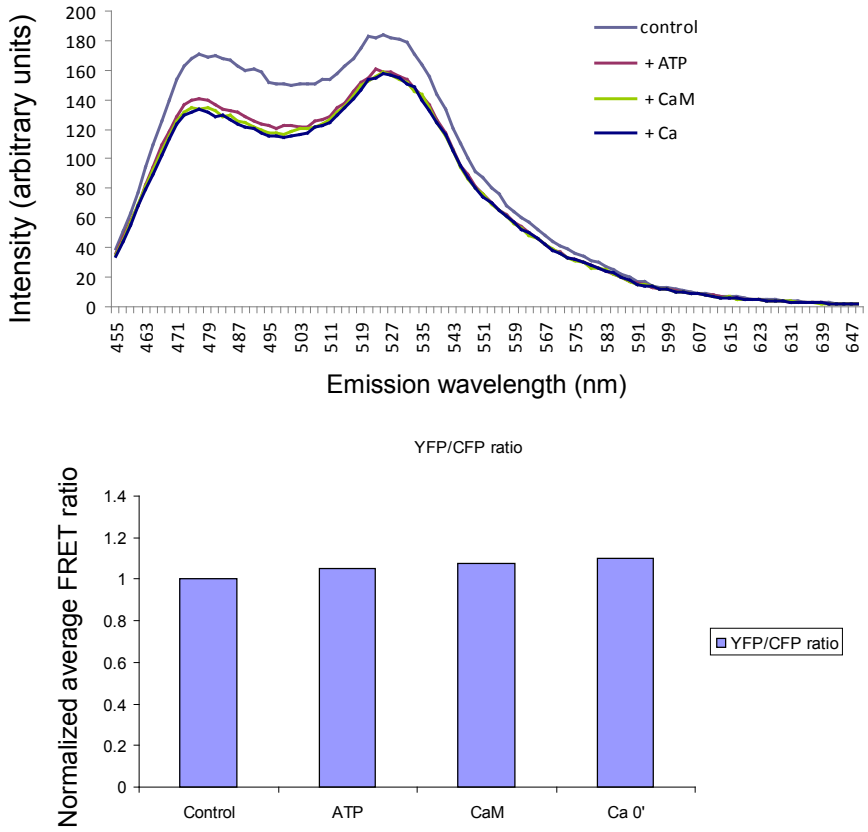

Figure A7. ***In vitro*** **spectral scan of CaMKAR in lysed cells.** Cos cells were transfected with the CaMKAR reporter, lysed, and then excitation/emission was measured. Measurements were taken following addition of ATP, Calmodulin and Ca and did not change the YFP/CFP ratio of the construct.

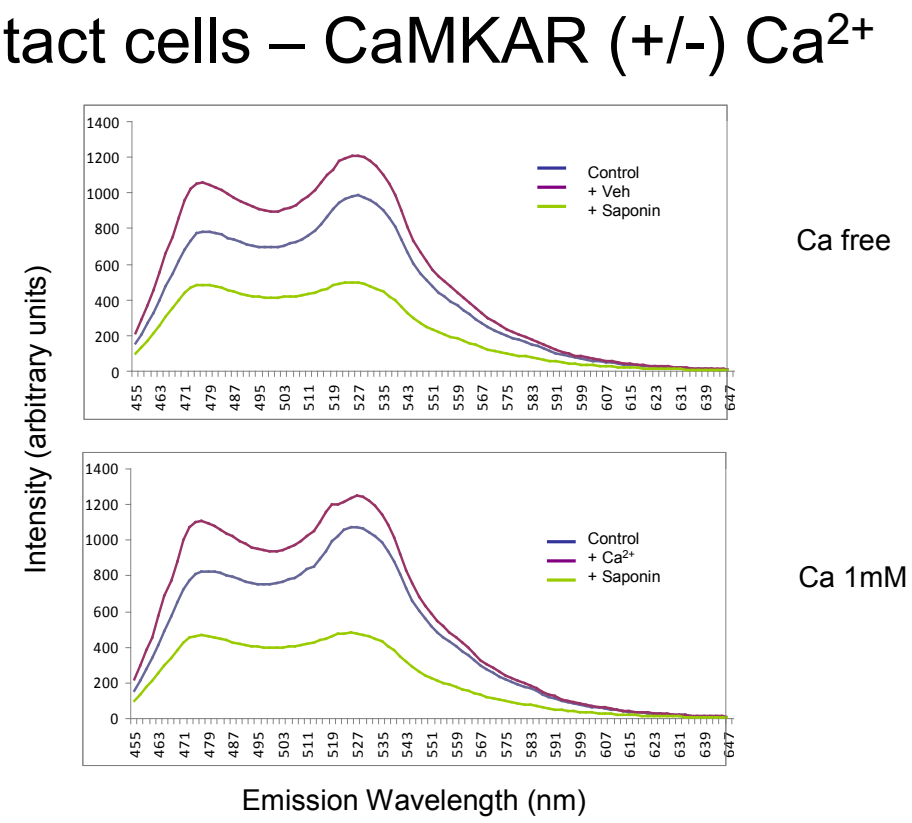

Figure A8. ***In vitro*** **spectral scan of CaMKAR in intact cells.** Spectral excitation/emission measurements were performed in intact Cos cells at baseline and following permeabilization with saponin. Measurements were taken in the presence and absence of 1mM Ca^{2+}.

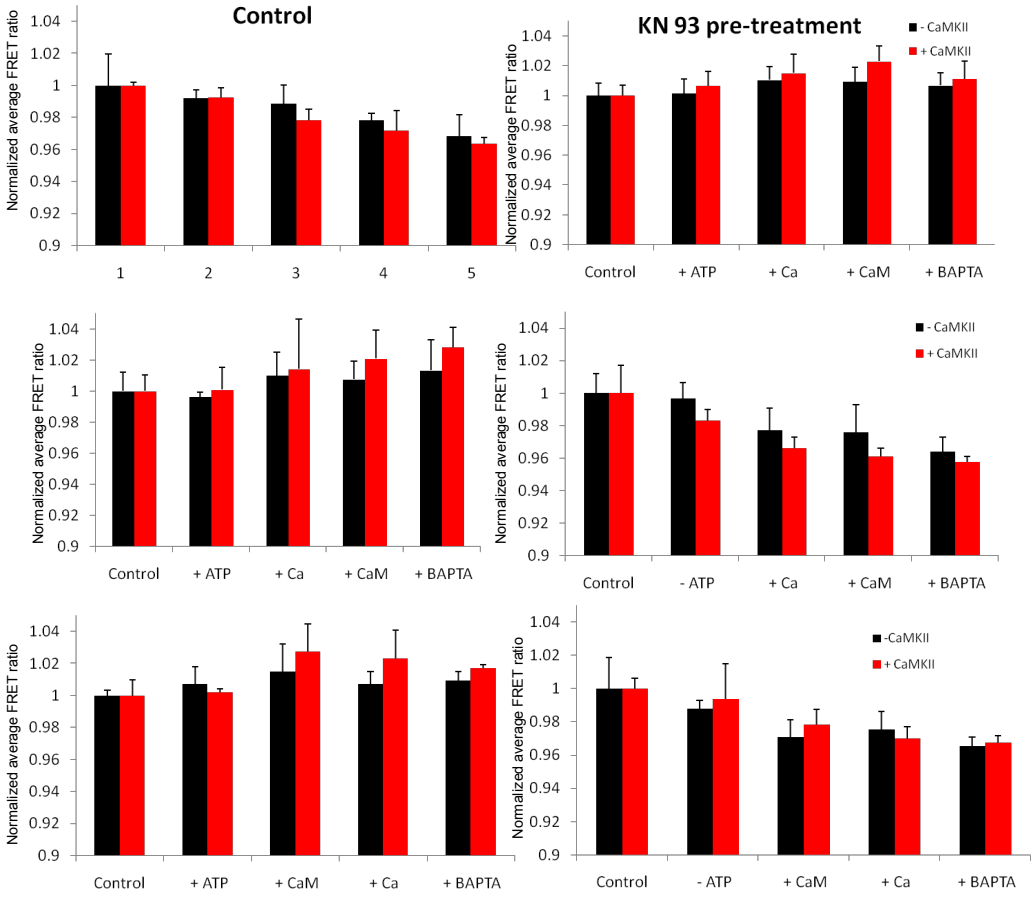

Figure A9. CaMKAR activation studies. In order to determine whether CaMKAR responded to CaMKII activity, cells with and without adenoviral CaMKII were used (Black and red bars). Cells were lysed and then control readings were made to determine bleaching, and then FRET ratio was measured following addition of ATP, Ca^{2+}, CaM, and BAPTA in several different addition orders. Measurements were also taken in the presence of CaMKII inhibitor KN-93.

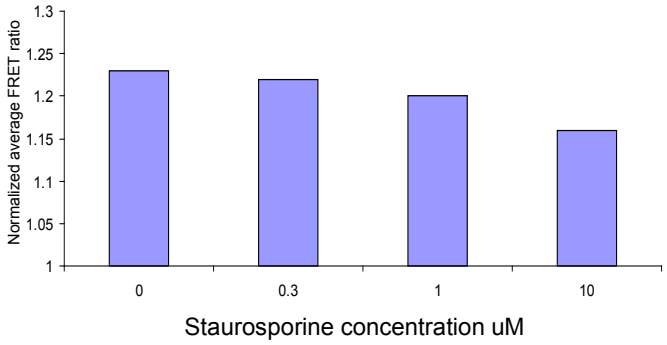

Figure A10. Kinase and phosphatase inhibitor effect on CaMKAR. Cos cells overexpressing CaMKAR were lysed and FRET ratio was measured following addition of kinase inhibitor staurosporine.

Reference List

(1) Zhang T, Brown JH. Role of Ca2+/calmodulin-dependent protein kinase II in cardiac hypertrophy and heart failure. *Cardiovasc Res* 2004 August 15;63(3):476-86.

(2) Zhang T, Maier LS, Dalton ND, Miyamoto S, Ross JJr, Bers DM, Brown JH. The δ_C isoform of CaMKII is activated in cardiac hypertrophy and induces dilated cardiomyopathy and heart failure. *Circ Res* 2003;92:912-9.

(3) Zhang T, Johnson EN, Gu Y, Morissette MR, Sah VP, Gigena MS, Belke DD, Dillmann WH, Rogers TB, Schulman H, Ross J, Jr., Brown JH. The cardiac-specific nuclear δ_B isoform of Ca^{2+}/calmodulin-dependent protein kinase II induces hypertrophy and dilated cardiomyopathy associated with increased protein phosphatase 2A activity. *J Biol Chem* 2002;277:1261-7.

(4) Frey N, Olson EN. Cardiac hypertrophy: the good, the bad, and the ugly. *Annu Rev Physiol* 2003;65:45-79.

(5) Heineke J, Molkentin JD. Regulation of cardiac hypertrophy by intracellular signalling pathways. *Nat Rev Mol Cell Biol* 2006 August;7(8):589-600.

(6) Olivetti G, Abbi R, Quaini F, Kajstura J, Cheng W, Nitahara JA, Di Loreto C, Beltrami CA, Krajewski S, Reed JC, Anversa P. Apoptosis in the failing human heart. *N Engl J Med* 1997;336:1131-41.

(7) Maier LS, Bers DM. Calcium, calmodulin, and calcium-calmodulin kinase II: heartbeat to heartbeat and beyond. *J Mol Cell Cardiol* 2002;34:919-39.

(8) Maier LS, Bers DM, Brown JH. Calmodulin and Ca2+/calmodulin kinases in the heart - physiology and pathophysiology. *Cardiovasc Res* 2007 March 1;73(4):629-30.

(9) Atar D, Backx PH, Appel MM, Gao WD, Marban E. Excitation-transcription coupling mediated by zinc influx through voltage-dependent calcium channels. *J Biol Chem* 1995 February 10;270(6):2473-7.

(10) Braun AP, Schulman H. The multifunctional calcium/calmodulin-dependent protein kinase: from form to function. *Annu Rev Physiol* 1995;57:417-45.

(11) Edman CF, Schulman H. Identification and characterization of δ_B-CaM kinase and δ_C-CaM kinase from rat heart, two new multifunctional Ca^{2+}/calmodulin-dependent protein kinase isoforms. *Biochim Biophys Acta* 1994;1221:89-101.

(12) Baltas LG, Karczewski P, Krause E-G. The cardiac sarcoplasmic reticulum phospholamban kinase is a distinct δ-CaM kinase isozyme. *FEBS Lett* 1995;373:71-5.

(13) Mayer P, Mohlig M, Idlibe D, Pfeiffer A. Novel and uncommon isoforms of the calcium sensing enzyme calcium/calmodulin dependent protein kinase II in heart tissue. *Basic Res in Cardiol* 1995;90:372-9.

(14) Schworer CM, Rothblum LI, Thekkumkara TJ, Singer HA. Identification of novel isoforms of the δ subunit of Ca^{2+}/calmodulin-dependent protein kinase II. *J Biol Chem* 1993;268:14443-9.

(15) Hudmon A, Schulman H. Structure-function of the multifunctional Ca^{2+}/calmodulin-dependent protein kinase II. *Biochem J* 2002 June 15;364(Pt 3):593-611.

(16) Erickson JR, Joiner ML, Guan X, Kutschke W, Yang J, Oddis CV, Bartlett RK, Lowe JS, O'Donnell SE, ykin-Burns N, Zimmerman MC, Zimmerman K, Ham AJ, Weiss RM, Spitz DR, Shea MA, Colbran RJ, Mohler PJ, Anderson ME. A dynamic pathway for calcium-independent activation of CaMKII by methionine oxidation. *Cell* 2008 May 2;133(3):462-74.

(17) Dzhura I, Wu Y, Colbran RJ, Balser JR, Anderson ME. Calmodulin kinase determines calcium-dependent facilitation of L-type calcium channels. *Nat Cell Biol* 2000;2:173-7.

(18) Witcher DR, Kovacs RJ, Schulman H, Cefali DC, Jones LR. Unique phosphorylation site on the cardiac ryanodine receptor regulates calcium channel activity. *J Biol Chem* 1991;266:11144-52.

(19) Hain J, Onoue H, Mayrleitner M, Fleischer S, Schindler H. Phosphorylation modulates the function of the calcium release channel of sarcoplasmic reticulum from cardiac muscle. *J Biol Chem* 1995 February 3;270(5):2074-81.

(20) Xu A, Hawkins C, Narayanan N. Phosphorylation and activation of the Ca^{2+}-pumping ATPase of cardiac sarcoplasmic reticulum by Ca^{2+}/calmodulin-dependent protein kinase. *J Biol Chem* 1993;268:8394-7.

(21) Toyofuku T, Curotto KK, Narayanan N, MacLennan DH. Identification of Ser38 as the site in cardiac sarcoplasmic reticulum Ca^{2+}-ATPase that is phosphorylated by Ca^{2+}/calmodulin-dependent protein kinase. *J Biol Chem* 1994 October 21;269(42):26492-6.

(22) LePeuch C, Haiech J, Demaille JG. Concerted regulation of cardiac sarcoplasmic reticulum calcium transport by cyclic adenosine monophosphate-dependent and calcium-calmodulin-dependent phosphorylations. *Biochem* 1979;18:5150-7.

(23) Simmerman HK, Collins JH, Theibert JL, Wegener AD, Jones LR. Sequence analysis of phospholamban. Identification of phosphorylation sites and two major structural domains. *J Biol Chem* 1986 October 5;261(28):13333-41.

(24) Lu J, McKinsey TA, Nicol RL, Olson EN. Signal-dependent activation of the MEF2 transcription factor by dissociation from histone deacetylases. *Proc Natl Acad Sci USA* 2000;97:4070-5.

(25) McKinsey TA, Zhang CL, Olson EN. Activation of the myocyte enhancer factor-2 transcription factor by calcium/calmodulim-dependent protein kinase-stimulated binding of 14-3-3 to histone deacetylase 5. *Proc Natl Acad Sci USA* 2000;97:14400-5.

(26) Huang W, Ghisletti S, Perissi V, Rosenfeld MG, Glass CK. Transcriptional integration of TLR2 and TLR4 signaling at the NCoR derepression checkpoint. *Mol Cell* 2009 July 10;35(1):48-57.

(27) Mani SK, Egan EA, Addy BK, Grimm M, Kasiganesan H, Thiyagarajan T, Renaud L, Brown JH, Kern CB, Menick DR. beta-Adrenergic receptor stimulated Ncx1 upregulation is mediated via a CaMKII/AP-1 signaling pathway in adult cardiomyocytes. *J Mol Cell Cardiol* 2009 November 27;48(2):342-51.

(28) Lu YM, Shioda N, Yamamoto Y, Han F, Fukunaga K. Transcriptional upregulation of calcineurin Abeta by endothelin-1 is partially mediated by calcium/calmodulin-dependent protein kinase IIdelta3 in rat cardiomyocytes. *Biochim Biophys Acta* 2010 May;1799(5-6):429-41.

(29) Luo W, Grupp IL, Harrer J, Ponniah S, Grupp G, Duffy JJ, Doetschman T, Kranias EG. Targeted ablation of the phospholamban gene is associated with markedly enhanced myocardial contractility and loss of beta-agonist stimulation. *Circ Res* 1994 September;75(3):401-9.

(30) Maier LS, Zhang T, Chen L, DeSantiago J, Brown JH, Bers DM. Transgenic CaMKIIδ_C overexpression uniquely alters cardiac myocyte Ca^{2+} handling: reduced SR Ca^{2+} load and activated SR Ca^{2+} release. *Circ Res* 2003;92:904-11.

(31) Brown JH, Trilivas I, Martinson EA. Muscarinic receptor regulation of protein kinase C distribution and phosphatidylcholine hydrolysis. *Symp Soc Exp Biol* 1990;44:147-56.

(32) Colomer JM, Mao L, Rockman HA, Means AR. Pressure overload selectively up-regulates Ca^{2+}/calmodulin-dependent protein kinase II in vivo. *Mol Endocrinol* 2003;17:183-92.

(33) Saito T, Fukuzawa J, Osaki J, Sakuragi H, Yao N, Haneda T, Fujino T, Wakamiya N, Kikuchi K, Hasebe N. Roles of calcineurin and

calcium/calmodulin-dependent protein kinase II in pressure overload-induced cardiac hypertrophy. *J Mol Cell Cardiol* 2003 September;35(9):1153-60.

(34) Sei CA, Irons CE, Sprenkle AB, McDonough PM, Brown JH, Glembotski CC. α-Adrenergic stimulation of atrial natriuretic factor expression in cardiac myocytes requires calcium influx, protein kinase C and calmodulin-regulated pathways. *J Biol Chem* 1991;266:15910-6.

(35) Ramirez MT, Zhao X, Schulman H, Brown JH. The nuclear δ_B isoform of Ca^{2+}/calmodulin-dependent protein kinase II regulates atrial natriuretic factor gene expression in ventricular myocytes. *J Biol Chem* 1997;272:31203-8.

(36) Kato T, Sano M, Miyoshi S, Sato T, Hakuno D, Ishida H, Kinoshita-Nakazawa H, Fukuda K, Ogawa S. Calmodulin kinases II and IV and calcineurin are involved in leukemia inhibitory factor-induced cardiac hypertrophy in rats. *Circ Res* 2000 November 10;87(10):937-45.

(37) Zhu W, Zou Y, Shiojima I, Kudoh S, Aikawa R, Hayashi D, Mizukami M, Toko H, Shibasaki F, Yazaki Y, Nagai R, Komuro I. Ca^{2+}/calmodulin-dependent kinase II and calcineurin play critical roles in endothelin-1-induces cardiomyocyte hypertrophy. *J Biol Chem* 2000;275:15239-45.

(38) Zhang T, Kohlhaas M, Backs J, Mishra S, Phillips W, Dybkova N, Chang S, Ling H, Bers DM, Maier LS, Olson EN, Brown JH. CaMKIIdelta isoforms differentially affect calcium handling but similarly regulate HDAC/MEF2 transcriptional responses. *J Biol Chem* 2007 November 30;282(48):35078-87.

(39) Ling H, Zhang T, Pereira L, Means CK, Cheng H, Gu Y, Dalton ND, Peterson KL, Chen J, Bers D, Heller BJ. Requirement for Ca2+/calmodulin-dependent kinase II in the transition from pressure overload-induced cardiac hypertrophy to heart failure in mice. *J Clin Invest* 2009 May;119(5):1230-40.

(40) Backs J, Backs T, Neef S, Kreusser MM, Lehmann LH, Patrick DM, Grueter CE, Qi X, Richardson JA, Hill JA, Katus HA, Bassel-Duby R, Maier LS, Olson EN. The {delta} isoform of CaM kinase II is required for pathological cardiac hypertrophy and remodeling after pressure overload. *Proc Natl Acad Sci U S A* 2009 January 28.

(41) Srinivasan M, Edman CF, Schulman H. Alternative splicing introduces a nuclear localization signal that targets multifunctional CaM kinase to the nucleus. *J Cell Biol* 1994;126:839-52.

(42) Little GH, Bai Y, Williams T, Poizat C. Nuclear calcium/calmodulin-dependent protein kinase IIdelta preferentially transmits signals to histone deacetylase 4 in cardiac cells. *J Biol Chem* 2007 March 9;282(10):7219-31.

(43) Peng W, Zhang Y, Zheng M, Cheng H, Zhu W, Cao CM, Xiao RP. Cardioprotection by CaMKII-{delta}B Is Mediated by Phosphorylation of Heat Shock Factor 1 and Subsequent Expression of Inducible Heat Shock Protein 70. *Circ Res* 2009 November 12.

(44) Zhu W, Woo AY, Yang D, Cheng H, Crow MT, Xiao RP. Activation of CaMKIIdeltaC is a common intermediate of diverse death stimuli-induced heart muscle cell apoptosis. *J Biol Chem* 2007 April 6;282(14):10833-9.

(45) Naya FJ, Wu C, Richardson JA, Overbeek P, Olson EN. Transcriptional activity of MEF2 during mouse embryogenesis monitored with a MEF2-dependent transgene. *Development* 1999 May;126(10):2045-52.

(46) Baines CP, Kaiser RA, Sheiko T, Craigen WJ, Molkentin JD. Voltage-dependent anion channels are dispensable for mitochondrial-dependent cell death. *Nat Cell Biol* 2007 May;9(5):550-5.

(47) Huke S, DeSantiago J, Kaetzel MA, Mishra S, Brown JH, Dedman JR, Bers DM. SR-targeted CaMKII inhibition improves SR Ca(2+) handling, but accelerates cardiac remodeling in mice overexpressing CaMKIIdelta(C). *J Mol Cell Cardiol* 2010 October 21.

(48) Means CK, Miyamoto S, Chun J, Brown JH. S1P1 receptor localization confers selectivity for Gi-mediated cAMP and contractile responses. *J Biol Chem* 2008 May 2;283(18):11954-63.

(49) Whittaker R, Glassy MS, Gude N, Sussman MA, Gottlieb RA, Glembotski CC. Kinetics of the translocation and phosphorylation of alphaB-crystallin in mouse heart mitochondria during ex vivo ischemia. *Am J Physiol Heart Circ Physiol* 2009 May;296(5):H1633-H1642.

(50) Couchonnal LF, Anderson ME. The role of calmodulin kinase II in myocardial physiology and disease. *Physiology (Bethesda)* 2008 June;23:151-9.

(51) Bers DM, Grandi E. Calcium/calmodulin-dependent kinase II regulation of cardiac ion channels. *J Cardiovasc Pharmacol* 2009 September;54(3):180-7.

(52) Adams JW, Migita DS, Yu MK, Young R, Hellickson MS, Castro-Vargas FE, Domingo JD, Lee PH, Bui JS, Henderson SA. Prostaglandin $F_{2\alpha}$ stimulates hypertrophic growth of cultured neonatal rat ventricular myocytes. *J Biol Chem* 1996;271:1179-86.

(53) Adams JW, Sah VP, Henderson SA, Brown JH. Tyrosine kinase and Jun NH_2-terminal kinase mediate hypertrophic responses to prostaglandin $F_{2\alpha}$ in cultered neonatal rat ventricular myocytes. *Circ Res* 1998;83(2):167-78.

(54) Ito H, Hirata Y, Adachi S, Tanaka M, Tsujino M, Koike A, Nogami A, Murumo F, Hiroe M. Endothelin-1 is an autocrine/paracrine factor in the mechanism of angiotensin II-induced hypertrophy in cultured rat cardiomyocytes. *J Clin Invest* 1993;92:398-403.

(55) Knowlton KU, Michel MC, Itani M, Shubeita HE, Ishihara K, Brown JH, Chien KR. The α1a-adrenergic receptor subtype mediates biochemical, molecular, and morphologic features of cultured myocardial cell hypertrophy. *J Biol Chem* 1993;268:15374-80.

(56) Shubeita HE, McDonough PM, Harris AN, Knowlton KU, Glembotski CC, Brown JH, Chien KR. Endothelin induction of inositol phospholipid hydrolysis, sarcomere assembly, and cardiac gene expression in ventricular myocytes: a paracrine mechanism for myocardial cell hypertrophy. *J Biol Chem* 1990;265:20555-62.

(57) Simpson P. Norepinephrine-stimulated hypertrophy of cultured rat myocardial cells is an α_1-adrenergic response. *J Clin Invest* 1983;72:732-8.

(58) Simpson P, McGrath A, Savion S. Myocyte hypertrophy in neonatal rat heart cultures and its regulation by serum and by catecholamines. *Circ Res* 1982;51:787-801.

(59) Passier R, Zeng h, Frey N, Naya FJ, Nicol RL, McKinsey TA, Overbeek PA, Richardson JA, Grant SR, Olson EN. CaM kinase signaling induces cardiac hypertrophy and activates the MEF2 transcription factor in vivo. *J Clin Invest* 2000;105:1395-406.

(60) Lantsman K, Tombes RM. CaMK-II oligomerization potential determined using CFP/YFP FRET. *Biochim Biophys Acta* 2005 October 30;1746(1):45-54.

(61) Wu X, Zhang T, Bossuyt J, Li X, McKinsey TA, Dedman JR, Olson EN, Chen J, Brown JH, Bers DM. Local InsP3-dependent perinuclear Ca2+ signaling in cardiac myocyte excitation-transcription coupling. *J Clin Invest* 2006 March;116(3):675-82.

(62) Little GH, Saw A, Bai Y, Dow J, Marjoram P, Simkhovich B, Leeka J, Kedes L, Kloner RA, Poizat C. Critical role of nuclear calcium/calmodulin-dependent protein kinase IIdeltaB in cardiomyocyte survival in cardiomyopathy. *J Biol Chem* 2009 September 11;284(37):24857-68.

(63) Zhang T, Guo T, Mishra S, Dalton ND, Kranias EG, Peterson KL, Bers DM, Brown JH. Phospholamban Ablation Rescues Sarcoplasmic Reticulum Ca2+ Handling but Exacerbates Cardiac Dysfunction in CaMKII{delta}C Transgenic Mice. *Circ Res* 2009 December 3;106(2):354-62.

(64) Wencker D, Chandra M, Nguyen K, Miao W, Garantziotis S, Factor SM, Shirani J, Armstrong RC, Kitsis RN. A mechanistic role for cardiac myocyte apoptosis in heart failure. *J Clin Invest* 2003 May;111(10):1497-504.

(65) Baines CP, Kaiser RA, Purcell NH, Blair NS, Osinska H, Hambleton MA, Brunskill EW, Sayen MR, Gottlieb RA, Dorn GW, Robbins J, Molkentin JD. Loss of cyclophilin D reveals a critical role for mitochondrial permeability transition in cell death. *Nature* 2005 March 31;434(7033):658-62.

(66) Palma E, Tiepolo T, Angelin A, Sabatelli P, Maraldi NM, Basso E, Forte MA, Bernardi P, Bonaldo P. Genetic ablation of cyclophilin D rescues mitochondrial defects and prevents muscle apoptosis in collagen VI myopathic mice. *Hum Mol Genet* 2009 June 1;18(11):2024-31.

(67) Millay DP, Sargent MA, Osinska H, Baines CP, Barton ER, Vuagniaux G, Sweeney HL, Robbins J, Molkentin JD. Genetic and pharmacologic inhibition of mitochondrial-dependent necrosis attenuates muscular dystrophy. *Nat Med* 2008 April;14(4):442-7.

(68) Fujimoto K, Chen Y, Polonsky KS, Dorn GW. Targeting cyclophilin D and the mitochondrial permeability transition enhances beta-cell survival and prevents diabetes in Pdx1 deficiency. *Proc Natl Acad Sci U S A* 2010 June 1;107(22):10214-9.

(69) Elrod J, Wong R, Mishra S, Vagnozzi R., Sakthievel B, Goonasekera S, Karch J, Gabel S, Farber J, Force T, Brown JH, Murphy E, Molkentin J. Cyclophilin-D controls mitochondrial pore-dependent Ca2+ exchange, metabolic flexibility and predisposition to heart failure in mice. J Clin Invest. In press 2010.

(70) Picht E, DeSantiago J, Huke S, Kaetzel MA, Dedman JR, Bers DM. CaMKII inhibition targeted to the sarcoplasmic reticulum inhibits frequency-dependent acceleration of relaxation and Ca2+ current facilitation. *J Mol Cell Cardiol* 2007 January;42(1):196-205.

(71) Kranias EG. Regulation of Ca2+ transport by cyclic 3',5'-AMP-dependent and calcium-calmodulin-dependent phosphorylation of cardiac sarcoplasmic reticulum. *Biochim Biophys Acta* 1985;844:193-9.

(72) Li L, Chu G, Kranias EG, Bers DM. Cardiac myocyte calcium transport in phospholamban knockout mouse: relaxation and endogenous CaMKII effects. *Am J Physiol* 1998;274:H1335-H1347.

(73) Janczewski AM, Zahid M, Lemster BH, Frye CS, Gibson G, Higuchi Y, Kranias EG, Feldman AM, McTiernan CF. Phospholamban gene ablation improves calcium transients but not cardiac function in a heart failure model. *Cardiovasc Res* 2004 June 1;62(3):468-80.

(74) Purcell NH, Wilkins BJ, York A, Saba-El-Leil MK, Meloche S, Robbins J, Molkentin JD. Genetic inhibition of cardiac ERK1/2 promotes stress-induced apoptosis and heart failure but has no effect on hypertrophy in vivo. *Proc Natl Acad Sci U S A* 2007 August 28;104(35):14074-9.

(75) Bers DM. Altered cardiac myocyte Ca regulation in heart failure. *Physiology (Bethesda)* 2006 December;21:380-7.

(76) Chien KR, Ross J, Jr., Hoshijima M. Calcium and heart failure: the cycle game. *Nat Med* 2003 May;9(5):508-9.

(77) del Monte F, Harding SE, Dec GW, Gwathmey JK, Hajjar RJ. Targeting phospholamban by gene transfer in human heart failure. *Circ*105(8):904-7.

(78) Engelhardt S, Hein L, Dyachenkow V, Kranias EG, Isenberg G, Lohse MJ. Altered calcium handling is critically involved in the cardiotoxic effects of chronic beta-adrenergic stimulation. *Circ* 2004 March 9;109(9):1154-60.

(79) Hoshijima M, Ikeda Y, Iwanaga Y, Minamisawa S, Date MO, Gu Y, Iwatate M, Li M, Wang L, Wilson JM, Wang Y, Ross J, Chien KR. Chronic suppression of heart-failure progression by a pseudophosphorylated mutant of phospholamban via in vivo cardiac rAAV gene delivery. *Nat Med* 2002 August;8(8):864-71.

(80) Iwanaga Y, Hoshijima M, Gu Y, Iwatate M, Dieterle T, Ikeda Y, Date MO, Chrast J, Matsuzaki M, Peterson KL, Chien KR, Ross J, Jr. Chronic phospholamban inhibition prevents progressive cardiac dysfunction and pathological remodeling after infarction in rats. *J Clin Invest* 2004 March;113(5):727-36.

(81) Minamisawa S, Hoshijima M, Chu G, Ward CA, Frank K, Gu Y, Martone ME, Wang Y, Ross JJr, Kranias EG, Giles WR, Chien KR. Chronic phospholamban-sarcoplasmic reticulum calcium ATPase interaction is the critical calcium cycling defect in dilated cardiomyopathy. *Cell* 1999;99:1-20.

(82) Sato Y, Kiriazis H, Yatani A, Schmidt AG, Hahn H, Ferguson DG, Sako H, Mitarai S, Honda R, Mesnard-Rouiller L, Frank KF, Beyermann B, Wu G, Fujimori K, Dorn GW, Kranias EG. Rescue of contractile parameters and myocyte hypertrophy in calsequestrin overexpressing myocardium by phospholamban ablation. *J Biol Chem* 2001 March 23;276(12):9392-9.

(83) Adams JW, Pagel AL, Means CK, Oksenberg D, Armstrong RC, Brown JH. Cardiomyocyte apoptosis induced by Gαq signaling is mediated by permeability transition pore formation and activation of the mitochondrial death pathway. *Circ Res* 2000;87:1180-7.

(84) Chen X, Zhang X, Kubo H, Harris DM, Mills GD, Moyer J, Berretta R, Potts ST, Marsh JD, Houser SR. Ca2+ influx-induced sarcoplasmic reticulum Ca2+ overload causes mitochondrial-dependent apoptosis in ventricular myocytes. *Circ Res* 2005 November 11;97(10):1009-17.

(85) Crompton M. The mitochondrial permeability transition pore and its role in cell death. *Biochem J* 1999;341:233-49.

(86) Green DR, Reed JC. Mitochondria and apoptosis. *Science* 1998;281:1309-12.

(87) Baines CP. The mitochondrial permeability transition pore and ischemia-reperfusion injury. *Basic Res Cardiol* 2009 March;104(2):181-8.

(88) Dorn GW. Apoptotic and non-apoptotic programmed cardiomyocyte death in ventricular remodelling. *Cardiovasc Res* 2009 February 15;81(3):465-73.

(89) Nakayama H, Chen X, Baines CP, Klevitsky R, Zhang X, Zhang H, Jaleel N, Chua BH, Hewett TE, Robbins J, Houser SR, Molkentin JD. Ca2+- and mitochondrial-dependent cardiomyocyte necrosis as a primary mediator of heart failure. *J Clin Invest* 2007 September;117(9):2431-44.

(90) Diwan A, Matkovich SJ, Yuan Q, Zhao W, Yatani A, Brown JH, Molkentin JD, Kranias EG, Dorn GW. Endoplasmic reticulum-mitochondria crosstalk in NIX-mediated murine cell death. *J Clin Invest* 2009 January;119(1):203-12.

(91) Demaurex N, Distelhorst C. Cell biology. Apoptosis--the calcium connection. *Science* 2003 April 4;300(5616):65-7.

(92) Szalai G, Csordas G, Hantash BM, Thomas AP, Hajnoczky G. Calcium signal transmission between ryanodine receptors and mitochondria. *J Biol Chem* 2000 May 19;275(20):15305-13.

(93) Kokoszka JE, Waymire KG, Levy SE, Sligh JE, Cai J, Jones DP, MacGregor GR, Wallace DC. The ADP/ATP translocator is not essential for the mitochondrial permeability transition pore. *Nature* 2004 January 29;427(6973):461-5.

(94) Zhu WZ, Wang SQ, Chakir K, Yang D, Zhang T, Brown JH, Devic E, Kobilka BK, Cheng H, Xiao RP. Linkage of β_1-adrenergic stimulation to apoptotic heart cell death through protein kinase A-independent activation of Ca^{2+}/calmodulin kinase II. *J Clin Invest* 2003;111:617-25.

(95) Yang Y, Zhu WZ, Joiner ML, Zhang R, Oddis CV, Hou Y, Yang J, Price EE, Gleaves L, Eren M, Ni G, Vaughan DE, Xiao RP, Anderson ME. Calmodulin kinase II inhibition protects against myocardial cell apoptosis in vivo. *Am J Physiol Heart Circ Physiol* 2006 December;291(6):H3065-H3075.

(96) Vila-Petroff M, Salas MA, Said M, Valverde CA, Sapia L, Portiansky E, Hajjar RJ, Kranias EG, Mundina-Weilenmann C, Mattiazzi A. CaMKII inhibition protects against necrosis and apoptosis in irreversible ischemia-reperfusion injury. *Cardiovasc Res* 2007 March 1;73(4):689-98.

(97) Kushnareva YE, Wiley SE, Ward MW, Andreyev AY, Murphy AN. Excitotoxic injury to mitochondria isolated from cultured neurons. *J Biol Chem* 2005 August 12;280(32):28894-902.

(98) Igbavboa U, Pfeiffer DR. EGTA inhibits reverse uniport-dependent Ca2+ release from uncoupled mitochondria. Possible regulation of the Ca2+ uniporter by a Ca2+ binding site on the cytoplasmic side of the inner membrane. *J Biol Chem* 1988 January 25;263(3):1405-12.

(99) Liu T, O'Rourke B. Regulation of mitochondrial Ca2+ and its effects on energetics and redox balance in normal and failing heart. *J Bioenerg Biomembr* 2009 April;41(2):127-32.

(100) Denton RM. Regulation of mitochondrial dehydrogenases by calcium ions. *Biochim Biophys Acta* 2009 November;1787(11):1309-16.

(101) Brandes R, Bers DM. Intracellular Ca2+ increases the mitochondrial NADH concentration during elevated work in intact cardiac muscle. *Circ Res* 1997 January;80(1):82-7.

(102) Unitt JF, McCormack JG, Reid D, MacLachlan LK, England PJ. Direct evidence for a role of intramitochondrial Ca2+ in the regulation of oxidative phosphorylation in the stimulated rat heart. Studies using 31P n.m.r. and ruthenium red. *Biochem J* 1989 August 15;262(1):293-301.

(103) Ji Y, Li B, Reed TD, Lorenz JN, Kaetzel MA, Dedman JR. Targeted inhibition of Ca^{2+}/calmodulin-dependent protein kinase II in cardiac longitudinal sarcoplasmic reticulum results in decreased phospholamban phosphorylation at threonine 17. *J Biol Chem* 2003 July 4;278(27):25063-71.

(104) Ji Y, Zhao W, Li B, DeSantiago J, Picht E, Kaetzel MA, Schultz JJ, Kranias EG, Bers DM, Dedman JR. Targeted inhibition of sarcoplasmic reticulum CaMKII activity results in alterations of Ca2+ homeostasis and cardiac contractility. *Am J Physiol Heart Circ Physiol* 2006 February;290(2):H599-H606.

(105) Ai X, Curran JW, Shannon TR, Bers DM, Pogwizd SM. Ca2+/calmodulin-dependent protein kinase modulates cardiac ryanodine receptor phosphorylation and sarcoplasmic reticulum Ca2+ leak in heart failure. *Circ Res* 2005 December 9;97(12):1314-22.

(106) Kirchhefer U, Schmitz W, Scholz H, Neumann J. Acitivity of cAMP-dependent protein kinase and Ca^{2+}/calmodulin-dependent protein kinase in failing and nonfailing human hearts. *Cardiovasc Res* 1999;42:254-61.

(107) Hoch B, Meyer R, Hetzer R, Krause E-G, Karczewski P. Identification and expression of δ-isoforms of the multifunctional Ca^{2+}/calmodulin dependent protein kinase in failing and nonfailing human myocardium. *Circ Res* 1999;84:713-21.

(108) Bossuyt J, Helmstadter K, Wu X, Clements-Jewery H, Haworth RS, Avkiran M, Martin JL, Pogwizd SM, Bers DM. Ca2+/calmodulin-dependent protein kinase IIdelta and protein kinase D overexpression reinforce the histone deacetylase 5 redistribution in heart failure. *Circ Res* 2008 March 28;102(6):695-702.

(109) Sossalla S, Fluschnik N, Schotola H, Ort KR, Neef S, Schulte T, Wittkopper K, Renner A, Schmitto JD, Gummert J, El-Armouche A, Hasenfuss G, Maier LS. Inhibition of elevated Ca2+/calmodulin-dependent protein kinase II improves contractility in human failing myocardium. *Circ Res* 2010 October 29;107(9):1150-61.

(110) Wehrens XH, Lehnart SE, Reiken SR, Marks AR. Ca2+/Calmodulin-Dependent Protein Kinase II Phosphorylation Regulates the Cardiac Ryanodine Receptor. *Circ Res* 2004 April 2;94(6):E61-E70.

(111) Guo T, Zhang T, Mestril R, Bers DM. Ca2+/Calmodulin-dependent protein kinase II phosphorylation of ryanodine receptor does affect calcium sparks in mouse ventricular myocytes. *Circ Res* 2006 August 18;99(4):398-406.

(112) Zhang R, Khoo MS, Wu Y, Yang Y, Grueter CE, Ni G, Price EE, Thiel W, Guatimosim S, Song LS, Madu EC, Shah AN, Vishnivetskaya TA, Atkinson JB, Gurevich VV, Salama G, Lederer WJ, Colbran RJ, Anderson ME. Calmodulin kinase II inhibition protects against structural heart disease. *Nat Med* 2005 April;11(4):409-17.

(113) Zhang J, Ma Y, Taylor SS, Tsien RY. Genetically encoded reporters of protein kinase A activity reveal impact of substrate tethering. *Proc Natl Acad Sci U S A* 2001 December 18;98(26):14997-5002.

(114) Violin JD, Zhang J, Tsien RY, Newton AC. A genetically encoded fluorescent reporter reveals oscillatory phosphorylation by protein kinase C. *J Cell Biol* 2003 June 9;161(5):899-909.

(115) Kunkel MT, Toker A, Tsien RY, Newton AC. Calcium-dependent regulation of protein kinase D revealed by a genetically encoded kinase activity reporter. *J Biol Chem* 2007 March 2;282(9):6733-42.

(116) Kunkel MT, Ni Q, Tsien RY, Zhang J, Newton AC. Spatio-temporal Dynamics of Protein Kinase B/Akt Signaling Revealed by a Genetically Encoded Fluorescent Reporter. *J Biol Chem* 2005 February 18;280(7):5581-7.

(117) Allen MD, Zhang J. Subcellular dynamics of protein kinase A activity visualized by FRET-based reporters. *Biochem Biophys Res Commun* 2006 September 22;348(2):716-21.